

The role of GRAS proteins in light signalling

Dissertation
zur Erlangung des Doktorgrades der Naturwissenschaften
(Dr. rer. nat.)
der Fakultät für Biologie der Ludwig-Maximilian-Universität
München

vorgelegt von
Patricia Torres Galea,
aus Spanien

2007

eingereicht am: 9. Juli 2007

- 1. Gutachter: Prof. Dr. Reinhold G. Herrmann**
- 2. Gutachter: PD Dr. Cordelia Bolle**

Tag der mündlichen Prüfung: 22. November 2007

TABLE OF CONTENTS

TABLE OF CONTENTS	1
ABBREVIATIONS	5

1. INTRODUCTION

1.1. Light and photoreceptors	8
1.2. Evolution of phytochromes	10
1.3. Classification of phytochromes	12
1.4. Two reversible forms of phytochromes	12
1.5. Structure of phytochromes	14
1.5.1. Structure-function relationships of phytochromes	16
1.6. Physiological functions of phytochromes	17
1.6.1. Phytochromes can initiate high, low and very low fluence responses	17
1.6.2. Phytochromes and seed germination	18
1.6.3. Phytochromes and de-etiolation	19
1.6.4. Phytochromes and shade avoidance	20
1.6.5. The complex interplay among the photoreceptors	21
1.7. Signal transduction by photoreceptors	22
1.8. PAT 1 (Phytochrome A Signal Transduction 1), a GRAS protein, is involved in phytochrome signalling	25

2. MATERIALS

2.1. Chemicals and enzymes	28
2.2. Enzymes	28
2.3. Kits	28
2.4. Antibiotic stock solutions	29
2.5. Oligonucleotides	29
2.6. Length and weight standards	29
2.7. Bacterial strains	29
2.8. Yeast strains	30
2.9. Antibodies	30
2.10. Plasmids	30
2.11. Hybridisation probes for Northern analysis	31
2.12. Plant material	31

3. METHODS

I. General Techniques of Molecular Biology

3.1. Preparation of competent bacterial cells	32
3.2. Transformation of bacteria	33
3.2.1. Culture of <i>E. coli</i> DH5 α cells for plasmid growth	33
3.2.2. Small-scale plasmid isolation from <i>E. coli</i> (Miniprep)	33
3.2.3. Restriction analysis of plasmid DNA	33
3.3. Analysis of DNA by agarose gel electrophoresis	34
3.3.1. Isolation of DNA fragments from agarose gels	34
3.4. Ligation of DNA fragments	34

II. DNA analyses

3.5. Isolation of genomic DNA	34
3.6. Polymerase chain reaction (PCR)	35
3.6.1. Preparation of PCR-derived DNA fragments for ligation	36
3.7. Determination of nucleic acid concentrations	36

III. RNA analyses

3.8. Isolation of total RNA	36
3.8.1 DNase I treatment of RNA preparations	36
3.9. Semiquantitative reverse transcription polymerase chain reaction (RT-PCR)	37
3.10. Northern analyses	37
3.10.1. Staining of Northern Blots	38
3.10.2. Generation and purification of ³² P-labelled radioactive probes	38
3.10.2.1. Hybridisation of nucleic acids	38

IV. Protein analyses

3.11. Extraction of total proteins for Western Blots	38
3.12. Preparation of Tris-Glycine SDS-Polyacrylamide Gel Electrophoresis (PAGE)	39
3.12.1. Separation of proteins by PAGE	39
3.12.2. Western analysis	40
3.12.3. Coomassie Blue R-250 staining of protein gels	40

V. Protein detection

3.13. Immunoblotting	41
----------------------	----

VI. Manipulation of yeast cells

3.14. Preparation of competent yeast cells	41
3.15. Yeast transformation	42
3.16. Plasmid DNA extraction from yeast cells	42
3.17. Yeast Two-Hybrid and One-Hybrid assays	43

VII. Growth conditions and physiological characterization

3.18. Seed sterilization, growth conditions and mutant selection	44
3.19. Physiological measurements	44
3.20. Cellular and subcellular localization	45

VIII. Analysis of mutants and Plant transformation

3.21. Analysis of mutants46
 3.22. Plant transformation47

IX. Generation of constructs

3.23. Transgenic plants47

X. Sequence analysis, Databases and Computer programmes

3.24. Sequence Analysis48
 3.25. Analysis of microarray data
 48
 3.26. Databases48
 3.27. Computer Programmes48

4. RESULTS

4.1. Phylogenetic analysis50
 4.1.1. Phylogenetic tree50
 4.1.2. Alignment of the *Arabidopsis* PAT1 branch of the GRAS protein family51
**4.2. Generation of transgenic *Arabidopsis* lines with defects in *SCL1*, *5*, *13*,
 21 and *PAT1*52**
 4.2.1. Identification of homozygous insertion lines52
 4.2.2. Generation of antisense and RNAi lines54
4.3. Physiological characterization of *SCL1*, *SCL5*, *SCL21* and *PAT1*56
 4.3.1. Hypocotyl elongation under different light conditions56
 4.3.2. Response to different FR light fluences57
 4.3.3. Hook opening and cotyledon unfolding58
4.4. Physiological characterization of *SCL13* antisense lines59
 4.4.1. Inhibition of hypocotyl elongation under R light conditions is specifically impaired
 in *SCL13* antisense lines59
 4.4.2. Response to different R light fluences60
4.5. Expression pattern of all genes of the *PAT1* branch61
 4.5.1. Role of the Intron in the 5'-UTR61
 4.5.2. Analysis of the *SCL1*, *SCL21* and *SCL13* promoter activities with the
 β -Glucuronidase (*GUS*) reporter gene62
 4.5.3. Expression pattern of all genes coding for proteins of the *PAT1* branch64
4.6. Analysis of the subcellular localization by expressing GFP fusions70
 4.6.1. Analysis of the subcellular localization by fluorescence microscopy70
**4.7. Detailed physiological analysis of the function of *SCL21* and *PAT1* in the
 Phytochrome A signalling72**
 4.7.1. Block of greening after FR irradiation72
 4.7.2. Germination efficiency73
 4.7.3. Expression of light regulated genes in *SCL21* and *PAT1*74
 4.7.4. Regulation of the expression of *SCL21* by light75

4.8. Expression of the genes on the protein level	77
4.8.1. Confirmation of the loss of SCL21 and PAT1 in the knock-out lines	77
4.8.2. Expression of SCL21 and PAT1 at the protein level	78
4.9. Yeast Two-Hybrid analysis	78
4.9.1. SCL21 activates transcription in yeast	78
4.10. SEUSS-LIKE (SL)1, a putative interactor of PAT1 and SCL21	79
4.10.1. Physiological analysis of the <i>seuss-like (sl)1</i> mutants	80
4.10.2. Response to different FR light fluences	81
4.10.3. SEUSS-Like1 can transactivate in yeast Two-Hybrid assay	81
4.10.4. Interaction between SEUSS-Like1 and the GRAS proteins, PAT1 and SCL21	82
5. DISCUSSION	
5.1. All members of the PAT1 sub-branch of the GRAS protein family are involved in light signalling	83
5.1.1. Detailed physiological analysis of the phyA responses in the mutant lines	84
5.1.2. Detailed analysis of the R light responses in SCL13 antisense lines	85
5.1.3. Interaction between phyA and phyB signal transduction cascades	86
5.2. Subcellular localization studies suggest that SCL1, 5, 13, 21 and PAT1 could play a biological role in the cytoplasm and nucleus	86
5.3. Tissue-specific expression of the PAT1-related genes	88
5.4. SCL21 gene expression is negatively regulated by phyA	89
5.5. Role of introns in the 5'-untranslated region of the genes	89
5.6. Protein stability	90
5.7. Seuss-Like 1, a putative interaction partner of PAT1 and SCL21	90
5.8. SCL21 and PAT1 as potential factors involved in activation of transcription	91
5.9. Are GRAS proteins transcription factors?	92
5.10. GRAS proteins and light signalling	93
6. SUMMARY	94
7. REFERENCES	96
8. APPENDIX 1	109
ACKNOWLEDGEMENT	113
Curriculum vitae	114
Ehrenwörtliche Versicherung	116

ABREVIATIONS

A	adenine
A	absorbance
AA	amino acid
AD	activation domain
amp	ampicillin
APS	ammonium persulfate
3AT	3-amino-1,2,4,-triazole
ATE	amino terminal extension
ATP	adenosine 5'-triphosphate
att	attachment sites (Gateway System)
B	blue light
Bar	basta
BarR	basta resistance
bp	base pairs
BLD	bilin lyase domain
BSA	bovine serum albumin
C	cytosine
°C	centigrade
CAB	<i>chlorophyll a/b-binding protein gene</i>
cDNA	complementary DNA
Chl	chlorophyll
CHS	<i>chalcone synthase gene</i>
cm	centimetres
Col-0	Columbia wild type
Cry	cryptochrome
CTAB	hexadecyltrimethyl-amonium bromide
C-term	carboxyl terminal
D	dark
d	day
DAPI	4'-6-diamidino-2-phenylIndole
dATP	desoxy-adenosintriphosphate
DB	DNA binding domain
dCTP	desoxy-cytosintriphosphate
dGTP	desoxy-guanosintriphosphate
dH ₂ O	deionised water
DNA	deoxyribonucleic acid
DNase	desoxyribonuclease
dNTP	desoxy-nucleotidetriphosphate
DTE	dithioerythitol
DDT	dichlordiphenyltrichlorethan
EDTA	ethylenediaminetetraacetic acid
ESTs	expressed sequence tags
f	forward
FR	far-red light
FRc	continuous far-red light
F1, F2, F3	first generation, second generation, third generation
G	guanine
g	gram
GAI	<i>gibberellin insensitive gene</i>
g	gravity force
GFP	green fluorescent protein
GUS	β- glucuronidase

h	hour
H	hinge region
<i>HAM</i>	<i>hairy meristem maintenance</i> gene
HEPES	N-[2-hydroxyethyl]piperazine-N'-[2-ethanesulfonic acid]
HIR	high irradiance response
His	histidine
<i>His3</i>	<i>histidine</i> reporter gene
HKRD	histidine kinase-related domain
IgG	immunoglobulin G
kan	kanamycin
KanR	kanamycin resistance
Kb	kilo bases
kDa	kilo Dalton
λ	lambda
l	litre
LB	left border
LB-Medium	luria-broth medium
LED	light emitting diode
LFR	low fluence response
LR	leucine-rich
<i>Ls</i>	<i>lateral suppressor</i> gene
M	molar
mA	milliamper
MB	methylene blue
mg	milligram
μ g	microgram
ml	millilitres
μ l	microlitres
μ M	micromolar
μ mol	micromol
min.	minutes
mM	millimolar
mm	millimetres
MOPS	2-morpholinoethansulfonic acid
mRNA	messenger RNA
MS	murashige-and-skoog medium
ng	nanogram
nm	nanometre
nt	nucleotides
N-term	amino terminal
OD	absorbance
ON	over night
ORF	open reading frame
P	phosphor
PAGE	polyacrylamide gel electrophoresis
PAS	per-arnt-sim domain
PAT1	phytochrome A signal transduction 1 protein
PBS	phosphate buffer saline
PCR	polymerase chain reaction
PEG	polyethylene glycol
Pfr	far-red light absorbing form of phytochrome
<i>PhHam</i>	<i>hairy meristem (HAM)</i> gene of petunia
Phot	phototropin
pM	picomolar
pmol	picomol

Pr	red light absorbing form of phytochrome
PRD	per-arnt-sim related domain
PVDF	polyvinylidene fluoride
<i>P35S</i>	<i>35S-CaMV</i> promoter
rev	reverse
R	red light
Rc	continuous red light
RB	right border
<i>RGA</i>	<i>repressor of ga-1</i> gene
RNA	ribonucleic acid
RNAse	ribonuclease
RNAi	RNA interference
rpm	revolutions per minute
rRNA	ribosomal RNA
RT	room temperature
RT-PCR	reverse transcription polymerase chain reaction
Sec.	seconds
SC media	synthetic complete dropout media
<i>SCL</i>	<i>scarecrow-like</i> gene
<i>SCR</i>	<i>scarecrow</i> gene
SD	standard deviation
SDS	sodium dodecyl sulphate
SDS-PAGE	SDS-polyacrylamide gel electrophoresis
<i>SHR</i>	<i>short-root</i> gene
<i>SL1</i>	<i>seuss-like 1</i> gene
<i>sl</i>	seuss-like
SSC	sodium chloride-sodium citrate
T	thymine
TBS buffer	tris buffered saline buffer
T-DNA	transferred DNA
TEMED	N,N,N',N'-tetramethylethylenediamine
Tm	melting temperature
Tris	tris-(hydroxymethyl)-aminomethane, 2-amino-2-(hydroxymethyl)-1,3-propanediol
<i>T35S</i>	<i>35S-CaMV</i> terminator
Tween 20	polyoxyethylene-sorbitane monolaurate
U	unit, enzyme activity
UAS	upstream activator sequences
5'-UTR	5'-untranslated region
UV-A/UV-B	ultraviolet light A/B
V	volt
VLFR	very low fluence response
Vol	volume
v/v	volume per volume
λ	wavelength
W	white light
WT	wild type
w/v	weight per volume
w/w	weight per weight
X-Gal	5-bromo-4-chloro-3-indolyl- β -D-galactopyranoside
X-Gluc	5-bromo-4-chloro-3-indolyl- β -D-glucuronide
<i>XTR7</i>	<i>xyloglucan endotransglycosylase</i> gene

1. INTRODUCTION

1.1. Light and photoreceptors

The survival of unicellular or multicellular organisms depends on their ability to sense and respond to their extracellular environment. As sessile organisms, plants are unable to move actively towards favourable or away from unfavourable environmental conditions. Therefore, by means of their evolution, plants have adapted a high degree of developmental plasticity to optimize their growth and reproduction in response to their surrounding environments.

Plants are exposed to a variety of different biotic and abiotic factors in their environment such as light, temperature, water abundance, salt, nutrient and toxic content of the soil, infection by pathogens, predators and competition with neighbouring plants. Light is one of the major environmental signals that influences plant growth and development. Not only is light the primary energy source for plants, it also provides them with information to modulate their developmental processes such as seed germination, seedling de-etiolation, gravitropism and phototropism, chloroplast movement, shade avoidance, circadian rhythms and flowering time (Smith 1995, Parks *et al.* 1996, Robson and Smith 1996, Chen and Fankhauser 2004). After germination, the very young seedling must choose between two developmental pathways depending on the availability of light. In the absence of light, the seedling grows heterotrophically, using the resources from the seed in an effort to reach light. This so called “etiolated stage” is characterized by a long hypocotyl, an apical hook and unopened cotyledons. Once the seedling perceives sufficient light, it will “de-etiolate”, a developmental process that optimizes the seedling for efficient photosynthetic growth (Tab. 1 and Fig. 1). During de-etiolation, the rate of hypocotyl growth decreases, the apical hook opens, cotyledons expand, chloroplasts develop, and a new gene expression program is induced.

Table 1. Comparison of the phenotypes of dark-grown (etiolated) and light-grown (de-etiolated) seedlings.

Etiolated characteristics	De-etiolated characteristics
Apical hook (dicot) or coleoptile (monocot)	Apical hook opens or coleoptile splits open
No leaf growth	Leaf growth promoted
No chlorophyll	Chlorophyll produced
Rapid hypocotyl elongation	Hypocotyl elongation suppressed
Reduced radial expansion of stem	Radial expansion of stem
Reduced root elongation	Root elongation promoted
Reduced production of lateral roots	Lateral root development accelerated

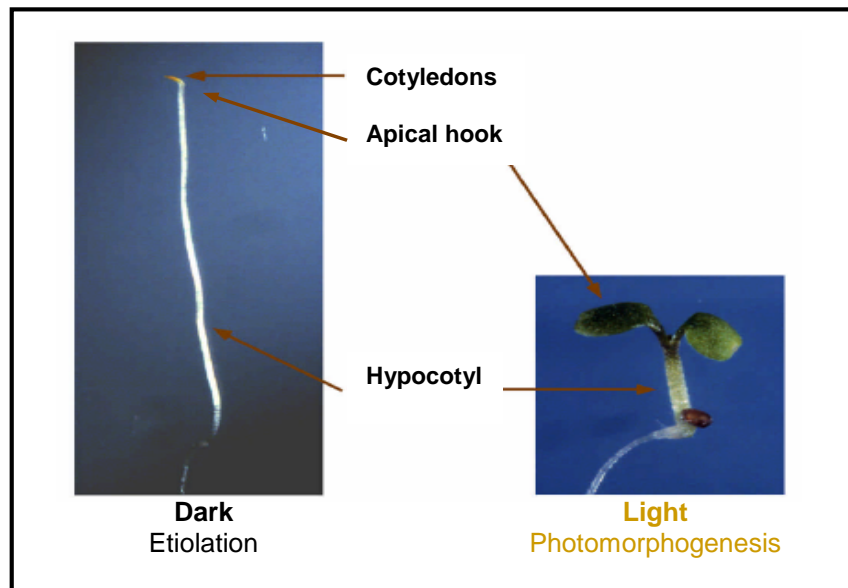


Figure 1. The phenotypes of dark- and light-grown *Arabidopsis thaliana* seedlings. In darkness seedlings undergo etiolation: elongated hypocotyls, closed cotyledons and apical hooks. By contrast, when seedlings perceive light they undergo photomorphogenesis: short hypocotyls, open and expanded green cotyledons. Adapted from Wang and Deng, 2004.

Using specialized photoreceptors, plants can monitor the quantity, quality, direction, duration and wavelength of the incoming light. Three principal families of signal-transducing photoreceptors have been identified and characterized in higher plants. These are the red (R)/far-red (FR) light (600 - 730 nm) absorbing phytochromes (phy), the blue (B)/UV-A (320 - 500 nm) absorbing cryptochromes (cry) and phototropins (phot), and as yet unidentified UV-B (282 - 320 nm) sensing receptors (Kendrick and Kronenberg 1994, Briggs and Olney 2001; Fig. 2). These photoreceptors perceive, interpret, and transduce light signals *via* intracellular signalling pathways to photoresponsive genes, which modulate plant growth and development (Ma *et al.* 2001, Tepperman *et al.* 2001).

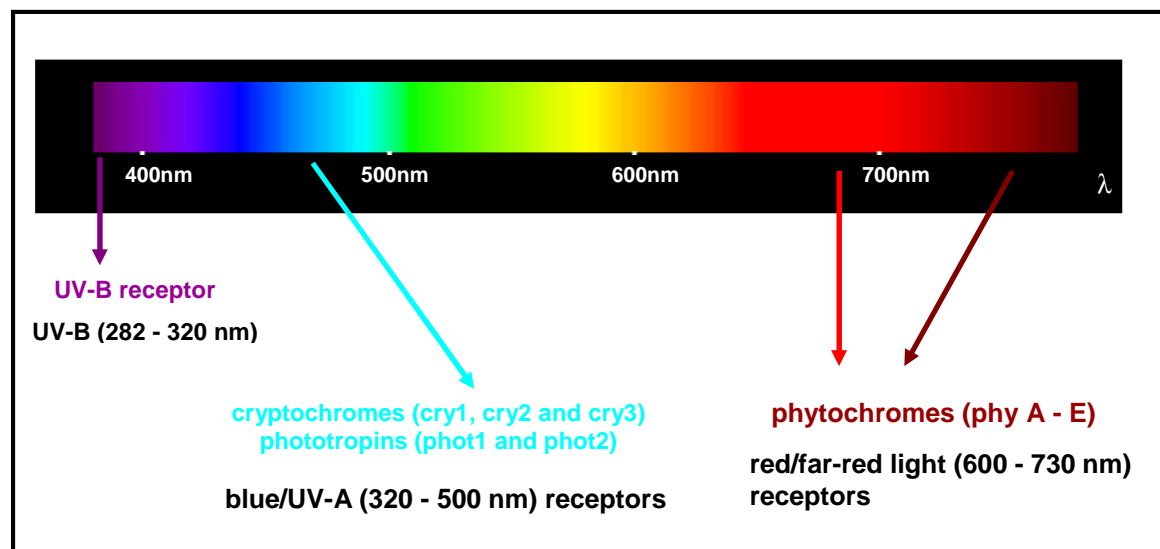


Figure 2. Principal families of photoreceptors in higher plants, as identified in *Arabidopsis thaliana*. The wavelength of their maximal absorption is given (nm).

The light-dependent development of plants, a process called photomorphogenesis, has been studied for more than a century in a wide variety of plant species. Due to its small structure and genome size, its short life cycle, and the ease with which it can be propagated, *Arabidopsis thaliana* has become a model plant in the study of photomorphogenesis. The *Arabidopsis thaliana* genome encodes receptors absorbing B and UV-A light (Christie 2006) and the phytochromes covering the R and FR part of the spectrum (Butler *et al.* 1959, Furuya 1993, Quail *et al.* 1995, Rockwell and Lagarias 2006). Phytochromes are encoded in *Arabidopsis thaliana* by a gene family of five members, called phytochromes A, B, C, D and E (phy A - E) (Sharrock and Quail 1989, Clack *et al.* 1994).

1.2. Evolution of phytochromes

Phytochromes have been found in all taxa of lower and higher plants examined (angiosperms, gymnosperms, mosses, ferns and green algae) and photosynthetic bacteria (cyanobacteria and purple bacteria; Kehoe *et al.* 1996, Hughes *et al.* 1997, Yeh and Lagarias 1997) as well as in non-photosynthetic eubacteria (Mathews and Sharrock 1997, Hughes and Lamparter 1999, Vierstra and Davis 2000). However, their role in prokaryotes is not very clear.

Phytochrome evolution in land plants is marked by a series of gene duplications that have led to independently evolving and functionally distinct lines (Mathews 2006). A duplication preceding the origin of seed plants resulted in two distinct lines that persist in all seed plants. Phylogenetic analyses suggest that subsequent duplications occurred in each of these lines, leading to the four major forms found in angiosperms, phytochromes A, B, C, and E (Mathews *et al.* 1995, Mathews and Sharrock 1997). The first duplication occurring about the time of the origin of seed plants, generated the *PHYA/C* and *PHYB/D/E* lines (Fig. 3). Two later duplications, at about the time of the origin of the flowering plants, separated *PHYA* from *PHYC* and *PHYB/D* from *PHYE*. *PHYB* and *PHYD* diverged more recently (Fig. 3).

In cycads, Ginkgo, and conifers, a duplication in the *PHYA/C*-related line led to *PHYN* and *PHYO*, but the *PHYB/E*-related line, *PHYP*, did not diversify in other seed plants except in Pinaceae (Schneider-Poetsch *et al.* 1998, Clapham *et al.* 1999, Schmidt and Schneider-Poetsch 2002). Phylogenetic analyses also suggest that the duplication leading to *PHYA* and *PHYC* occurred prior to the origin of angiosperms (Mathews *et al.* 1995, Mathews and Sharrock 1997, Mathews and Donoghue 1999).

Gene duplications are considered to be a significant force in genome evolution (Wagner 2001) and may also play a significant role in speciation (Lynch and Conery 2000). When a gene duplicates, one copy may be silenced or evolve a novel function, or the two copies may subdivide functions of the ancestral gene (Ohno 1970, Walsh 1995, Force *et al.* 1999, Lynch and Force 2000). In the case of *PHYA* and *PHYC*, both copies have been maintained but they exert

different functions. However, recent results showed that the functions of phyA and phyC in the dicot *A. thaliana* are more diverse than in the monocot rice (Takano *et al.* 2005).

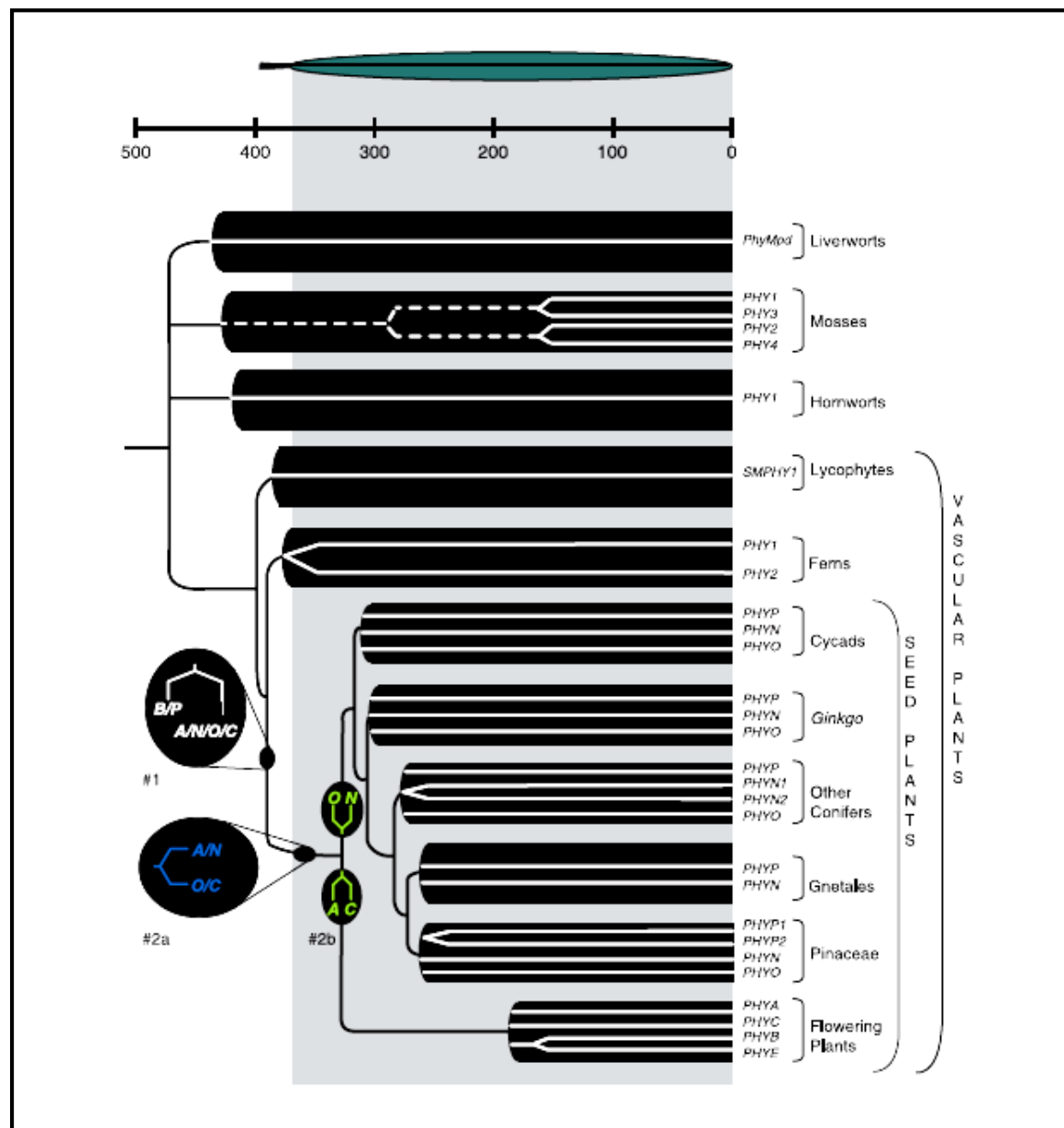


Figure 3. Ancestry of phytochromes among land plants. The first duplication of the land plant phytochrome occurred near the origin of seed plants (#1). A later duplication occurred before the divergence of angiosperms and extant gymnosperms (#2a), separate duplications occurred in angiosperms and gymnosperms (#2b). Timeline indicates million years ago. Dashed lines indicate unknown ancestry. Adapted from Mathews, 2006.

In mosses and ferns, phytochromes seem to be particularly involved in phototropism (Esch *et al.* 1999), a function mediated exclusively by the B light absorbing phototropin in the angiosperms (Christie *et al.* 1998). Indeed, in the fern *Adiantum*, a gene has been characterized that encodes both a typical phytochrome and a protein with sequence similarity to NPH1 (the *Arabidopsis* phototropin) (Nozue *et al.* 1998). Another chimaeric phytochrome gene has been identified in the moss *Ceratodon* (Thümmel and Dittrich 1992), encoding a protein kinase carboxy-terminal segment, but its function has not been determined.

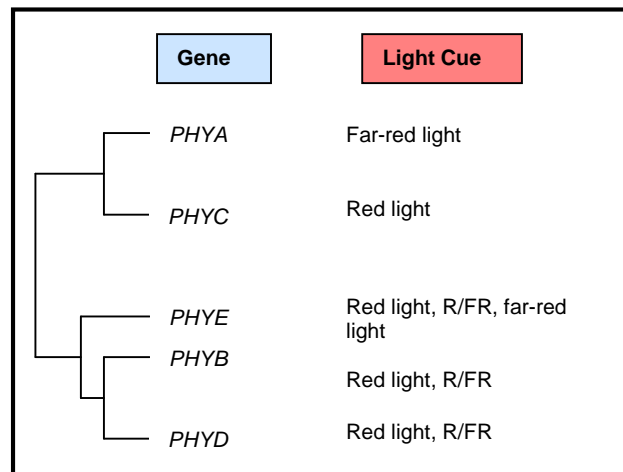


Figure 4. Phylogenetic relationships of the phytochrome genes of *Arabidopsis thaliana*, where the encoded proteins phyA and phyB have been demonstrated to be the principal mediators of responses to far-red (FR) and red (R) light, respectively.

1.3. Classification of phytochromes

All five phytochromes of *Arabidopsis* are expressed throughout the plant with only minor differences in their expression patterns, however, their abundance and stability differ dramatically (Somers and Quail 1995). The protein products of the *PHYB* and *PHYD* genes share approximately 80% sequence similarity and these are more related to *PHYE* than they are to either *PHYA* or *PHYC* proteins (about 50% identity; Fig. 4) (Clack *et al.* 1994, Sharrock and Quail 1989, Mathews and Sharrock 1997).

In the 1980's, spectrophotometric studies indicated that there are at least two distinct pools of phytochromes, Type I (light labile) and Type II (light stable). Type I phytochromes, phyA in *Arabidopsis*, are highly abundant in dark-grown seedlings and their protein level drops 100 times in light-grown plants (Clough *et al.* 1999, Hennig *et al.* 1999, Somers and Quail 1995). This downregulation is effective at several levels: a feedback control reduces the *PHYA* gene expression, the mRNA is unstable and furthermore the protein is degraded by a ubiquitin/26S proteasome dependent process (Seo *et al.* 2004). Type II phytochromes are relatively light stable and phyB is the most abundant phytochrome in light-grown plants. Phy C - E also belong to this group, but are much less abundant (Clark *et al.* 1994, Hirschfeld *et al.* 1998).

1.4. Two reversible forms of phytochromes

The physiological functions of phytochromes are determined by their photosensory characteristics, which depend on photochemistry. The striking characteristic of the phytochromes is their reversible photochromism, the property of changing colour on photon absorption and of reverting to the original form on the absorption of another photon. The absorption maximum of the phytochrome Pr form is close to that of the chlorophylls at 660 nm (R light), but the Pfr form

absorbs at a longer wavelength with an absorption maximum at 730nm (FR light). Phytochromes can exist *in vivo* in these two isoforms. The Pr form of phytochrome is generally considered to be inactive and accumulates to relatively high levels in dark-grown tissues. Upon exposure to R light, the Pr form is converted to the Pfr form, which is considered as the biologically active form (Quail *et al.* 1995). The active Pfr form can be converted back to the inactive Pr form by a slow non-photoinduced reaction (dark reversion) or much faster upon absorption of FR light (Fig. 5). This photoconversion of phytochrome involves a number of intermediate forms in both directions, and the establishment of an equilibrium between Pr and Pfr takes several minutes even at daylight irradiance levels (Smith 2000). The phytochromes are cytosolically localised in their Pr form, but are triggered to translocate to the nucleus upon photoconversion to their Pfr form (Kircher *et al.* 1999, Nagy and Schäfer 2000).

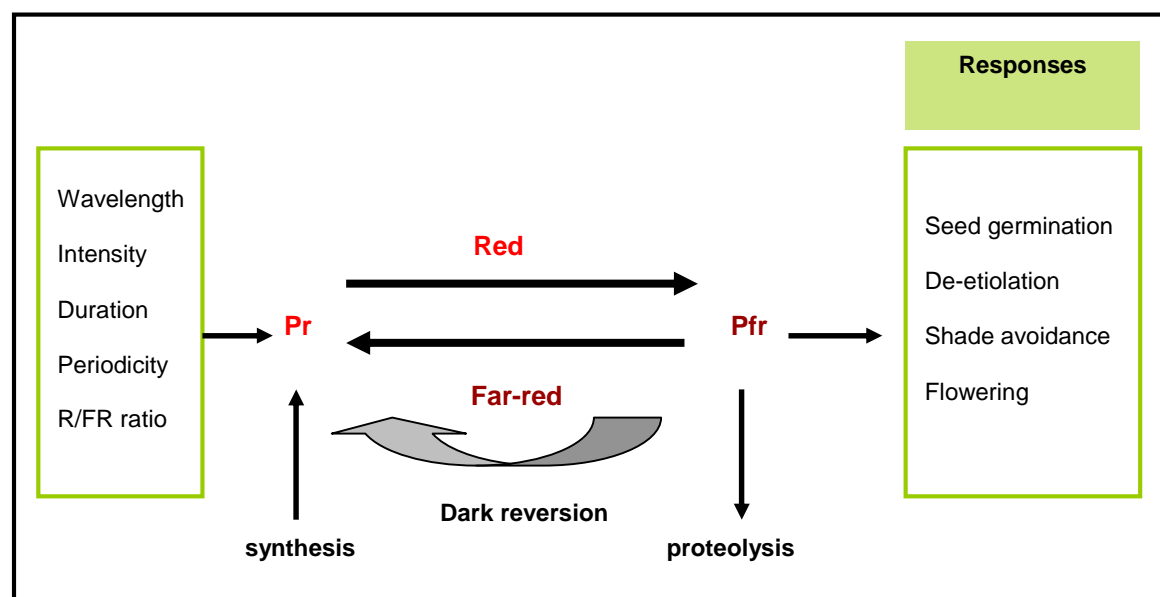


Figure 5. Phytochromes can act as photoconvertible switches. Pr is biologically inactive and upon absorption of red photons is converted to Pfr, the active form. Pfr is converted back to Pr by absorption of far-red photons or dark reversion.

Phytochromes can be used as sensitive estimators of the spectral changes that happen within plant communities when daylight interacts with photosynthetic structures (Smith 1982). Daylight contains equal proportions of R and FR light (R/FR ratio ≈ 1.2), but under a canopy this ratio is lowered by the absorption of R light by photosynthetic pigments of leaves (Fig. 6). Changes in the R/FR ratio due to scattering or reflection from leaves are much more reliable indicators of the proximity of potentially competing neighbours than the reduction in the total amount of light penetrating the canopy (Ballaré *et al.* 1987, Gilbert *et al.* 1995). Plants use phytochromes as proximity sensors and modify their growth and development, constituting the “shade avoidance syndrome” (Smith *et al.* 1995). Upon sensing a low R/FR ratio, a shade avoiding plant will exhibit enhanced elongation growth and, if the strategy is successful, will project its leaves into regions of unattenuated daylight. If elongation is unsuccessful, other aspects of the shade avoidance syndrome cause accelerated flowering and early production of seeds, enhancing the probability of survival. Shade avoidance is a strategy employed by the majority of angiosperms, ranging from

small herbs to large trees, and is of major ecological importance. The ability of phytochrome-mediated proximity sensing provides the plant with positional information with respect to potentially competing neighbours. This can also lead to negative implications for farmers, who grow their crops too close on the field.

Phytochromes also provide plants with temporal signals that entrain the phases of the biological clock, and others that ensure crucial developmental steps are initiated at appropriate points of the life cycle. Endogenous circadian rhythms synchronize development to the changing seasons, as exemplified in the photoperiodic control of flowering and dormancy. Even when employed as simple light detectors, such as in the stimulation of seed germination or the conversion of the etiolated seedling to photosynthetic competence, the phytochromes may be thought of as timing agents.

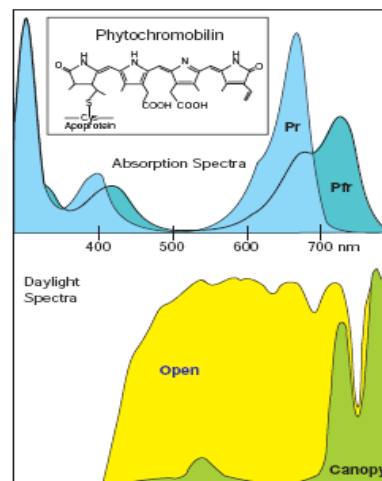


Figure 6. Absorption spectra of the Pr and Pfr forms of phytochromes (top) and the light spectra perceived in the open field or under a canopy. The X-axis shows the wavelength in nm. Adapted from Smith, 2000.

From action spectra it becomes obvious that phytochromes do not only absorb R and FR light (Fig. 6; Shinomura *et al.* 1996). Phytochromes also weakly absorb B light (Furuya and Song 1994, Fig. 6) and they act to modulate phototropin-mediated phototropic bending and cryptochrome-mediated seedling de-etiolation in response to B light (Ahmad and Cashmore 1997, Casal 2000, Lariguet and Fankhauser 2004).

1.5. Structure of phytochromes

The phytochrome molecule is a soluble, dimeric chromoprotein that consists of two polypeptides of approximately 125 kDa. Each polypeptide has two main structural domains: a photosensory, globular amino-terminal (N-terminal) chromophore-binding domain, which is sufficient for light

absorption and photoreversibility (~ 70 kDa), and a regulatory, conformationally more extended carboxy-terminal (C-terminal) domain functioning in dimerization and downstream signalling (~ 55 kDa).

The photosensory domain (N-terminal domain) is highly conserved throughout phytochrome species (>50% sequence identity between proteins), and it exhibits photoreversible spectral changes that are indistinguishable from those observed for full-length phytochrome. This domain can be divided into three regions: a short N-terminal extension (ATE, 6 - 10 kDa) which is plant specific, the central bilin lyase domain (BLD, ~40 kDa), and a C-terminal PHY domain (~20 kDa) (Montgomery and Lagarias 2002). The C-terminal domain can also be subdivided into a Per-Arnt-Sim (PAS)-related domain (PRD) containing two PAS repeats and a histidine kinase-related domain (HKRD). PAS domains can either be used as protein-protein interaction platforms or as response modules to small ligands or changes in light conditions, oxygen levels, and redox potentials (Quail 1997, Neff *et al.* 2000). The putative dimerization motifs (D1 and D2) of phytochrome are also localized in the C-terminal half of phytochrome molecules (Quail 1997). These two main domains are connected by a flexible hinge region (H) (Fig. 7).

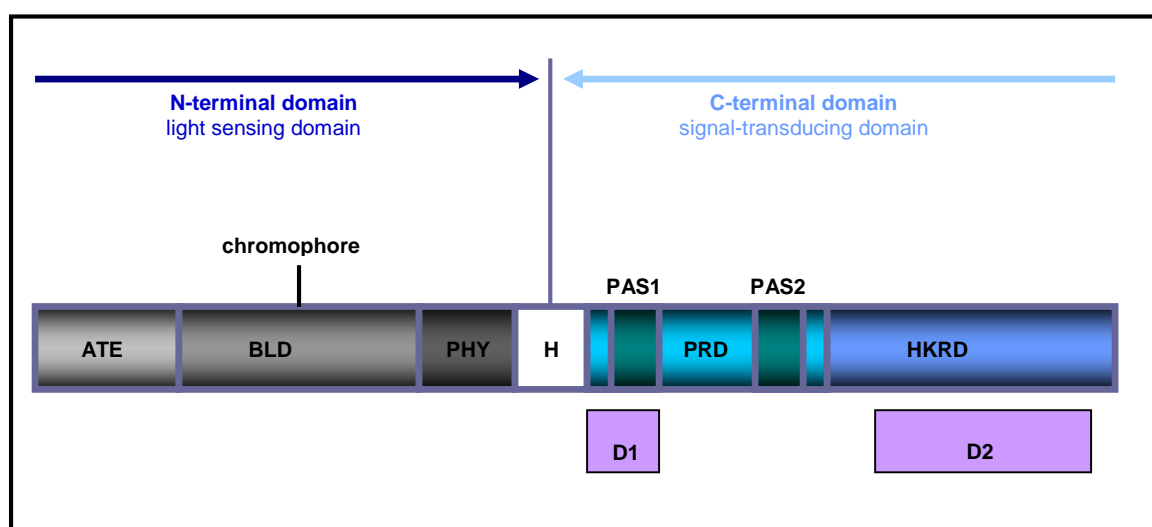


Figure 7. Structure of phytochromes. The N-terminal and the C-terminal domains are connected by a flexible hinge region (H). Regions of these two domains are marked: amino-terminal extension (ATE), a central bilin lyase domain (BLD), a PHY domain, a PAS-related domain (PRD) containing two PAS repeats and a histidine kinase-related domain (HKRD). Two putative dimerization motifs (D1 and D2) are located in the C-terminal half of the molecule. Adapted from Wang and Deng, 2004.

Each monomer is attached to a light-absorbing linear tetrapyrrole chromophore, via a thioether linkage to a conserved cysteine residue (Furuya and Song 1994). The chromophore is attached with the help of the lyase activity of the BDL domain. The structure of the phytochrome chromophore was determined to be a linear tetrapyrrole, phytochromobilin ($P\Phi B$). $P\Phi B$ was shown to ligate *via* the A-ring to a cysteine residue located within the BDL domain (Lagarias and Rapoport 1980). Phytochrome is synthesized in the Pr form in dark-grown seedlings. Exposure to R light causes a “Z” to “E” isomerization in the C-15 double bond between the C and D rings of the linear tetrapyrrole, resulting in the FR absorbing form Pfr (Andel *et al.* 1996; Fig. 8). Recently,

the three-dimensional structure of the chromophore-binding domain of *Deinococcus radiodurans* phytochrome assembled with its chromophore biliverdin in the Pr form has been crystallized (Wagner *et al.* 2005). These data confirmed the predicted cysteine residue as the chromophore attachment site and identified those amino acids that form the solvent-shielded bilin-binding pocket providing the first model for the photochromic behaviour of these photoreceptors.

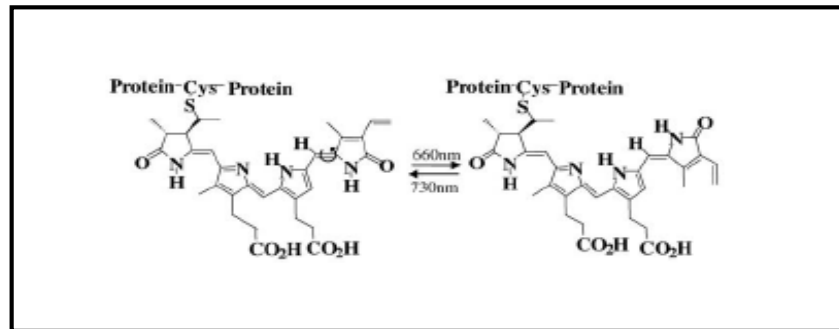


Figure 8. Photochemical property of phytochromes. The “Z” to “E” isomerization of phytochromobilin in the Pr-Pfr transformation of phytochromes is indicated. Adapted from Kim *et al.* 2002.

1.5.1. Structure-function relationships of phytochromes

Analysis has shown that determinants for wavelength specificity of phyA and phyB are located in the photosensory domain (Wagner *et al.* 1996). In the N-terminal domain, the ATE is poorly conserved among different phytochromes, in phyA the ATE might be implicated in stabilization of the Pfr form of the photoreceptor (Song 1999; Fig. 7). The BDL domain processes chromophore lyase activity required for attachment of the chromophore to the apoprotein (Fankhauser 2001, Wu and Lagarias 2000). The PHY domain also contributes to the integrity and stability of Pfr, and may be also involved in interactions with downstream signalling components and/or in light induced nuclear translocation of phytochromes.

The C-terminal domain is believed to be important in dimerization and essential for proper downstream signalling (Park *et al.* 2000, Ni *et al.* 1998). The PRD domain is required for interaction with a number of phy signalling partners, and it also plays a role in stabilization of the Pfr form of phyB (Choi *et al.* 1999, Ni *et al.* 1998, Quail *et al.* 1995). However, recent studies suggest that the N-terminal domain of phyB is enough to transduce the light signal to downstream targets, and the C-terminal domain attenuates the activity of phyB (Matsushita *et al.* 2003).

Higher plant phytochromes have an HKRD region distantly related to bacterial histidine kinases; however they seem to lack several residues essential for kinase activity (Fankhauser 2000, Quail 1997). A recombinant oat phyA protein was found to display kinase activity that is light dependent and modulated by the chromophore, with Pfr being more active than Pr (Yeh and Lagarias 1998). Oat phyA is also phosphorylated *in vivo*, and two *in vivo* phosphorylation sites have been mapped (Stockhaus *et al.* 1992, Lapko *et al.* 1997, 1999). Potential physiological roles

of phosphorylation modification of phytochromes could include regulation of their stability (for phyA), their subcellular localization, or their interaction with downstream signalling partners (Kim *et al.* 2002, 2004).

1.6. Physiological functions of phytochromes

1.6.1. Phytochromes can initiate high, low and very low fluence responses

In the 1950's, phytochromes were characterized as a protein pigment that mediates the reversible control of night-break of short day flowering plants (such as tobacco and soybean) and lettuce seed germination by R and FR light (Borthwick *et al.* 1952). The R/FR reversibility and reciprocity constitute the hallmarks of the classical phytochrome responses. This class of phytochrome responses is defined as the low fluence responses (LFR, fluence requirement 1-1.000 $\mu\text{mol}/\text{m}^2/\text{s}$). The classical example for LFR is the R light induced germination of lettuce seeds and this induction can be inhibited by a subsequent FR light treatment. Thus, photoreversibility is one characteristic feature of LFR. Low fluence of R light also induces other transient responses, such as changes in ion flux, leaf movement, chloroplast rotation, and gene expression (Roux 1994, Haupt and Häder 1994). PhyB to phyE regulate light responses under continuous R and white (W) light, and most of their responses can be grouped into the classical LFR.

PhyA is unique among all phytochromes because it is solely responsible for the very-low-fluence response (VLFR, fluence requirement 0.001-1.000 $\mu\text{mol}/\text{m}^2/\text{s}$) and for the FR light dependent high irradiance response (HIR, fluence requirement $>1.000 \mu\text{mol}/\text{m}^2/\text{s}$). The VLFR includes light effects on the expression of some genes such as light-induced expression of the *CAB* (chlorophyll *a/b* binding protein) gene, seed germination, and the gravitropic control of hypocotyl growth, and it can be induced with R, FR and B light pulses. The HIR requires relatively high photon fluence rates of FR light and a longer duration of irradiation. This response mode operates in the regulation of many aspects of seedling de-etiolation, including inhibition of hypocotyls elongation, opening of the apical hook, the expansion of cotyledons, changes in gene expression, the synthesis of the anthocyanin and a FR light block of greening in subsequent W light (Casal *et al.* 1998, Neff *et al.* 2000; Tab. 2). Both the VLFR and the HIR are not photoreversible.

Table 2. Different roles of phytochrome family members in seedling and early vegetative development.

Phytochrome member	Primary photosensory activities	Primary physiological roles
PhyA	VLFR	seed germination under a broad spectra of light conditions
	FR-HIR	seedling de-etiolation under FRc; promoting flowering under long day condition
PhyB	LFR	seed germination under Rc
	R-HIR	seedling de-etiolation under Rc
	EOD-FR	shade avoidance response
PhyC	R-HIR	primary leaf expansion
PhyD	EOD-FR (R/FR ratio)	shade avoidance response
phyE	EOD-FR (R/FR ratio)	shade avoidance response

1.6.2. Phytochromes and seed germination

The role of light signals in regulating seed germination has long been established. In natural light environments, the timing of seed germination is influenced by multiple factors. These include ambient temperature, water availability, the position of seeds in the soil profile, soil disturbance and the degree of vegetational shading.

Germination of the seeds and maturation of the developing seedlings, both dependent upon limited storage reserves, are probably the most vulnerable stages of the plant life cycle. In these processes, the phytochromes do not operate alone, but seem to be predominant. Phytochromes are mainly responsible for initiating germination and they have important roles in de-etiolation, perhaps because longer wavelengths of light more readily penetrate the seed coats and the initial few millimetres of soil (Shinomura *et al.* 1996, 1998).

In *Arabidopsis*, analyses of loss-of-function mutants and their respective double, triple or even quadruple mutants have revealed differential, as well as overlapping, physiological roles for the members of the phytochrome family (Franklin *et al.* 2003, Monte *et al.* 2003, Quail *et al.* 1995, Whitelam and Devlin 1997). PhyA, phyB and phyE are involved in the control of *Arabidopsis* seed germination. PhyA mediates FR-HIR germination, with phyE playing a secondary role (Botto *et al.* 1996, Shinomura *et al.* 1996, Hennig *et al.* 2002). Additionally, phyA uniquely mediates VLFR germination, which allows dark-imbibed seeds to germinate in response to millisecond pulses of light, irrespective of wavelength (Botto *et al.* 1996, Shinomura *et al.* 1996), whereas phyB plays a major role in the LFR and promotion of seed germination under prolonged R light, which is a R/FR responsible response (Botto *et al.* 1996, Reed *et al.* 1994, Shinomura *et al.* 1996).

Analysis of *phyAphyBphyD* and *phyAphyBphyE* triple mutant combinations uncovered a significant role for phyE in mediating R/FR reversible promotion of seed germination and in the promotion of germination by FR light, a response previously considered to be mediated solely by phyA. Surprisingly, given the high sequence similarity between phyB and phyD, the additional absence of phyD did not further impair the germination of *phyAphyB* seeds (Hennig *et al.* 2002).

1.6.3. Phytochromes and de-etiolation

De-etiolation is an interplay of several responses, including inhibition of extension growth, unfolding of cotyledons, development of the photosynthetic apparatus, expression of anthocyanins, and leaf development, all of which are critical for seedling establishment. Phytochromes also perform distinct functions in mediating seedling de-etiolation. Following seed germination, light signals inhibit hypocotyl extension, promoting the opening and expansion of cotyledons. The coordinated synthesis of chlorophyll, chloroplast development and opening of stomata enable plants to initiate photosynthetic activity and become photoautotrophic.

In *Arabidopsis*, until a light signal is received, seedlings are etiolated and negatively gravitropic. This allows seedlings buried beneath soil and/or leaf litter to devote the limited resources in the seed to rapidly reaching the light necessary for them to switch from heterotrophic to autotrophic growth.

As in germination, phyA and phyB are the principal mediators of R- and FR-induced de-etiolation in *Arabidopsis thaliana* (Reed *et al.* 1994), and it is likely that phyB-mediated LFR predominates in open habitats while phyA-mediated FR-HIR predominates in shaded habitats. PhyC, phyD and phyE also contribute to R-induced de-etiolation (Franklin and Whitelam 2005).

The unique role of phyA in inhibiting hypocotyl elongation in prolonged FR light was established through analysis of *phyA*-deficient mutants in a variety of species including *Arabidopsis thaliana* (Nagatani *et al.* 1993, Parks and Quail 1993, Whitelam *et al.* 1993), tomato (Van Tuinen *et al.* 1995) and rice (Takano *et al.* 2001, 2005). When grown in continuous FR light, *Arabidopsis phyA* mutants display long hypocotyls and are unable to open and expand their cotyledons (Fig. 9A). This phenotype has been used extensively for screening mutant populations for lesions in phyA-signalling.

Mutants deficient in phyB have been also characterised in a variety of species including *Arabidopsis thaliana* (Koornneef *et al.* 1980, Somers *et al.* 1991), *Brassica rapa* (Devlin *et al.* 1992), cucumber (López-Juez *et al.* 1992), tomato (Van Tuinen *et al.* 1995), pea (Weller *et al.* 2000) and *Nicotiana plumbagnifolia* (Hudson *et al.* 1997). Analyses of these mutants have revealed a significant role for phyB in the de-etiolation of seedlings in R, but not in prolonged FR light. Under R light conditions, *phyB* null mutants display elongated hypocotyls and

smaller cotyledons when compared to wild-type controls (Fig. 9B). Such phenotypes have been used as the basis of genetic screens for mutants deficient in phyB-signalling components.

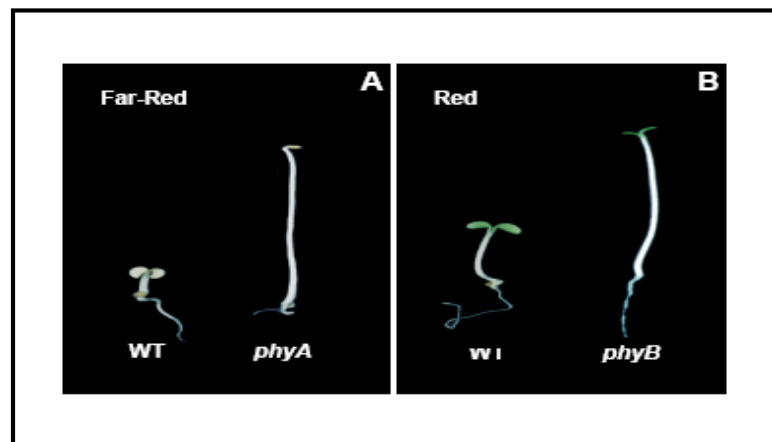


Figure 9. Phytochrome photoreceptor mutants of *Arabidopsis*. (A) *phyA* seedlings compared with WT seedlings grown under far-red light. (B) *phyB* seedlings compared with WT seedlings grown under red light (adapted from Franklin *et al.* 2005).

Redundancy between *phyA* and *phyB* has also been reported in the R light-mediated opening and expansion of cotyledons (Neff and Van Volkenburgh 1994, Reed *et al.* 1994, Neff and Chory 1998). The generation of double, triple and quadruple mutants, deficient in multiple species of phytochrome, have revealed that all five phytochrome family members promote cotyledon expansion in continuous R light (Franklin *et al.* 2003). Despite showing high sequence similarity to *phyB*, the role of *phyD* in R-mediated de-etiolation appears minor. When grown in continuous R light, *phyD* mutants displayed marginally longer hypocotyls than plants containing an overexpressed *PHYD* gene (Aukerman *et al.* 1997). The role of *phyE* in seedling de-etiolation appears negligible, when treated with R, FR or W light, etiolated *phyE* mutant seedlings display no obvious mutant phenotype (Devlin *et al.* 1998). The recent identification of null mutants at the *PHYC* locus has provided insights into the role of this phytochrome in seedling de-etiolation (Franklin *et al.* 2003). When grown in continuous R, *phyC* mutants displayed elongated hypocotyls, suggesting a role for this phytochrome in modulating extension growth. Despite the relatively close phylogenetic relationship between *PHYA* and *PHYC*, no identifiable role was identified for *phyC* in FR sensing (Franklin *et al.* 2003, Monte *et al.* 2003). This is in contrast to the rice *phyC*, which is involved in the photoperception of FR for the de-etiolation as well as the induction of *CAB* (chlorophyll *a/b* binding protein) genes and has little effect on the R light-mediated responses (Takano *et al.* 2005).

1.6.4. Phytochromes and shade avoidance

One of the most ecologically important capacities of phytochromes is their adaptation to their surroundings. In response to neighbour detection shade-intolerant plants increase extension growth, suppress branches, produce thinner leaves with less chlorophyll, flower early, and

decrease allocation to storage organs, a set of responses collectively known as “shade avoidance”.

Experiments with field-grown *Arabidopsis* and *Brassica* mutants have defined a clear role for phyB in detection of reflected FR light (Schmitt *et al.* 1995, Ballaré 1999). While phyA may enhance the sensitivity to subtle changes in the R/FR ratio caused by reflected light from non-shading neighbours (Ballaré 1999), the role of phyA in promoting de-etiolation under dense canopies may be antagonistic to some shade avoidance responses (Smith and Whitelam 1997). Moreover, analyses of mutants under canopies of lower density indicate a primary role for phyB in mediating shade avoidance responses, by increasing the elongation growth of petioles and stems, the length-to-width ratio of leaves, and accelerating flowering (Devlin *et al.* 1996, Smith and Whitelam 1997). Lesser roles are attributed to the phyB-related photoreceptors, phyD and phyE (Ballaré 1999). Under denser canopies, *phyB* mutants still retain measurable responses to shade, perhaps indicating a greater role for phyD and phyE, and/or for other perception systems, in shade avoidance in deep shade (Ballaré 1999; Fig. 10B).

A saturating pulse of FR light given at the end of the day simulating the enrichment of FR in the incandescent sunlight induces enhanced hypocotyl elongation in *Arabidopsis* (Robson *et al.* 1993, Aukerman *et al.* 1997, Franklin and Whitelam 2005). This end-of-day (EOD)-FR response is greatly diminished in *phyB*, *phyD* and *phyE* mutants and is a way to assess shade avoidance responses and to determine how plants can react to changing R/FR ratios.

1.6.5. The complex interplay among the photoreceptors

As well as having independent functions, phytochromes also show redundancy of functions and can also antagonize the action of each other (Reed *et al.* 1994, Smith 1995). Clearly, phytochromes also interact and coact with other photoreceptors. It has been reported that the inhibition of hypocotyl elongation under B light by cryptochrome was dependent upon the presence of phyA or phyB (Casal *et al.* 2002). However, it was later shown that cry1 had biological activity in a *phyA phyB* null mutant background in B light, especially at higher fluence rates (Shao *et al.* 2005). Cryptochromes and phytochromes also interact in phototropic curvature: prior stimulation of phytochrome by R light enhances the B light-mediated response, and this appears to be regulated by phyA (Ballaré *et al.* 1987, Gilbert *et al.* 1995). Additionally, phyB and cry2 act antagonistically in regulating flowering: phyB appears to repress whereas cry2 stimulates floral induction (Mouradov *et al.* 2002). In addition to these genetic studies indicating interactions between phytochromes and cryptochromes there is also evidence that cry1 can physically interact with phyA in yeast two-hybrid assays and that cry2 can interact with phyB. It is not only clear that phytochromes interact directly with other photoreceptors, but it has also been demonstrated that there is an interconnected signal transduction network among phytochromes, cryptochromes, phytohormones and environmental stresses (Franklin and Whitelam 2004).

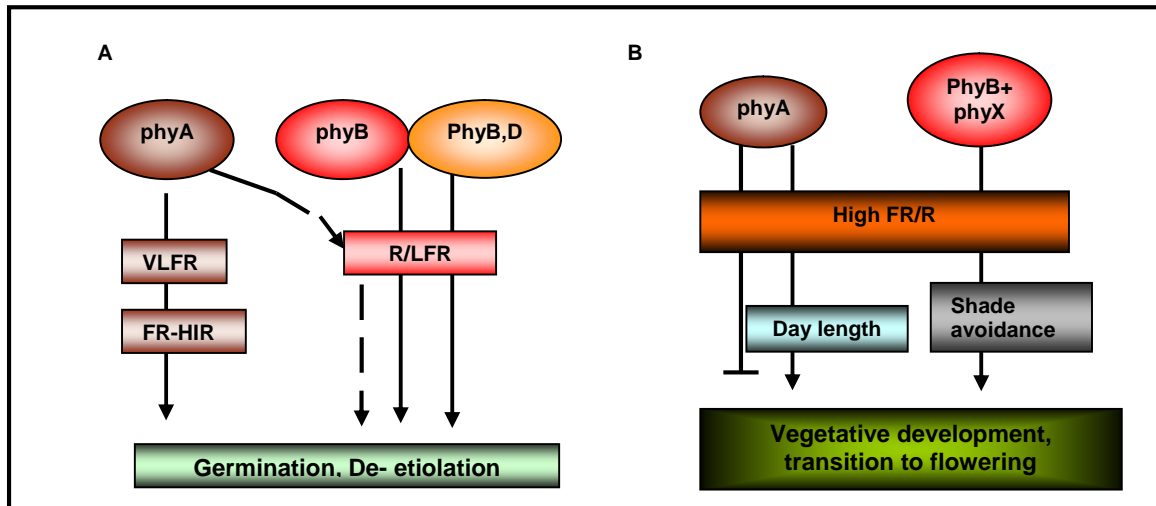


Figure 10. Phytochrome functions throughout a plant's development. (A) The role of phyA, phyB and phyD in the juvenile stages. **(B)** Phytochromes influencing vegetative development and the transition to flowering in adult plants. Red, R; far-red, FR; very low fluence response, VLFR; low fluence response, LFR; high irradiance response, HIR.

1.7. Signal transduction by photoreceptors

Between the sensing of an environmental impulse (signal) and an appropriate response the information is processed and integrated with other information obtained through different sources. This process is called signal transduction. The signal transduction pathway for light is best studied for phyA signalling (Bowler and Chua 1994, Millar *et al.* 1994, Barnes *et al.* 1997, Mustilli and Bowler 1997). Approaches to elucidate this pathway were made using genetic (Fankhauser and Chory 1997, Deng and Quail 1999) and biochemical strategies (microinjections: Neuhaus *et al.* 1993, Bowler *et al.* 1994; two-hybrid screens: Ni *et al.* 1998, Fankhauser *et al.* 1999, Choi *et al.* 1999) as well as promoter analysis (Terzhagi and Cashmore 1995). It has been demonstrated that the *Arabidopsis* phytochromes are localized in the cytosol in the dark and up on light activation translocate to the nucleus where they form speckles whose biological function is not known (Nagatani 2004). The mechanisms of photoreceptor signal transduction are far from being completely elucidated, but are believed to involve both cytosolic and nuclear components (Nagy and Schäfer 2000).

Photoactivation of phyA is linked to cellular and molecular events that elicit changes in gene expression patterns. Several protein intermediates have been isolated to date that are important for phyA signalling (Chen *et al.* 2004). In most cases, genetic screens exploited the hypocotyl elongation as a parameter for mutant selection. Only three mutants, *fhy1*, *fhy3* and *pat1-1*, have been isolated that have a nearly abolished inhibition of hypocotyl elongation specifically under FR light, very similar to a *phyA* photoreceptor mutant. Several other mutants have been isolated with weaker or intermediate responses (*laf1*, *laf3*, *laf6*, *far1*, *far3*, *fhl*, *hfr1/rsf1rep1*, *fin2*, *fin219*). Other mutants have been isolated because of their hypersensitivity towards FR light such as *eid1*, *spa1*

and *spa4*. Although most mutants have been characterized at the molecular level it is still not clear how the light signal is transduced (Fig. 11).

Phosphorylation and dephosphorylation are mechanisms widely used by organisms in signalling cascades. The presence of putative kinase domains within photoreceptor proteins has suggested a role for phosphorylation in light signalling. The C-terminal domain of phytochromes contains a region of sequence with homology to histidine kinases, suggesting that phytochrome may act as a light-regulated kinase (Yeh *et al.* 1997). In addition to autophosphorylation, phyA and phyB also phosphorylate the protein PKS1 (Phytochrome Kinase Substrate 1) in a light-dependent manner *in vitro* (Fankhauser *et al.* 1999). The phosphorylation of PKS1 acts negatively to regulate phytochrome function, suggesting an important role for phytochrome kinase activity in light signalling (Fankhauser *et al.* 1999). In addition, studies in *Arabidopsis* have revealed the binding of the Pfr form of phyA to increase the phosphate exchange activity of nucleoside diphosphate kinase 2 (NDPK2) *in vitro* (Choi *et al.* 1999). Such studies suggest NDPK2 to be a positive signalling component of the phytochrome-mediated light signal transduction pathway in *Arabidopsis thaliana*. Furthermore, a type 5 protein phosphatase (PAPP5) has been identified that specifically dephosphorylates biologically active phytochromes and thereby enhances phytochrome-mediated photoresponses and the affinity for NDPK2 (Ryu *et al.* 2005).

In the nucleus, many proteins that have been identified as signalling intermediates are transcription factors: basic helix-loop-helix proteins such as PIF1/PIL5, PIF3, PIF4, PIF5/PIL6 and PIL1, many of which can directly interact with phytochromes (Duek and Fankhauser 2005); the leucine zipper proteins HY5 and HYH (Oyama *et al.* 1997, Holm *et al.* 2002); homeobox proteins such as ATHB2, which is involved in the shade avoidance response (Steindler *et al.* 1999); MYB factors such as CCA1 and LHY and transcription factors with DOF domains such as COG1 and OBP3 (Wang *et al.* 1997, Schaffer *et al.* 1998, Park *et al.* 2003, Ward *et al.* 2005). The binding of phytochromes to bHLH transcription factors in the nucleus is believed to form an early signalling step in the de-etiolation of dark grown seedlings. The DNA sequence motif recognised by most bHLH transcription factors is termed the E-box, a hexameric sequence, CANNTG. In *Arabidopsis*, the most commonly recognized type of E-box is the sequence CACGTG, termed the G-box (Toledo-Ortiz *et al.* 2003).

Light also regulates photomorphogenesis via the specific targeting of proteins for ubiquitination and proteasome-mediated degradation. One of the key regulators of this process is the COP1 (Constitutive Photomorphogenesis 1) E3 ubiquitin protein ligase which acts downstream of both phytochromes and cryptochromes (Ang and Deng 1994, Seo *et al.* 2004). In the dark, COP1 is associated with a nuclear-localised twelve subunit complex, the COP9 signalosome, involved in targeting proteins for degradation (Wei and Deng 2003). In the light, COP1 moves out of the nucleus allowing proteins involved in the positive regulation of photomorphogenesis, such as the transcriptional regulator HY5, to accumulate and photomorphogenesis to occur. In addition, there

is physical interaction of photoreceptors (Wang *et al.* 2002, Yang *et al.* 2000) with COP1 in a light-dependent manner leading to their degradation (Seo *et al.* 2004)

The regulation of gene expression by phytochrome may also involve chromatin remodelling. This pathway of phytochrome signalling was discovered by analysis of *det1* mutants. Plants lacking this gene exhibit a constitutive de-etiolation in darkness, suggesting that DET1 encodes a negative regulator of light signalling, like the COP proteins. Biochemical experiments revealed that DET1 could interact with the N-terminal tail of histone H2B in a nucleosome context (Benvenuto *et al.* 2002). This finding indicates that DET1 may regulate light-inducible gene expression by modulating chromatin architecture. Furthermore, DET1, together with another protein (DDB1), has now been found to interact with COP1, COP10 and the COP9 signalosome (Yanagawa *et al.* 2004), suggesting that polyubiquitin-dependent proteolysis of regulatory factors may be closely coupled with chromatin-level control of photoregulated gene expression.

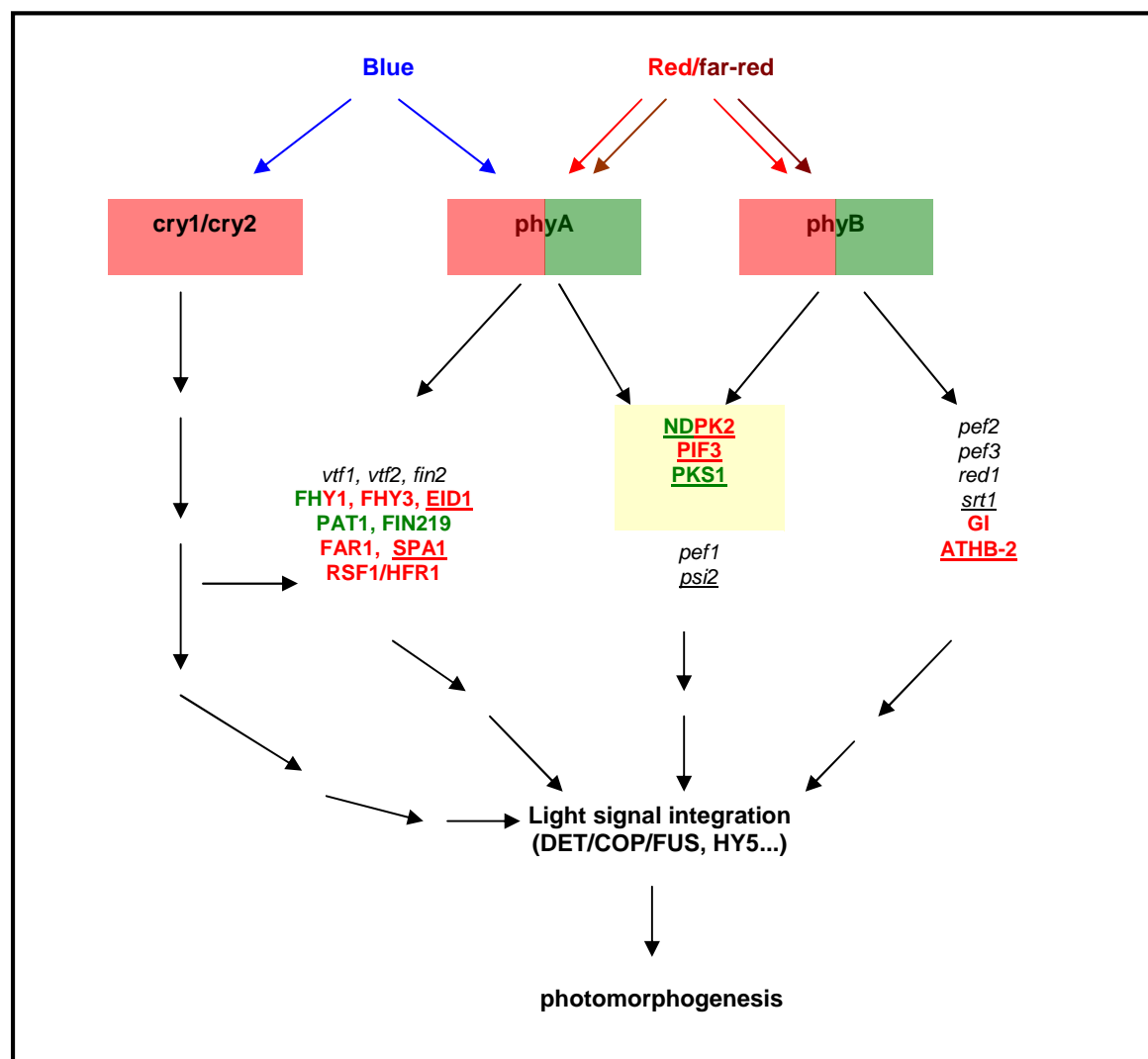


Figure 11. A simplified model for phytochrome-mediated light signalling. Cloned genes are indicated in CAPITALS. Genetic loci affecting specific branches of phytochrome signalling are *italicized*. Proteins that can directly interact with phytochromes are *boxed*. Negative regulators are underlined. Cytoplasmic localization is indicated in green and nuclear localization in red.

1.8. PAT 1 (Phytochrome A Signal Transduction 1), a GRAS Protein, is involved in phytochrome signalling

One of the phyA-dependent signalling intermediates that have been identified is PAT1 (Bolle *et al.* 2000). The *Arabidopsis thaliana* mutant *phytochrome A signal transduction (pat)1-1*, acts in a semi-dominant negative way. Molecular analysis demonstrated that a carboxy-terminally truncated *PAT1* mRNA is still expressed. Several responses to FR-HIR light are severely reduced in this mutant, such the FR light induced gene expression of *CHS* and *CAB*. Hypocotyl elongation under FR light is strongly enhanced, leading to a phenotype similar to that of the *phyA* photoreceptor mutant. No effect on hypocotyl elongation and gene expression was noted under any other light conditions, suggesting specificity for the phyA signalling pathway. This protein belongs to the class of GRAS proteins, which constitutes a large protein family. GRAS proteins have been found in many higher plants such as *Arabidopsis*, tomato, petunia, lily, rice, barley and also in *Physcomitrella*. However, GRAS proteins are plant-specific as they cannot be found outside this clade. The family name is derived from the first three members to be cloned, GAI (Gibberellin-insensitive), RGA (Repressor of *ga1-3*) and SCR (Scarecrow) (Pysh *et al.* 1999).

GRAS proteins are typically composed of 400 – 770 amino acid residues and exhibit considerable sequence homology to each other in their respective C-termini (Fig. 12). The distinguishing domains of GRAS proteins, two leucine-rich areas flanking a VHIID motif (named after the most prominent amino acid residues), are present in all members of the family. The two leucine-rich domains of approximately 100 amino acid residues length are characterized by leucines, which in most cases do not occur as heptad repeats. If heptad repeats can be found, their number is small, usually one or two, although in AtSCR a stretch of four leucines is positioned in the correct spacing for a leucine zipper. Nonetheless, the presence of conserved leucines suggests that these domains could be important for protein–protein interactions. An LXXLL sequence appears in several GRAS proteins at the beginning of the first leucine-rich domain. The significance of this motif in plants is not yet known, although it fits the consensus sequence demonstrated to mediate the binding of steroid receptor co-activator complexes to nuclear receptors (Heery *et al.* 1997). Several additional amino acid residues are invariant in most or all members of the GRAS protein family. These include the PFYRE and RVER motifs, designated after the respective conserved amino acids (Pysh *et al.* 1999), and the C-terminal SAW motif, which contains three pairs of conserved residues: R-(x)₄-E,-W-(x)₇-G,-W-(x)₁₀-W. After the second leucine-rich domain a consensus sequence for a tyrosine phosphorylation site [RK]-x_(2,3)-[DE]-x_(2,3)-Y] (Patschinsky *et al.* 1982) is present in many members of the family, overlapping with the tyrosine in the PFYRE motif (Fig. 12). Its function as a phosphorylation site, however, has yet to be demonstrated. Despite the substantial homology between GRAS proteins in the C-terminal part, the N-terminal amino acid sequences are highly divergent.

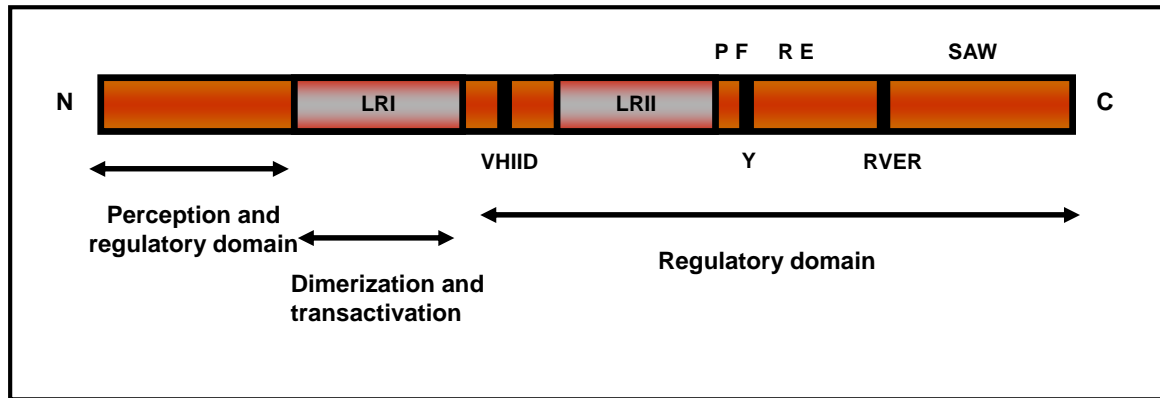


Figure 12. Presentation of the different domains of GRAS Proteins.

The GRAS protein family is relatively large with at least 33 identified ORFs in the *Arabidopsis thaliana* genome (Bolle 2004, Tian *et al.* 2004) and at least 57 genes identified in the *Oryza sativa* genome. Comparative analysis revealed duplication and divergence of the GRAS gene family between monocots and eudicots, which have diverged from a common ancestor 150 - 300 million years ago.

Sequence alignment and phylogenetic analysis of the GRAS gene family reveal several subfamilies: the "DELLA" proteins, the SCR-branch, the Ls-branch, the HAM-branch, the PAT1-branch, the SHR-branch and the SCL9-branch. The phylogenetic trees are very similar if based on full-length sequences or only on the conserved C-termini of the proteins (Fig. 13).

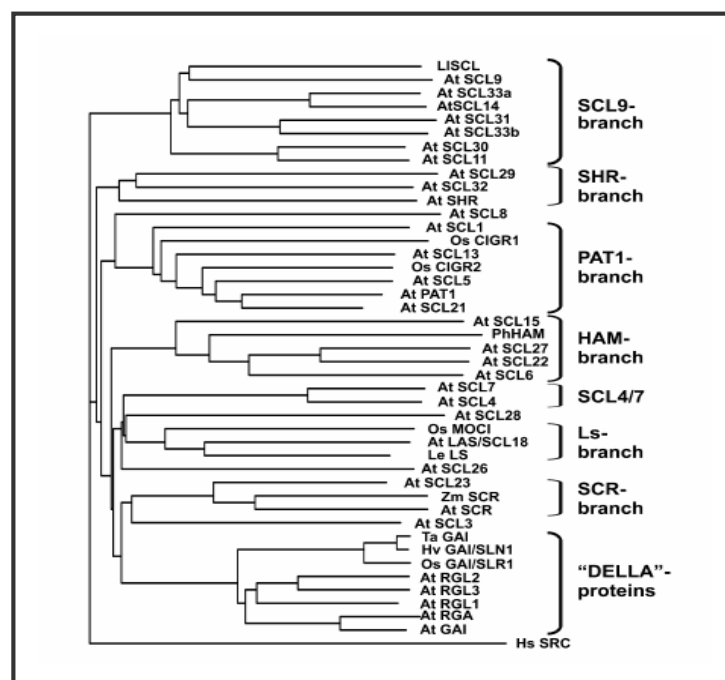


Figure 13. Phylogenetic tree of GRAS proteins. Evolutionary relationship among the 33 members of the *Arabidopsis thaliana* GRAS protein family (At) including several GRAS proteins from *Petunia hybrida* (petunia; Ph), *Lycopersicon esculentum* (tomato; Le), *Lilium longiflorum* (lily; Ll), *Oryza sativa* (rice; Os), *Hordeum vulgare* (barley; Hv) and *Zea mays* (maize; Zm). Adapted from Bolle, 2004.

Several GRAS genes have been cloned and functionally characterized in a variety of plant species. GRAS proteins are involved in many developmental processes such as axillary meristem initiation (LS/LAS; Schumacher *et al.* 1999, Greb *et al.* 2003), shoot meristem maintenance (HAM; Stuurman *et al.* 2002) or radial organization of the root (SCR, SHR; Di Laurenzio *et al.* 1996, Helariutta *et al.* 2000), whilst others are involved in signal transduction pathways such as the members of the DELLA protein sub-branch (GAI, RGA, RGL1-3), which are negative regulators of the gibberellin signal transduction (Peng *et al.* 1997, 1999, Silverstone *et al.* 1998, Ikeda *et al.* 2001) or such as PAT1, which is involved in light signal transduction (Bolle *et al.* 2000). Others have been found to be important for nodulation in *Medicago* and *Lotus* (Kalo *et al.* 2005, Smit *et al.* 2005, Heckmann *et al.* 2006).

Four proteins in *Arabidopsis* show high similarity to PAT1, namely SCARECROW-LIKE (SCL)1, SCL5, SCL13 and SCL21 (Fig. 13). These proteins cluster to the PAT1-branch of the GRAS protein family. The aim of this analysis was to determine if whether these proteins are also involved in light signal transduction. Furthermore, the biological and biochemical role of GRAS proteins involved in light signalling could be elucidated.

2. MATERIALS

2.1. Chemicals and enzymes

All chemicals used in this work had a degree of purity suitable *pro analyse* and were provided by Merck GmbH (Darmstadt, Germany), Pharmacia GmbH (Uppsala, Sweden), Roth GmbH (Karlsruhe, Germany), Serva GmbH (Heidelberg, Germany) and Sigma-Aldrich Chemie GmbH (Taufkirchen, Germany).

Radioactive nucleotides were purchased from Amersham Biosciences Europe GmbH (Freiburg, Germany). Other chemicals, buffers, and additional materials are described under the respective methods.

2.2. Enzymes

Enzymes were obtained from the following companies, if not otherwise mentioned: Invitrogen GmbH (Karlsruhe, Germany), MBI Fermentas GmbH (St.Leon-Rot, Germany), New England Biolabs GmbH (Frankfurt/Main, Germany), Promega GmbH (Mannheim, Germany), Qiagen GmbH (Hilden, Germany), Roche Diagnostics GmbH (Mannheim, Germany), and Stratagene GmbH (Heidelberg, Germany).

T4 DNA ligase	MBI Fermentas GmbH, St.Leon-Rot, Germany
DNase I, RNase-free	Roche Diagnostics GmbH, Penzberg, Germany
DNA polymerase	TaKaRa Ex Taq™, Takara Bio INC., Shiga, Japan
BioTherm DNA polymerase	GeneCraft GmbH, Lüdinghausen, Germany
Shrimp alkaline phosphatase	USB, Cleveland, OH, USA
Gateway™ LR Clonase Enzyme Mix	Invitrogen GmbH, Carlsbad, CA, USA
Gateway™ BP Clonase Enzyme Mix	Invitrogen GmbH, Carlsbad, CA, USA
Protease Inhibitor Cocktail	Sigma, Missouri, USA
RNase A	Roche GmbH, Mannheim, Germany
RNase Inhibitor	Roche GmbH, Mannheim, Germany
Proteinase K	Invitrogen GmbH, Karlsruhe, Germany

2.3. Kits

ProQuest Two-Hybrid System	Invitrogen GmbH, Carlsbad, CA, USA
SuperSignal West Pico Chemiluminiscent Substrate Kit	Perbio GmbH, Bonn, Germany
Random Primed DNA Labeling Kit	Roche GmbH, Penzberg, Germany
QIAprep Spin Miniprep Kit	Qiagen GmbH, Hilden, Germany
QIAquick PCR Purification Kit	Qiagen GmbH, Hilden, Germany
QIAquick Gel Extraction Kit	Qiagen GmbH, Hilden, Germany

RNeasy Plant Mini Kit	Qiagen GmbH, Hilden, Germany
Omniscript Reverse Transcriptase Kit	Qiagen GmbH, Hilden, Germany
DIG High Prime DNA Labeling and Detection Starter Kit	Roche GmbH, Penzberg, Germany
Mini Quick Spin DNA Columns	Roche GmbH, Mannheim, Germany
pENTR Directional TOPO Cloning Kit	Invitrogen GmbH, Carlsbad, CA, USA
Gateway™ pENTR™ Vectors	Invitrogen GmbH, Carlsbad, CA, USA
PCR Cloning System with Gateway Technology with pDONR221/pDONR 201/pDONR 207	Invitrogen GmbH, Carlsbad, CA, USA

2.4. Antibiotic stock solutions

ampicillin	100 mg/ml dissolved in water
chloramphenicol	40 mg/ml dissolved in 70% ethanol
kanamycin	50 mg/ml dissolved in water
gentamycin	10 mg/ml dissolved in water
streptomycin	50 mg/ml dissolved in water
spectinomycin	50 mg/ml dissolved in water

2.5. Oligonucleotides

All oligonucleotides used for PCR reactions, cloning or sequence analyses have been synthesized by MWG-Biotech GmbH (Ebersberg, Germany). The list of primers is given in the Appendix 1.

2.6. Length and weight standards

GeneRuler™ 1Kb DNA ladder (MBI Fermentas, St. Leon-Rot, Germany) yielding fragments between 250 to 10,000 bp and λ DNA restricted with *EcoRI* and *HindIII* yielding fragments between 564 to 21,226 bp were used as DNA length standards.

As a standard for the determination of the molecular weight of proteins, Prestained Protein Marker, broad range (New England BioLabs, Frankfurt/Main, Germany) was utilized.

2.7. Bacterial strains

E.coli DH5" (Bethesda Res. Lab., 1986)

One Shot® TOP10 Chemically Competent *E. coli* (Invitrogen GmbH, Karlsruhe, Germany)

Agrobacterium tumefaciens GV 3101 (pMK90RK) (Koncz *et al.* 1994)

2.8. Yeast strains

Saccharomyces cerevisiae, strain MaV203, has been used for the routine introduction of plasmid DNA into yeast cells for use with the Proquest Two-Hybrid System with the Gateway Technology (Invitrogen GmbH, Carlsbad, CA, USA).

2.9. Antibodies

Primary antibodies were generated by Pineda Antikörper-Service (Berlin, Germany) in rabbit against peptides of SCL21 (NH₂-CSSIYKSLQSREPES-CONH₂) and PAT1 (NH₂-CVTDELNDFKH KIRE-CONH₂). Preimmunsera and bleeds were tested on extracts from wild-type plants and knock-out mutants. Secondary antibodies such as goat anti-mouse IgG (H+L) were obtained from Molecular Probes Europe BV (Leiden, The Netherlands). A goat anti-rabbit IgG (whole molecule) peroxidase conjugate was obtained from Sigma-Aldrich Chemie GmbH (Taufkirchen, Germany).

2.10. Plasmids

Vectors for standard cloning and plant binary expression vectors used in this work are described below.

Table 3. Vectors for standard cloning procedures

Name	Application	Enzyme	Selection marker	Company/Description
pGEM-T Easy Vector	For cloning of PCR products	DNA T4 ligase	ampicillin	Promega (Mannheim, Germany)
pENTR/D-TOPO	Directionally introduces blunt-end PCR products containing a CACC at the 5'-end. Generates <i>attB</i> flanked donor clones	topoisomerase	kanamycin	Invitrogen (Carlsbad, CA, USA)
PENTR 4	Allows restriction cloning of the gene of interest for entry into the Gateway system	DNA T4 ligase	kanamycin	Invitrogen (Carlsbad, CA, USA)
pDONR 201/207/221	Gateway-adapted vectors designed to generate <i>attL</i> -flanked entry clones containing the gene of interest following recombination with an <i>attB</i> expression clone or an <i>attB</i> -linker containing PCR product	BP-clonase	kanamycin gentamycin kanamycin	Invitrogen (Carlsbad, CA, USA)
PDEST 32	DNA Binding Domain (DB) Gateway Destination Vector derived from pDBLeu. The vector is used to clone the gene of interest in frame with the sequence encoding the DNA Binding Domain (DB) of the GAL4 protein (generating DB-X)	LR-clonase	gentamycin	Invitrogen (Carlsbad, CA, USA)
PDEST 22	Activation Domain (AD) Gateway Destination Vector. The vector is used to clone the gene of interest in frame with the sequence encoding the Transcription Activation Domain (AD) of the GAL4 protein (generating AD-Y)	LR-clonase	ampicillin	Invitrogen (Carlsbad, CA, USA)

pDBLeu	DNA Binding Domain (DB) cloning vector derived from pPC97. It contains a multiple cloning site with blunt end-generating restriction sites in each of the three reading frames	DNA T4 ligase	kanamycin	Invitrogen (Carlsbad, CA, USA)
PEXP-AD502	Activation Domain (AD) Gateway Expression Vector. This plasmid is used to construct a cDNA or genomic library for identifying proteins (AD-Y) that interact with the fusion protein (DB-X)	DNA T4 ligase	ampicillin	Invitrogen (Carlsbad, CA, USA)
PGFP	To generate N-terminal fusion to GFP	DNA T4 ligase	ampicillin	Kost <i>et. al</i> 1998

Table 4. Plant binary expression vectors

Name	T-DNA structure	Application	Selection marker in bacteria	Selection marker in plants	Description
pK7GWIWG2(I)	LB-(Tnos-KanR-Pnos)-T35S-(attR1,GW,attR2)-intron-(attR2,GW,attR1)-p35S)-RB	RNA expression	spectinomycin/streptomycin	kanamycin	Karimi <i>et al.</i> 2002
pB7GWIWG2(I)	LB-(Tnos-BarR-Pnos)-T35S-(attR1,GW,attR2)-intron-(attR2,GW,attR1)-p35S)-RB	RNA expression	spectinomycin/streptomycin	Basta	Karimi <i>et al.</i> 2002
pKGWFS7	LB-(Tnos-KanR-Pnos)-(attR1,GW,attR2)-Egfp:gus-T35S)-RB	Promoter analysis	spectinomycin/streptomycin	kanamycin	Karimi <i>et al.</i> 2002
pK7FWG2	LB-(Tnos-KanR-Pnos)-(T35S-Egfp:(attR2,GW,attR1)-P35S)-RB	N-terminal fusion to GFP	spectinomycin/streptomycin	kanamycin	Karimi <i>et al.</i> 2002

att = attachment sites (Gateway System), LB = left border, RB = right border, GW = reading frame of inserted gene, T35S = 35S-*CaMV* terminator, p35S = 35S-*CaMV* promoter, KanR = kanamycin resistance, BarR = Basta resistance.

After cloning, all resulting plasmids were sequenced to ensure no errors were introduced into the gene during the amplification reactions.

2.11. Hybridisation probes for Northern analysis

Hybridisation probes are listed in Appendix 1 (Tab. 5). DNA probes were generated by PCR, amplifying specific regions of the genes of interest using oligonucleotide primers synthesized by MWG-Biotech GmbH (Ebersberg, Germany).

2.12. Plant material

All lines used in this study, are in the *Arabidopsis thaliana* Columbia background (Col-0). Insertion lines were derived from the SALK (<http://signal.salk.edu/about.html>) or SAIL-collection (http://www.tmri.org/en/partnership/sail_collection.aspx).

Table 5. List of the different lines used for physiological analysis. At, *Arabidopsis thaliana*

MIPS-Code	Gene	Name of the mutant	SAIL or NASC number or reference	Resistance
At1g21450	<i>AtSCL1</i>	<i>scl1-1</i>	760 F10	Basta
At1g21450	<i>AtSCL1</i>	<i>scl1-2</i>	1296 B07	Basta
At1g21450	<i>AtSCL1</i>	<i>scl1-3</i>	N602071	kanamycin
At1g50600	<i>AtSCL5</i>	<i>scl5-1</i>	N582550	kanamycin sensitive
At2g04890	<i>AtSCL21</i>	<i>scl21-1</i>	313 G09	Basta
At2g04890	<i>AtSCL21</i>	<i>scl21-2</i>	N503630	kanamycin
At5g48150	<i>AtPAT1</i>	<i>pat1-1</i>	Bolle <i>et al.</i> 2000	hygromycin
At5g48150	<i>AtPAT1</i>	<i>pat1-2</i>	N568176	kanamycin
At5g62090	<i>Seuss-like1</i>	<i>sla</i>	N585761	kanamycin
At5g62090	<i>Seuss-like1</i>	<i>slb</i>	N589954	kanamycin

3. METHODS

I. General Techniques of Molecular Biology

3.1. Preparation of competent bacterial cells

LB-MgSO₄: 1% (w/v) Bacto-tryptone, 0.5% (w/v) Yeast extract, 1% (w/v) NaCl, 1% (v/v) 1M MgSO₄

Tfb-I buffer: 30 mM K-acetate, 50 mM MgCl₂, 100 mM KCl, 10 mM CaCl₂, 15% glycerol

Tfb-II buffer: 10 mM Na-MOPS, pH 7.0, 75 mM CaCl₂, 10 mM KCl, 15% glycerol

E. coli DH5 α cells were streaked on LB-plates without antibiotics and incubated overnight at 37°C. Single colonies were selected and used for inoculation of 100 ml of an overnight culture. 1 ml of the overnight culture was added to 200 ml of pre-warmed LB-MgSO₄ and incubated on the rotary shaker until an absorbance of 0.5 at 600 nm was reached (approx. 90 – 120 min.). The culture was chilled on ice, transferred to sterile round-bottom tubes and centrifuged at low speed (4,000 x g, 5 min., 4°C). The supernatants were discarded and the cells resuspended in ice-cold Tfb-I buffer (30 ml for a 100 ml culture). The suspension was kept on ice for an additional 90 min. Then, the cells were collected by centrifugation (4,000 x g, 5 min., 4°C), the supernatant was discarded again and the cells resuspended in 4 ml ice-cold Tfb-II buffer. Aliquots of 100 μ l were prepared, frozen in liquid nitrogen and stored at –80°C.

3.2. Transformation of bacteria

LB-medium: 10 g Tryptone, 5 g Yeast extract, 10 g NaCl, dH₂O up to 1 l

LB-plates: LB-medium with 1.5% (w/v) agar

Appropriate antibiotic(s)

To 100 µl of competent *E. coli* DH5α cells, 2 - 3 µl of ligation mixture were added and incubated for 30 min. on ice. After a heat shock (1.5 min., 42°C) and successive incubation on ice (3 min.), 500 µl LB-medium were added and the bacteria incubated at 37°C for 1 h on a rotary shaker. The cells were then centrifuged (10,000 x g, 30 sec., RT) and the supernatant removed. Cells were resuspended in 200 µl of LB-medium and plated onto LB-plates containing the appropriate antibiotics. Plates were incubated overnight at 37°C.

Transformation of One Shot® TOP10 Chemically Competent *E. coli* (Invitrogen GmbH, Karlsruhe, Germany) was performed according to the manufacturer's protocol.

3.2.1. Culture of *E. coli* DH5α cells for plasmid growth

In a conical flask, 4 ml of LB-medium with an appropriate antibiotic were inoculated with a single colony of *E. coli* DH5α harbouring the plasmid of interest. The culture was incubated overnight on a platform shaker at 37°C and 210 rpm. From this culture the cells were harvested by centrifugation (18,000 x g, 5 min., RT) and the plasmid DNA was purified as described below.

3.2.2. Small-scale plasmid isolation from *E. coli* (Miniprep)

Plasmids were isolated from bacterial cells using QIAprep Spin Miniprep Kit (Qiagen, Hilden, Germany) according to the manufacturer's protocol. DNA was eluted from the columns by addition of 50 µl elution buffer and subsequent centrifugation (14,000 x g, 2 min., RT).

3.2.3. Restriction analysis of plasmid DNA

Superdo restriction buffer (10x) : 330 mM Tris-HCl, pH 7.8, 625 mM K-acetate, 100 mM MgCl₂, 40 mM spermidine, 5 mM dithioerythritol (DTE)

Plasmid DNA was digested with restriction endonuclease(s) by mixing 2 µl of plasmid preparation, 10 units of each restriction endonuclease and 1 µl of 1x Superdo buffer and the reaction mix was brought to a final volume of 10 µl. After incubation at 37°C for 2 h the DNA was analyzed on an agarose gel as described below. If the conditions for two enzymes were incompatible with each other, the DNA was digested successively with the respective enzymes and buffers provided by the company.

3.3. Analysis of DNA by agarose gel electrophoresis

50x TAP buffer: 242 g/l Tris-HCl, 0.5 M EDTA, pH 8.0, 57.1 ml pure acetic acid
10x Loading buffer: 1x TAP buffer, 50% (v/v) glycerin, 0.1% (w/v) bromophenol blue,
0.1% (v/v) xylene cyanol

Agarose gel electrophoresis of DNA was performed in submarine gel tanks of appropriate size. All agarose gels used throughout this work were run in 1x TAP buffer and were prepared by dissolving from 0.8% to 1.0% agarose and 0.5 µg/ml ethidium bromide in 1x TAP buffer. Samples containing an appropriate amount of DNA were mixed with 10x loading buffer prior to sample application. The gels were run at 60 - 70 V until optimal separation was achieved. The DNA was visualized *via* fluorescence excitation by illumination with UV light (302 nm). A 1 kb DNA ladder was applied as a size standard.

3.3.1. Isolation of DNA fragments from agarose gels

After separation by agarose gel electrophoresis, DNA fragments used for cloning were cut out from the gel and extracted by using the QIAquick® Gel Extraction Kit™ (Qiagen GmbH, Hilden, Germany) according to the supplier's protocol.

3.4. Ligation of DNA fragments

Standard ligation of DNA fragments was performed by mixing 50 ng vector DNA with a five-fold molar excess of insert DNA, 1 µl of T4 DNA ligase and 1 µl of 10x ligation buffer and the reaction mix was brought to a final volume of 10 µl. The reaction was incubated in a water bath at 16°C or at 4°C for ligations in pGEM vector. The assay was used directly for transformation of *E.coli* cells without any further purification.

Cloning reactions using pENTR Directional TOPO Cloning Kit and Gateway LR-/BP-Clonase Enzyme Mix (Invitrogen GmbH, Carlsbad, CA, USA) were performed according to the supplier's protocol.

II. DNA analyses

3.5. Isolation of genomic DNA

CTAB-buffer: 2% CTAB, 1.4 M NaCl, 20 mM EDTA, 100 mM Tris/HCl, pH 8.0, 100 mM
β-mercaptoethanol (added before use)
TE (Tris/EDTA) buffer: 10 mM Tris-HCl, pH 7.5 or 8.0, 1 mM EDTA

Isolation of DNA from plants was performed according to Doyle and Doyle (1990) using CTAB as detergent. The leaf material (approx. 300 mg) was homogenised in 1.5 ml-Eppendorf tubes using a mechanical stirrer RW16 basic (Kika Labortechnik, Staufen, Germany) for approx. 10 sec. DNA was extracted using 400 µl of the CTAB-buffer and continued grinding. Afterwards, the slurry was incubated at 65°C for 30 - 60 min. The reaction was centrifuged to remove cellular debris (12,000 x g, 10 min.) and DNA precipitated from the supernatant with isopropanol (4°C, 30 min., 18,000 x g). For PCR amplification usually 0.2 µg DNA were used.

3.6. Polymerase chain reaction (PCR)

Amplification of DNA fragments was performed in a 50 µl reaction mixture with thinwalled PCR tubes in a PCR cycler (Advanced Primus 96, PeqLab Biotechnologie GmbH, Erlangen, Germany). The following reaction mixture was used:

template:	2 - 10 ng
primer 1 (10 pM):	1 µl (final concentration 0.2 – 1 µM)
primer 2 (10 pM):	1 µl (final concentration 0.2 – 1 µM)
dNTP Mixture (10 mM each):	4 µl (final concentration 200 µM)
PCR buffer (10x):	5 µl
<i>Taq</i> polymerase:	2.5 units/µl
add. H ₂ O ultra pure to 50 µl	

The PCR was performed with the following steps, if not otherwise stated:

- 1) initial denaturing at 94°C for 3 min.,
- 2) denaturing at 94°C for 30 sec.,
- 3) annealing usually at 50 - 65°C for 45 sec.,
- 4) elongation at 72°C for approx. 1 min./1kb DNA,
- 5) termination at 72°C for 10 min.,
- 6) cooling to 8°C.

The amplification procedure (steps 2 - 4) was repeated 30 times. The melting temperature of the primers depends on their GC content and was calculated by the following formula:

$$T_m = n(G+C) \times 4^\circ\text{C} + (A+T) \times 2^\circ\text{C}$$

If the two primers chosen had different melting temperatures, the lower one was used. The quality of PCR products was monitored by gel electrophoresis.

3.6.1. Preparation of PCR-derived DNA fragments for ligation

DNA fragments produced by PCR (see Section 3.6.) to be used for cloning were purified with the QIAquick^R PCR purification Kit (Qiagen GmbH, Hilden, Germany) or precipitated with ½ Vol 30% PEG 8000 (Sigma-Aldrich Chemie GmbH, Taufkirchen, Germany) containing 30 mM MgCl₂. The DNA was then resuspended in 50 µl dH₂O.

3.7. Determination of nucleic acid concentrations

DNA and RNA concentrations were determined spectroscopically using an Amersham Pharmacia Biotech (Freiburg, Germany) Ultraspec 3000 spectrometer. The minimal volume necessary for measuring was 100 µl. Concentrations were determined by measuring the absorbance at 260 and 280 nm. For clean double stranded DNA the absorption ratio A₂₆₀/A₂₈₀ is approx. 1.8.

Concentrations were calculated as follows:

double stranded DNA [mg/µl] = 50 x A₂₆₀ x dilution factor

RNA [mg/µl] = 40 x A₂₆₀ x dilution factor

III. RNA analyses

3.8. Isolation of total RNA

Total cellular RNA was isolated from plant tissue using TRIzol reagent (Invitrogene GmbH, Karlsruhe, Germany) following the supplier's protocol. The concentration of isolated RNA was checked by spectroscopic measurement (see Section 3.7.). As a quality control of isolated RNA, aliquots (1 µg) were fractionated on agarose gels containing ethidiumbromide to visualise the RNA.

For far-red (FR) light gene expression experiments, seedlings were prepared as described in Section 3.19. After induction of germination, seedlings were grown for 4 d in darkness before being transferred (0 h) to FR light (0.7 µM m⁻²s⁻¹) for 3, 6 or 18 h. Tissue was collected and frozen in liquid nitrogen and RNA was extracted using the Qiagen Plant RNeasy Kit (Qiagen GmbH, Valencia, CA, USA) according to the manufacturer's instructions. The RNA solutions were stored at -20°C until further use.

3.8.1. DNase I treatment of RNA preparations

DNaseI (Roche Diagnostics GmbH, Penzberg, Germany) treatment of RNA preparations to remove contaminating genomic DNA was performed by adding 1 µg/ml of RNase free/DNaseI. The reaction was incubated for 30 min. at 37°C and the enzyme was inactivated by heating the sample for 10 min. at 65°C.

3.9. Semiquantitative reverse transcription-polymerase chain reaction (RT-PCR)

For the analysis of transcript levels of low abundant genes (e.g. *SCL21* and *PAT1*) a semiquantitative reverse transcription (RT) reaction was performed with total RNA extracted from wild type (WT) and mutant lines. An oligo(dT)₁₈ primer (10 μM) was hybridized to 1 μg of total RNA. Reverse transcription was performed with the Omniscript RT Kit (Qiagen GmbH, Hilden, Germany) according to the manufacturer's instruction. After the RT reaction, 1 μl of the cDNA was used for the PCR reaction with gene specific primers for *SCL21*, *PAT1* and *SCL13*: (*PAT1*: 5'-GAACTCTCCATGTGGCCTG-3'; 5'-GCACACGAGGCAACCAA AT-3'; *SCL21*: 5'-CCCTTATC GACTTCCACCG-3'; 5'-GATTCGAACATTGCCGTG-3'; *SCL13*: 5'-CTCCCATTCAACAAAATTT CTTCA-3'; 5'-CCAGCAATACACTACACAGCTC-3'). To be able to discriminate between genomic DNA and cDNA amplification products, the 5'-forward primer was located 5' of the intron in the leader sequence, which also prevented amplifying the respective RNAi and antisense constructs. PCR reactions were stopped after 25 or 30 cycles and analyzed on agarose gels. The number of cycles used was optimized dependent on the abundance of the respective RNA. Each PCR was repeated three times.

One μl of the cDNA was also used for a control PCR with the *18S rRNA* (*18S rRNA-f*: 5'-GCTCA AAGCAAGCCTACGCTCTGG-3'; *18S rRNA-r*: 5'-GGACGGTATCTGATCGTCTTCGAG-3') or the *actin2* (*actin2-f*: 5'-GCAACTGGGATGATATGGAAAAGA-3'; *actin2-r*: 5'-CAAACGAGGGCTG GAACAAGACT-3'). In this case the PCR reaction was stopped after 20 cycles and quantified on agarose gels.

3.10. Northern analyses

MOPS buffer: 20 mM MOPS, pH 7.0, 5 mM Na-acetate, 1 mM Na₂ EDTA, pH 7.0, final pH 5.5 to 7.0

20x SSC buffer: 3M NaCl, 3M sodium citrate, pH 7.0 with HCl

For Northern analysis 5 to 10 mg of total cellular RNA was used. RNA was denaturated through incubation with 30% glyoxal (McMaster and Carmichael 1977), electrophoretically separated on 1.2% agarose gels in MOPS buffer and transferred by capillary force onto a Hybond-N nylon membrane (Amersham Pharmacia Biotech GmbH, Freiburg, Germany) in 20x SSC buffer. RNA was fixed to the membrane by UV crosslinking (2x Autocrosslink on "UV-StratalinkerTM 2400", Stratagene GmbH, Heidelberg, Germany). *EcoRI/HindIII*-digested and glyoxylized λ DNA was used as a molecular weight standard.

3.10.1. Staining of Northern Blots

Methylene Blue (MB) stain: 0.03% (w/v) methylene blue, 0.3 M NaOAc, pH 5.2

After RNA was fixed to the membrane by UV crosslinking, the membrane was stained with Methylene Blue to visualize rRNA bands. The blot was soaked in MB stain for 30 - 60 sec. and destained in repeated changes of water (usually 3 changes over 2 min.) until background was reduced. The membrane was air dried and documented using a digital camera (Coolpix 700, Nikon, Tokyo).

3.10.2. Generation and purification of ³²P-labelled radioactive probes

DNA labelling of PCR fragments was performed using the Random Primed DNA Labelling Kit (Roche Molecular Biochemicals GmbH, Mannheim, Germany) according to the method of Feinberg and Vogelstein (1983). Briefly, the fragment to be labelled and the random primers provided by the kit were heated in a water bath for 10 min. at 95°C to separate the DNA strands. Unlabeled dNTP stock mix as well a reaction buffer, Klenow enzyme and ³²P α -dCTP were added. After incubation for 30 min. at 37°C the labelled DNA fragments were separated from unincorporated nucleotides using Mini Quick Spin DNA Columns (Roche Molecular Biochemicals GmbH, Mannheim, Germany) probe purification columns. The probe was denaturated at 95°C for 5 min. prior to addition to the pre-heated hybridization buffer.

3.10.2.1. Hybridisation of nucleic acids

“Church Hyb” hybridisation buffer: 7% (w/v) SDS, 0.5 M NaPhosphate, pH 7.0, 1 mM EDTA

All hybridisations were performed overnight in hybridisation buffer “Church Hyb” (similar buffer first described by Church and Gilbert (1984) at 68°C. Prehybridisations were carried out in the same buffer for at least two hours. After hybridisation, washing steps were carried out to a final stringency of 0.5x SSC and 0.1% (w/v) SDS at RT. For exposure, filters were sealed in plastic bags and quantified by phosphorimaging (BASIII Fuji Bio Imaging plates, BAS2000 software package and the AIDA software package v3.25 beta; Raytest, Straubenhardt, Germany).

IV. Protein analyses

3.11. Extraction of total proteins for Western Blots

Homogenisation buffer: 50 mM Tris acetate, pH 7.9, 100 mM potassium acetate, 1 mM EDTA, 1 mM DDT (always added before use), 20% (v/v) glycerol and protease inhibitors (2.5 μ l in 1 ml).

Proteins were isolated from young *Arabidopsis thaliana* leaves (50 - 100 mg). Plant material was homogenised in homogenisation buffer (1 v/w) in 1.5 ml-Eppendorf tubes using a mechanical stirrer RW16 basic (Kika Labortechnik, Staufen, Germany) for approx. 10 sec. The extract was centrifuged for 10 min. at maximum speed at 4°C. The supernatant was transferred to a new Eppendorf tube and stored at -20°C.

3.12. Preparation of Tris-Glycine SDS-Polyacrylamide Gel electrophoreses (PAGE)

Solutions for preparing 10% resolving gels :

H ₂ O ultra pure	4.8 ml
40% acrylamide mix	2.5 ml
1.5 M Tris, pH 8.8	2.5 ml
10% SDS	100 µl
10% APS	100 µl
TEMED	4 µl

Solutions for preparing 5% stacking gels :

H ₂ O ultra pure	3.6 ml
40% acrylamide mix	630 µl
1.0 M Tris, pH 6.8	630 µl
10% SDS	50 µl
10% APS	50 µl
TEMED	5 µl

Minigels with 0.75 mm thickness were cast in the Mini-PROTEAN 3 Cell (Bio-Rad Laboratories GmbH, Germany) following the instructions manual. The resolving gel was poured and polymerized with an overlay of isobutanol. Polymerisation time was at least 30 min., after removal of the isobutanol the stacking gel was cast. Mini gels, wrapped in a plastic foil, can be stored at 4°C for at least one week.

3.12.1. Separation of proteins by PAGE

Tris/glycine/SDS buffer:	250 mM Tris, 1.92 M Glycine, 1% (w/v) SDS, dH ₂ O up to 1 l
10x Laemmli buffer:	30.25 g Tris, 14.4 g glycerol, 10 g SDS, dH ₂ O up to 1 l
Laemmli sample buffer:	4% (w/v) SDS, 50 mM Tris/HCl, pH 6.8, 10% (v/v) β-mercaptoethanol
Tris-glycine electrophoresis buffer:	25 mM Tris, 250 mM glycine (electrophoresis grade), pH 8.3, 0.1% (w/v) SDS

Gels were assembled in a Mini-PROTEAN 3 Cell Running Chamber (Bio-Rad Laboratories GmbH, Germany) and filled with running buffer following the manufacturer's instructions. Tris/glycine/SDS or Laemmli buffer were used as running buffer systems. Protein samples were treated with Laemmli sample buffer in a 1:2 ratio, boiled at 95°C for 5 min. and loaded into the wells of the gel. The electrophoresis was run constant at 120 V until the Bromophenol Blue reached the bottom of the gel. Prestained protein marker, broad range (New England BioLabs GmbH, Frankfurt/Main, Germany), was used for the determination of molecular masses.

3.12.2. Western analysis

Transfer buffer, pH 8.3: 39 mM glycine, 48 mM Tris, 0.037% (w/v) SDS, 20% (v/v) methanol in dH₂O

Electrophoretic transfer of proteins from the polyacrylamide gels to a polyvinylidene fluoride (PVDF) membrane was performed using the mini Trans-Blot Electrophoretic Transfer Cell (Bio-Rad Laboratories GmbH, Germany). The PVDF membrane (Hyond-P, Amersham Biosciences Europe GmbH, Freiburg, Germany) was activated in methanol and soaked in transfer buffer together with two filter paper sheets and the fibre pads. Gel sandwich was prepared in the cassette following the instructions manual. Electrophoresis was performed at 150 mA for 120 min. or at 20 V overnight at 4°C. Upon completion of the run, the membrane was stained with Coomassie Blue R-250 (see below). Detection of proteins on the PVDF membrane was accomplished by using antibodies (see Section 3.13.).

3.12.3. Coomassie Blue R-250 staining of protein gels

Coomassie Blue R-250 staining solution: 50% (v/v) methanol, 0.05% (w/v) Coomassie Brilliant Blue R-250 dissolved in methanol, 10% (v/v) acetic acid, 40% (v/v) dH₂O

Methanol/acetic acid destaining solution: 5% (v/v) methanol, 7% (v/v) acetic acid, 88% (v/v) dH₂O

After SDS-PAGE, the gels were stained in Coomassie staining solution at RT for 1h with constant agitation. The gels were then incubated in destaining solution until the background of the gel appeared nearly transparent.

V. Protein detection

3.13. Immunoblotting

10x TBS Buffer:	200 mM Tris-HCl, pH 7.6, 1370 mM NaCl, dH ₂ O up to 2 l
Blocking solution:	1x TBS, 0.1 - 1% (v/v) Tween20, 5% (w/v) nonfat dried milk or BSA
Washing solution:	1x TBS, 0.1 - 1% (v/v) Tween20
Solution I:	2.5 mM Luminol, 0.4 mM coomarcic acid, 0.1 M Tris/HCl, pH 8.5
Solution II:	5.4 mM hydrogen-peroxide, 0.1 M Tris/HCl, pH 8.5

Proteins covalently bound to a PVDF membrane can be detected with the help of antibodies. Dried membranes were pre-wetted in methanol and equilibrated with 1x TBS buffer. Membranes were blocked in blocking solution for 1 h to suppress non-specific adsorption of antibodies. Proteins were incubated for 2 h at RT or overnight at 4°C with the specific polyclonal antibody diluted in washing solution (1:500). Antibodies are detailed in Section 2.9. Membranes were washed (1x 15 min. and 2x 10 min.) and incubated for 1 h with a secondary goat anti-rabbit IgG peroxidase conjugate antibody (Sigma GmbH, Missouri, USA) diluted 1:10.000 in 1x TBS buffer. Again the membranes were washed (1x 15 min. and 2x 10 min.). Incubations were performed at RT or at 4°C on a shaker. Antigen-antibody complexes were viewed by chemiluminescent reactions using the SuperSignal West Pico Chemiluminiscent Substrate Kit (Perbio GmbH, Bonn, Germany) following the manufacturer's instructions, or by chemiluminescent reactions soaking the membrane for 1 min. in detection solution (1:1 mixture of solutions I and II). The solution was removed and the blot was placed between two Saran wrap foils. Then the membrane was exposed to a high performance autoradiography film, Hyperfilm™ (Amersham Biosciences Europe GmbH, Freiburg, Germany) for varying periods and the films were developed to detect the signals.

VI. Manipulation of yeast cells

3.14. Preparation of competent yeast cells

YPAD medium:	6 g yeast extract, 12 g peptone, 12 g glucose, 60 mg adenine hemisulfate, dH ₂ O to 600 ml. For plates, 10 g bacto-agar was added.
Buffered lithium solution:	150 µl 10x TE buffer, pH 7.5, 150 µl 1 M lithium acetate, 1200 µl dH ₂ O
10x TE buffer:	0.1 M Tris-HCl, 10 mM EDTA, pH 7.5

MaV203 yeast cells were streaked on YPAD-plates and incubated overnight at 30°C. A single yeast colony was picked and used for inoculation of 300 ml of an overnight culture. Approx. 3 ml of the overnight culture was added to 300 ml of YPAD medium and shaken until an absorbance of

1.0 to 1.2 at 600 nm was reached (approx. 120 – 180 min.). The culture was transferred to sterile round-bottom tubes and centrifuged at low speed (4,000 x g, 5 min., RT). The supernatants were discarded and the cells resuspended in 10 ml highest-quality sterile water. Then, the cells were collected by centrifugation (5,000 to 6,000 x g, 5 min., RT), the supernatant was discarded again and the cells were resuspended in 1.5 ml buffered lithium solution (freshly prepared). Aliquots of 150 µl were stored at 4°C until transformation (no more than 4 days).

3.15. Yeast transformation

PEG solution: 120 µl 10x TE buffer, 120 µl 1 M lithium acetate, 960 µl 50% PEG 4000 (Sigma-Aldrich Chemie GmbH, Taufkirchen, Germany)

SC medium: 6.7 g yeast nitrogen base without amino acids (Sigma-Aldrich Chemie GmbH, Taufkirchen, Germany); 1.4 g yeast synthetic drop-out media supplement without histidine, leucine, tryptophan and uracil (Sigma-Aldrich Chemie GmbH, Taufkirchen, Germany); 40 ml 50% (w/v) glucose; 8 ml 20 mM uracil; 8 ml 100 mM histidine-HCl and dH₂O to 1 l. The medium was autoclaved for 15 min. only. The agar was autoclaved separately from the drop-out mix and yeast nitrogen base according to the manufacturer's instructions. For plates, 20 g agar was added.

For each transformation, 200 µg of carrier DNA with 5 µg transforming DNA were mixed in a sterile 1.5 ml microcentrifuge tube. 150 µl of yeast suspension and 1.2 ml of PEG solution (freshly prepared) were added to each microcentrifuge tube. Cells were incubated for 30 min. under continuous agitation at 30°C. After a heat shock (20 min., 42°C) the cells were centrifuged (5 sec. at RT), resuspended in 200 µl of 1x TE buffer (freshly prepared from 10x stock) and plated onto SC plates without leucine and tryptophan. Plates were incubated for 2 to 5 days at 30°C until transformants appear.

3.16. Plasmid DNA extraction from yeast cells

Solutions used: 3% (w/v) SDS
0.2 M NaOH
TE Buffer (10 mM Tris-HCl, pH 7.5, 1 mM EDTA)
3 M sodium acetate
chloroform: isoamyl: alcohol 25:24:1
isopropanol
70% (v/v) ethanol

Plasmid DNA was extracted from yeast cells according to the procedure provided with the Manual Invitrogen ProQuest Two-Hybrid System (Invitrogen, Karlsruhe, Germany). This protocol is a modification of the method described by Polaina and Adam, 1991.

3.17. Yeast Two-Hybrid and One-Hybrid assays

The full-length *SCL21* and *PAT1* reading frames and an N-terminal deleted *Seuss-like 1* gene resulting in a 1,560 bp long fragment, were amplified with the TAKARA Polymerase (TaKaRa Ex Taq™, Takara Bio INC., Shiga, Japan) from a cDNA library. Primers contained the *attB* sequences (underlined): (*SCL21*full-length): *SCL21-f*: 5'-GGGGACAAGTTTGTACAAAAAAGCAGGCTCGATGGACAATGTAAGAGGTTCAATAATG-3', *SCL21-rev*: 5'-GGGGACCACTTTGTACAAGAAAGCTGGGTATCACTTCCATGCACAAGATGAC-3', (*PAT1*full-length): *PAT1-f*: 5'-GGG GACAAGTTTGTACAAAAAAGCAGGCTCGATGTACAAGCAGCCTAGACAAGAG-3', *PAT1-rev*: 5'-GGGGACCACTTTGTACAAGAAAGCTGGGTACATTTCCAAGCACAAAGGAGC-3', (*SEUSS*-like): *TH77900-f*: 5'-GGGGACAAGTTTGTACAAAAAAGCAGGCTCGATGCAGTACCTATATCAT CAGC-3', *TH77-rev*: 5'-GGGGACCACTTTGTACAAGAAAGCTGGGTATCATGACTTCCAAGAAT ATCCTC-3'. After precipitation with ½ Vol 30% PEG 8000 containing 30 mM MgCl₂ and resuspension in TE buffer (30 µl), the PCR fragment was introduced with the help of the BP-Clonase Enzyme Mix (Invitrogen GmbH, Carlsbad, CA, USA) into the pDONR221-Vector (Invitrogen GmbH, Carlsbad, CA, USA).

An N-terminal deletion of *SCL21*, resulting in a 820 bp long fragment, was amplified with the Ex Taq™ Polymerase (TaKaRa, Takara Bio INC., Shiga, Japan) from the cDNA and cloned into the pENTR/D-TOPO cloning vector (Invitrogen GmbH, Carlsbad, CA, USA). For directed cloning a 5'-CACC-extension was added to the forward primer: *SCL21 delN-f*: 5'-CACCATGGTGGAGCCA ATATCAAG-3', *SCL21 del N-rev*: 5'-TCACTTCCATGCACAAGATGAGAC-3'.

In a next step the PCR fragments were transferred into the pDEST 32- and pDEST 22-vectors with the help of the LR-Clonase Enzyme Mix (Invitrogen GmbH, Carlsbad, CA, USA), thereby either generating an N-terminal fusion with the GAL4 DNA-binding domain (pDEST 32; "bait") or the GAL4 activation domain (pDEST 22; "prey"). For assaying dimerization the constructs were co-transformed and selected on Synthetic Complete Dropout (SC) media without leucine and tryptophane. For the one-hybrid assays only the "bait" was introduced in yeast cells and selected on SC media without leucine. GAL4-binding UAS drive the expression of the *HIS3* reporter gene. The ability to grow in the absence of histidine was tested on media without histidine and media supplemented with different concentrations of 3-Amino-1,2,4,-Triazole (3AT), 10, 25, 50 and 75 mM. Colonies were streaked or dropped on master plates and lifted onto plates containing different amounts of 3AT. Yeast was incubated at 30°C and growth was evaluated after 2 subsequent rounds of replica cleaning. The replica cleaning was performed according to the procedure provided with the Manual Invitrogen ProQuest Two-Hybrid System (Invitrogen, Karlsruhe, Germany). After the tests the plasmids were extracted from the yeast and rechecked for the correct fragment insertion via PCR.

VII. Growth conditions and physiological characterization

3.18. Seed sterilization, growth conditions and mutant selection

Seeds were surface-sterilized for 10 min. in 50% (v/v) commercial bleach with the addition of 0.05% Triton X-100, rinsed at least three times and sown on Petri dishes (11 cm diameter) containing half-strength Murashige and Skoog basal medium (Sigma, St. Louis) and 0.8% (w/v) agar. To select transgenic lines the medium was supplemented with kanamycin or Basta and 3% sucrose. Until use for germination assays, plates were stored at 4°C for 4 days and germination was induced by 2 h of W light followed by 22 h of darkness at 21°C. After this treatment plates were transferred into the appropriate light conditions for 4 days. The blue (B), red (R) and far-red light (FR) sources were generated by LED using diodes with a maximum at 469, 660 or 740 nm, respectively (Quantum Devices, Barneveld and PVP GmbH, Willich). White light (W) was provided by cool-white fluorescent bulbs (Osram L85W125 Universal White Fluorescent Lamps). Light intensities were determined with spectroradiometers (W, B und R light: model Li-1800, LiCor, Lincoln, NE; FR light: model SKP200 with a sensor for 730 nm, Skye Instruments, UK).

3.19. Physiological measurements

For fluence response experiments, briefly, seedlings were grown on 1x MS plates without sucrose and stratified at 4°C in the dark for 4 d. After 2 h in W light, to induce germination and 22 h in darkness at 21°C plates were transferred to the appropriate light conditions for 4 d at 21°C. Lines were always analysed in parallel with the appropriate controls. The experiments were repeated at least 3 times and each time a minimum of 50 seedlings was analysed. Hypocotyl, petiole lengths and cotyledon sizes were documented using a digital camera (Coolpix 700, Nikon, Tokyo) and measured with the NIH Image software (ImageJ, National Institutes of Health, Bethesda, MD). Data derived from hypocotyl length assays were subjected to statistical analysis included in Microsoft Office Excel 2003 such as the t-student-tests to verify hypotheses about differences between two mean values. Differences were assumed to be insignificant when the *P* values associated with these tests exceeded 0.05.

Germination assays were performed according to Shinomura *et al.* 1996. Seeds were sterilized and plated on half-strength MS medium without sucrose. After plating, the seeds were pulsed with FR light ($1 \mu\text{M m}^{-2}\text{s}^{-1}$) for 10 min. and transferred to darkness (D). To test for R light responsiveness seeds were illuminated again after 3 h with R light ($5 \mu\text{M m}^{-2}\text{s}^{-1}$) for 10 min. To test for FR light responsiveness a FR light pulse ($1 \mu\text{M m}^{-2}\text{s}^{-1}$) was given after 48 h for 10 min. After the appropriate light pulse the seedlings were kept in darkness for 6 days and germination was scored positive as soon as the radicle was visible. Germination efficiency was normalized for seeds that could germinate without the second light pulse and seeds that did not germinate under W light, the following formula was used: $[(\text{germination in FR or R}) - (\text{germination in D}) \times 100\%] / [(\text{germination in WL}) - (\text{germination in D})]$

For chlorophyll accumulation assays, seeds were sown on 1x MS plates without sucrose and vernalized for 4 d at 4°C in the dark. After 2 h in W light, to induce germination, and 22 h in darkness at 22°C plates were transferred to FR light at 22°C for 4 d. Plants were then shifted for an additional 2 - 3 d in W light. 25 seedlings for each of the different lines were harvested in 2 ml Eppendorf tubes and incubated overnight in the dark under continuous agitation in 1 ml of 80% (v/v) acetone. On the next day, the Eppendorf tubes were centrifuged (2 min., RT at maximum speed) and the supernatants were used for measurements of chlorophyll accumulation. Chlorophyll accumulation was determined by measuring the absorbances at 645 and 663 nm and was calculated according the following formula:

$$\text{Chl a mg/ml} = 12,7 * A_{663} - 2,69 * A_{645}$$

$$\text{Chl b mg/ml} = 22,9 * A_{645} - 4,68 * A_{663}$$

$$\text{Total Chl mg/ml} = \text{Chl a} + \text{Chl b}$$

$$\text{Total Chl (mg) in original tissue sample} = \text{Chl a (mg/ml)} * \text{final volume}$$

3.20. Cellular and subcellular localization

The *SCL21*, *PAT1* and *SCL13* open reading frames were amplified by PCR from cDNA using primers containing restrictions sites for *XbaI* and *KpnI* and inserted into the pGFP vector (Kost *et al.* 1998) generating *SCL21*-, *PAT1*- and *SCL13-GFP* fusions driven by the *35S-CaMV* promoter.

The full-length *SCL1* and *SCL5* reading frames, resulting in a 1,780 bp long fragment for *SCL1* and a 1,580 bp long fragment for *SCL5*, were amplified with the Ex Taq™ Polymerase (TaKaRa, Takara Bio INC., Shiga, Japan) from a cDNA library. Primers contained the *attB* sequences (underlined): (*SCL1* full-length): *SCL1-f*: 5'-GGGGACAAGTTTGTACAAAAAAGCAGGCTCCATG GTGGAACAAACTGTGGTTAGAG-3', *SCL1rev*: 5'- GGGGACCACTTTGTACAAGAAAGCTGGG TCCCTCCAAGCTGAAGCAACGATTAAG-3'); (*SCL5* full-length): *SCL5 f*: 5'-GGGGACAAGTTT GTACAAAAAAGCAGGCTCCATGGAAGCTACTCAGAAACATATG-3', *SCL5 rev*: 5'-GGGACC ACTTTGTACAAGAAAGCTGGGTCCCTCCAAGCACAAGAAGGATAAGAG-3').

After precipitation with ½ Vol 30% PEG 8000 (Sigma-Aldrich Chemie GmbH, Taufkirchen, Germany) containing 30 mM MgCl₂ and resuspension in TE buffer (30 µl), the PCR fragment was introduced with the help of the BP-Clonase Enzyme Mix (Invitrogen GmbH, Carlsbad, CA, USA) into the pDONR221-Vector (Invitrogen GmbH, Carlsbad, CA, USA). In a next step the fragments were combined into the Gateway-adapted binary vector pK7FWG2 (Karimi *et al.* 2002), which contains the coding sequence of GFP in the N-terminus.

Onion or leek epidermis cells were bombarded with gold particles loaded with DNA (10 µg) encoding GFP fusion proteins using a helium biolistic gun and incubated in darkness for 12 h. To test for possible effects of light the cells were subsequently incubated for 3 h either under FR, R

or W light. A *35S-GFP* construct was used as a control. To visualize GFP, fluorescence cells were examined using an Axioskop microscope (Carl Zeiss, Jena, Germany).

To examine the *SCL1*, *SCL21* and *SCL13 promoter* activity, the DNA fragments upstream of the ATG start codon were amplified by PCR and cloned into the pENTR/D-TOPO cloning vector (Invitrogen GmbH, Carlsbad, CA, USA). For *SCL1* the fragment was 1,385 bp long and for *SCL21* 1,946 bp. For directed cloning a 5'-CACC-extension was added to the forward primer [*SCL1*: (*SCL1 Prom-f*: 5'-CACCAGTGCCTACTGTCTAGGCAC-3'; *SCL1 ATG-rev*: 5'-CCACAGTTTGT TCCACCATTTCAG-3') and *SCL21*: (*SCL21 Prom-f*: 5'-CACCGCAACAACTGAACAAG-3'; *SCL21 Prom-rev*: 5'-CAGCTATCTCTGGCAGTGGCTG-3')]. For the *SCL13 promoter* two DNA fragments containing the *SCL13* 5' upstream sequences were used. The 5'-end of both fragments was located 2,514 bp upstream of the ATG start codon (5'-CACCGTCTGTCTCTTCTCTGGT AC-3'). One fragment had its 3'-end located at the beginning of the 5'-UTR, 882 bp upstream of the ATG start codon, leading to the promoter fragment lacking the 5'-UTR and the intron therein (5'-GCTGAAGAAATTTTGTGAATGGG-3'), whereas the 3'-end of the other fragment was located 117 bp downstream of the ATG generating the *SCL13-promoter-5'-UTR* construct (5'-CCAGCAATACACTACACAGCTC-3'). The 5'-end of the third construct, which contained only the 5'-UTR with the intron sequence began at the predicted transcription start site, 908 bp upstream of the ATG (5'-CACCTCCCATTCAACAAAATTTCTTCAG-3') and the 3'-end was located 117 bp downstream of the ATG. With the help of the LR-Clonase Enzyme Mix (Invitrogen GmbH, Carlsbad, CA, USA) the fragments were combined into the Gateway-adapted vector pKGWFS7 (Karimi *et al.* 2002), which contained the coding sequence of GFP and GUS downstream of the insertion site.

For GUS staining, transgenic seedlings or adults plants were incubated for 3 to 24 h in 0.1 M phosphate buffer, pH 7.0, containing 0.1% Triton X-100 (v/v), 10 mM EDTA, 0.5 mM ferrocyanide, 0.5 mM ferricyanide and 0.125 mM X-Gluc (Roth GmbH, Karlsruhe, Germany). Chlorophyll was removed with 70% (v/v) ethanol and the blue staining analysed with a microscope.

VIII. Analysis of mutants and Plant transformation

3.21. Analysis of mutants

Insertion lines were derived from the Sail- and Salk-collection and selected on Basta- or kanamycin-containing medium (see Appendix 1 Tab. 3). Genomic DNA was extracted from resistant plants and analysed by PCR to see if they contained the insertion. For *sc121-1*, *sc11-1* and *sc11-2* a primer at the 5'-end of the coding sequence (*SCL21 Intron-f*: 5'-CCCTTATCGACTT CCACCG-3', *SCL1 1110-f*: 5'-GCTGAGGCAGATAGTTTCTATCCAA-3', *SCL1-3*: 5'-CGAGAAG CGCTCTTTCAAGCTCTTG-3') and from the left border of the T-DNA insertion (Sail LB: 5'-GAAA TGGATAAATAGCCTTGCTTCC-3') were used to detect insertion sites. For *sc121-2*, *pat1-2*, *sc11-3* and *sc15-1* a primer at the 3'-end of the coding sequence (*SCL21 1000*:

5'-CGAGCAGCACTGCATGGCAAG-3', *PAT TGA-rev.* 5'-TTTCCAAGCACACGGCGAAACC-3', *SCL1 TGA-rev.* 5'-CGGTACCCCTCCAAGCTGAAGCAAC-3', *SCL5 TGA-rev.* 5'-CGGTACCCC CCAAGCACAAGAAG-3') and from the left border of the T-DNA insertion (Salk LB: 5'-GTTACG TAGTGGGCCATCG-3') were used to detect insertion sites.

Gene specific primers flanking the insertion sites were used to distinguish heterozygous from homozygous plants (see Results, Tab.1, and Appendix 1, Tab. 2). Homozygous plants were selfed and retested in the next generation.

3.22. Plant transformation

Infiltration medium: 5% (w/v) sucrose, 0.05% (w/v) Silwet L-77 (Clough and Bent 1998)

Antibiotics for transformed *Agrobacterium tumefaciens*: streptomycin (50 mg/ml),
spectinomycin (50 mg/ml)
and gentamycin (10 mg/ml)

Gateway-adapted binary vectors (Karimi *et al.* 2002) to be used for the stable transformation of *Arabidopsis thaliana* were introduced into *Agrobacterium tumefaciens* (Koncz *et al.* 1994). Homozygous Col-0 or mutant plants were used for *in planta* transformation via the *Agrobacterium tumefaciens* floral dip method (Clough and Bent 1998). Briefly, a 300 ml culture of *Agrobacterium tumefaciens* was grown in LB-medium with the corresponding antibiotics at 28°C and harvested by centrifugation (4.000 x g, 20 min., RT). The pellet was resuspended in 500 ml of infiltration medium. Flowering plants were placed upside down into the bacteria suspension excluding rosettes, leaves and soil for 20 sec. Plants were grown until the seeds were dried. Transformants were selected on kanamycin- or Basta-containing media, self-fertilized and homozygous progeny was selected.

IX. Generation of constructs

3.23. Transgenic plants

To generate *PAT1* and *SCL21 RNAi* lines a portion of the respective cDNA was amplified, resulting in a 665 bp long fragment for *PAT1* and a 855 bp long one for *SCL21*, and cloned into the pENTR/D-TOPO cloning vector (Invitrogen GmbH, Carlsbad, CA, USA). For directed cloning a 5'-CACC-extension was added to the forward primer (*PAT1*: 5'-CACCGACTTCAGCGTATGCT C-3'; 5'-GCACACGAGGCAACCAAATC-3'; *SCL21*: 5'-CACCAACTCTCCATGTGGCCTG-3'; 5'-GATTCGAACATTGCCGTG-3'). With the help of the LR-Clonase Enzyme Mix (Invitrogen GmbH, Carlsbad, CA, USA) the fragments were combined into the Gateway-adapted binary vector pK7GWIWG2(I) (Karimi *et al.* 2005), which contains two tail-to-tail insertion sites separated by an intron. The expression is driven by the 35S-*CaMV* promoter.

To generate *SCL13* antisense plants a portion of the *SCL13* cDNA was amplified with *Xba*I-*Kpn*I adaptors at the 5'- and 3'-end (5'-GCTCTAGAATGGAAGCCACAGTCAAAATATTC-3'; 5'-GGTACCTCATTCTGACCCTCCATTTC-3'). The resulting PCR fragment was cloned into the appropriate sites of a binary vector (Van der Krol and Chua 1991) in the reverse orientation under the control of a 35S-*CaMV* promoter.

All constructs were checked by restriction analysis and sequencing. Constructs were transformed into *Arabidopsis thaliana* plants via the *Agrobacterium tumefaciens* floral dip method (Clough and Bent 1998, see Section 3.22.). Transformants were selected on kanamycin- or Basta-containing media, self-fertilized and homozygous progeny was selected.

X. Sequence analysis, Databases and Computer programmes

3.24. Sequence analysis

Alignment of sequences was performed with the ClustalW program (DNASStar, MegAlign 6.1). The phylogenetic tree was generated with the help of the PHYLIP program 3.6 (<http://evolution.genetics.washington.edu/phylip.html>) using SEQBOOT for bootstrapping (100), PROTDIST, NEIGHBOR analysis and DRAWTREE.

3.25. Analysis of microarray data

The original data published by the AtGenExpress consortium (<http://web.uni-frankfurt.de/fb15/botanik/mcb/AFGN/atgenex.html>) were evaluated according to the analysis performed at NASC (<http://affymetrix.arabidopsis.info>). Values not marked with *P* were discharged. A mean value was generated from the triplicates and standard deviation was calculated. Furthermore, the data were compared using the Genevestigator program (Zimmermann *et al.* 2004).

3.26. Databases

GenBank <http://www.ncbi.nlm.nih.gov/Genbank/index.html>
NCBI <http://www.ncbi.nlm.nih.gov/>
PubMed <http://www.ncbi.nlm.nih.gov/entrez/query.fcgi>
Swiss-Prot <http://us.expasy.org/sprot/>

3.27. Computer programmes

ClustalW program (DNASStar, MegAlign 6.1) was used to perform the alignment and analyses of the sequences.

CorelDraw9 was used to edit the digital images.

Microsoft Excel was used for hypocotyl length analysis, graphics, statistical analysis and evaluation of the microarray data.

NIH Image software (ImageJ, National Institutes of Health, Bethesda, MD) was used for hypocotyl and cotyledon sizes measurements.

PHYLIP program 3.6 was used to generate the phylogenetic tree.

4. RESULTS

4.1. Phylogenetic analysis

4.1.1. Phylogenetic tree

The GRAS protein family is a relatively large family. The *Arabidopsis thaliana* genome encodes at least 33 members (Bolle 2004, Tian *et al.* 2004), but only a few GRAS proteins have been characterized so far. By comparing protein sequences aligned with ClustalW, a neighbour-joining phylogenetic tree was generated. The phylogenetic trees are very similar if based on full-length sequences or only on the conserved C-termini of the proteins (Bolle 2004). The GRAS protein family can be divided into several subfamilies, which have been designated after one of their members or a common feature. These subfamilies are: the DELLA proteins, the SCR branch, the Ls branch, the HAM branch, the PAT1 branch, the SHR branch and the SCL9 branch (Fig. 14). Some proteins do not seem to cluster to sub-branches such as SCL30, SCL11, SCL28, SCL4, SCL7, SCL23, SCL3, SCL26 and SCL8.

Four *Arabidopsis* proteins cluster to the PAT1 branch of the family, namely SCARECROW-LIKE (SCL)1, SCL5, SCL13 and SCL21 (Fig. 14), which show high similarity to PAT1. The *Arabidopsis* mutant *phytochrome A signal transduction (pat1-1)* is a semi-dominant mutant, which is disrupted in the phytochrome PhyA-specific signalling pathway (Bolle *et al.* 2000). Members of the PAT1 branch have an overall identity to other GRAS proteins of 15 to 26%, whereas within this group the identity is increased to between 37 to 66%. Because of sequence similarities it was reasoned that perhaps all proteins of the PAT1 branch may be involved in light signalling pathways. The closest homolog of PAT1 in *Arabidopsis thaliana* is SCL21 (68% identity).

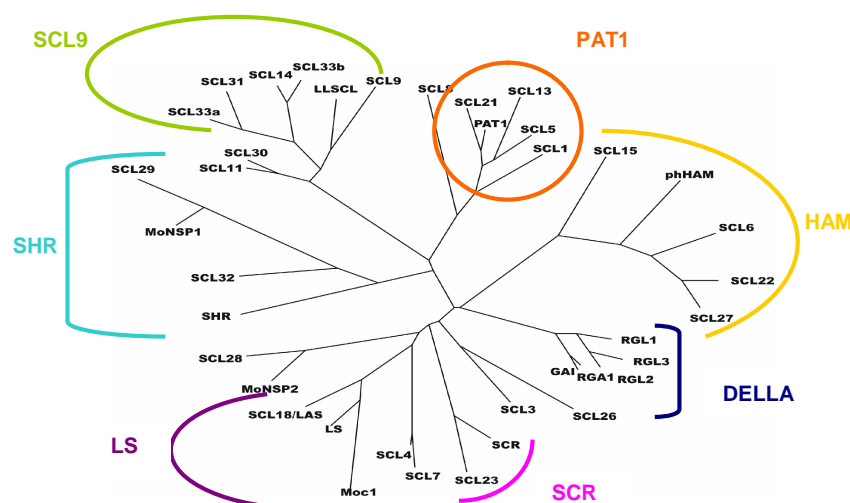


Figure 14. Members of the PAT1 branch of the GRAS protein family. Neighbour-joining tree of the GRAS protein family. All *Arabidopsis* GRAS proteins and known GRAS proteins from other plant organisms were aligned and the unrooted tree was generated with the PHYLIP program. All *Arabidopsis* proteins in the PAT1 cluster are indicated.

4.1.2. Alignment of the *Arabidopsis* PAT1 branch of the GRAS protein family

The conserved signature motifs described for GRAS proteins are present in all members of the PAT1 branch (Fig. 15). The C-terminal part of the GRAS proteins is highly conserved but their N-termini vary in sequence. The conserved C-terminal part of the proteins contains the signature motifs defined for GRAS proteins, namely two leucine-rich (LR) domains flanking a conserved domain around the amino acid residues "V/I HIID". Furthermore, the motifs PFYRE, RVER, SAW and a putative tyrosine phosphorylation site [R]-X(2)-[E]-X(3)-Y (Patschinsky *et al.* 1982), are highly conserved. Besides these motifs, whose functional implications are still unknown, no other functional domains could be determined. On the other hand, all genes encoding proteins for the PAT1 branch show a similar genomic structure, as these genes contain an intron upstream of the ATG start codon in the 5'-untranslated region (5'-UTR) (see Fig.16). The possible role of this intron for gene expression was analyzed with the aid of promoter-GUS fusions (see Section 4.5.). Additionally, *PAT1* is the only gene of this sub-branch with an additional intron in the coding region.

An alignment of sequences was performed with the ClustalW program (DNASStar, MegAlign. 6.1). The alignment shows that SCL21, SCL13, SCL1 and SCL5 also shares several conserved amino acids with PAT1 in the N-terminal part of the protein, especially the motif "EAISSRD", but its N-terminus is much shorter than PAT1 (Fig. 15). SCL21 is the shortest protein of all five with 413 amino acid residues (At2g04890). *SCL13* encodes a predicted protein of 529 amino acid residues (At4g17230), with a more variable N-terminal and a conserved C-terminal domain compared to other members of this branch. The *PAT1* cDNA encodes a protein of 490 amino acid residues (At5g48150) whereas *SCL5* encodes a predicted protein of 496 amino acid residues (At1g50600) and *SCL1* a predicted protein of 593 amino acid residues (At1g21450).

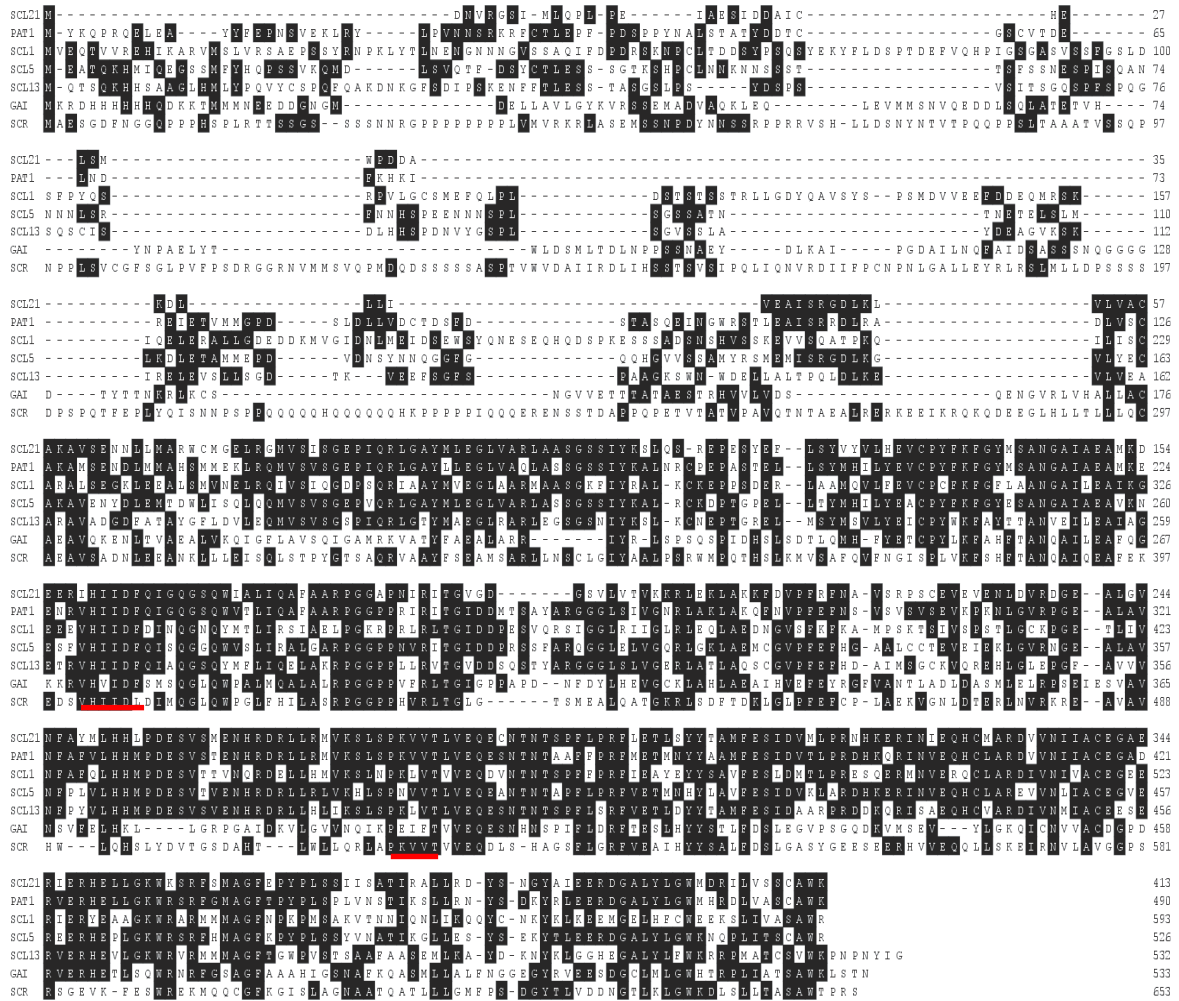


Figure 15. Alignment of the amino acid sequences of the proteins of the PAT1 branch with GAI and SCR as a more distant relatives. Conserved sequences are shaded. Gaps introduced to facilitate alignment of conserved residues are indicated as dashes in the sequence. Conserved motifs such as the VHIID domain, the putative phosphorylation site and the RVER motif are underlined in red.

4.2. Generation of transgenic *Arabidopsis* lines with defects in *SCL1*, *5*, *13*, *21* and *PAT1*

4.2.1. Identification of homozygous insertion lines

In order to evaluate the function of the different proteins of the PAT1 branch (PAT1, SCL21, SCL13, SCL1 and SCL5) *in vivo* and to determine, whether they contribute to the phyA-signalling pathway in a similar fashion as PAT1, we used reverse genetics to generate loss-of-function lines (Fig. 16). As the previously isolated *pat1-1* mutant was not a loss-of-function line, we isolated the *pat1-2* insertion line from the SALK collection (N568176), in which the open reading frame is disrupted at AA 37. For *SCL21* two insertion lines were identified: *sc/21-1* carries a T-DNA insertion 120 bp after the ATG start codon (SALK-collection 313_G09), whereas *sc/21-2* carries a T-DNA insertion 9 bp after the stop codon (SALK-collection N503630). As this second line

showed no differences in *SCL21* gene expression and was disregarded for the physiological analysis.

For *SCL1* three insertion lines were identified: *scl1-1* carries a T-DNA insertion 45 bp after the stop codon (SAIL-collection 760_F10), *scl1-2* a T-DNA insertion 840 bp in front of the ATG start codon (SAIL-collection 1296_B07) and the *scl1-3* insertion line from the SALK collection (N602071) a T-DNA insertion in the coding sequence, 1313 bp after the ATG. Lines *scl1-1* and *scl1-2* showed no differences in *SCL1* gene expression. As *scl1-3* was the only line with a disrupted the open reading frame, we continued the analysis with this line.

For *SCL5* only one insertion line from the SALK collection (N582550) was identified: *scl5-1*. It carries a T-DNA insertion in the open reading frame, 300 bp after the ATG start codon.

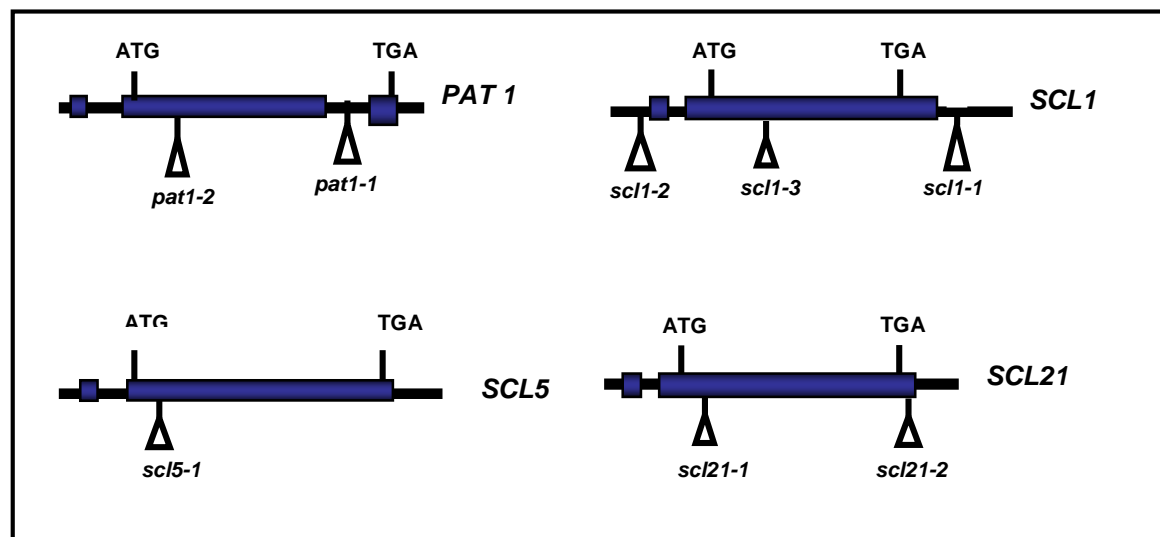


Figure 16. Genomic structure of the different genes of the PAT1 branch. The exon/intron structure and the T-DNA insertion sites are indicated. ATG and TGA depict the start and stop codons, respectively. Triangles indicate the position of the insertions in the different lines. Thick lines indicate transcribed regions.

To identify plants homozygous for the insertion, seeds from segregating populations of insertion lines were tested for their resistance marker. Lines from the SAIL-collection contained a resistance gene for Basta and were therefore grown on soil and sprayed with Basta (20 mg/ml) after 2 weeks, surviving plants were transferred into individual pots and grown to maturity on soil. In the other hand, lines from the SALK-collection contained a kanamycin resistance and therefore for selection they were sown on a Murashige and Skoog basal medium (MS) with 3% sucrose and kanamycin (50 µg/µl). After the vernalization for 3 days at 4°C, plates were transferred to white (W) light for 2 or 3 weeks until non-resistant plants bleached. Resistant plants were then transferred to soil and grown to maturity. Genomic DNA was extracted from adult resistant plants and PCR was used to identify homozygous lines for the insertion, utilizing primers flanking the insertion site and primers within the left border (LB) of the insertion and the respective gene (Tab. 6). Lines were regarded homozygous for the insertion when no PCR-product could be obtained with the primers flanking the insertion site, but when a

PCR-product could be obtained with a primer within the LB of the insertion and the gene specific primer. Furthermore, the position of the insertion was confirmed by sequence analysis.

Table 6. Primers used for the identification of the homozygous lines and the position of the T-DNA insertion for the different genes evaluated. n.d. = not determined.

Insertion line	Primers flanking insertion site	Fragment length (bp)	Primers within the LB and the gene	Fragment length (bp)
<i>scl21-1</i>	SCL21 Xho SCL21 Kpn	855	Salk LB SCL21 Intron-f	660
<i>scl21-2</i>	n.d.		Salk LB SCL21 1000	265
<i>scl1-1</i>	SCL1 1500 SCL1 1900	470	Salk LB SCL1 1110-f	1095
<i>scl1-2</i>	SCL1 Prom-f SCL1 ATG-rev	1380	Salk LB SCL 1-3	1335
<i>scl1-3</i>	SCL1 ATG-f SCL1 TGA-rev	1790	Salk LB SCL1 TGA-rev	900-950
<i>scl5-1</i>	SCL5 ATG-f SCL5 TGA-rev	1580	Salk LB SCL5 TGA-rev	300
<i>pat1-2</i>	PAT1 ATG-f PAT1 TGA-rev	1480	Salk LB PAT1 TGA-rev	n.d.

4.2.2. Generation of antisense and RNAi lines

To complement this analysis we generated several independent RNAi and antisense lines for *SCL21*, *PAT1* and *SCL13*, to decrease the endogenous gene expression and to determine a partial loss-of-function phenotype. For *SCL13* no insertion line could be identified, therefore we generated several antisense lines.

For the RNAi lines we chose partial cDNA sequences of *SCL21* and *PAT1* which were inserted into the Gateway-adapted binary expression vector pK7GWIWG2(I) (Karimi *et al.* 2002). By expressing the gene under the control of the 35S-*CaMV* promoter in a tail-to-tail manner separated by an intron, the resulting mRNA can form a stem-loop-structure which is recognized by the DICER complex (Brantl 2002, Voinnet 2002). By endonucleolytic cleavage the mRNA is reduced to short single stranded mRNAs which bind specifically to the endogenous mRNA and lead to its degradation.

The verification of the reduction of the RNA levels in all lines used for the following physiological experiments were confirmed with semiquantitative RT-PCR using primers which amplified part of the coding sequence, spanning the intron sequence. To be able to discriminate amplification of contaminating DNA, the 5'-forward primer was located 5' of the intron in the leader, which also prevented the amplification of the antisense construct. RT-PCR products were obtained with cDNA derived from wild-type seedlings, but not from RNA of insertion lines (Fig. 17). Independent RNAi and antisense lines showed a variety of different levels of reduction on the RNA level and lines, which had the strongest reduction (over 70%) such as *SCL21-RNAi-2*, were chosen for further experiments (Fig. 17). Taken together, these data demonstrate that the isolated lines are

disrupted in normal protein function. RNAi and antisense lines were further tested, whether the knock-down was also affecting similar genes. In no case interference was seen, not even between the most similar genes *PAT1* and *SCL21*.

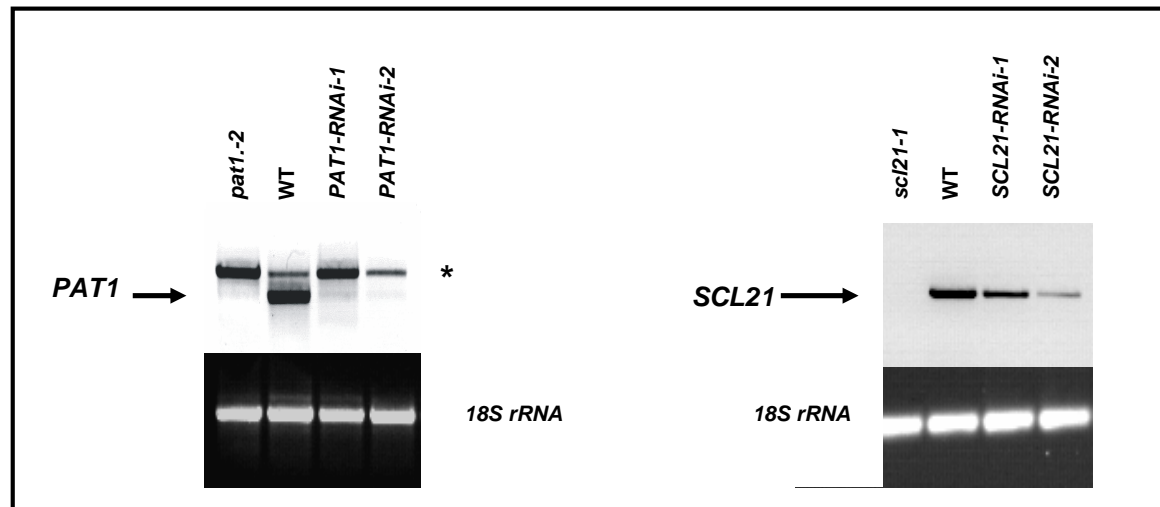


Figure 17. No expression of *SCL21* and *PAT1* was detected in the mutants by RT-PCR. RT-PCR analysis of RNA isolated from WT and *scl21-1*, *SCL21-RNAi* lines, *pat1-2* and *PAT1-RNAi* lines plants. RNA was reverse transcribed and subsequently amplified by PCR using *SCL21*- and *PAT1*-specific primers or *18S rRNA* specific-primers as a control. An asterisk (*) marks PCR-products derived from contamination with genomic DNA.

For antisense lines a portion of the *SCL13* cDNA was expressed in reverse orientation under the control of the *35S-CaMV* promoter. To analyse the reduction of the endogenous *SCL13* mRNA a RT-PCR was performed with total RNA extracted from WT and *SCL13* antisense lines. To avoid amplification of contaminating DNA the 5'-forward primer was located 5' of the intron in the *SCL13* leader, which also prevented the amplification of the antisense construct. Figure 18 indicates that the reduction of *SCL13* mRNA varied between 20 and 90%, but none of the transgenic lines showed a complete loss of expression. Both, seedlings under red light and adult plants showed a similar reduction of the mRNA levels. To verify that only the targeted mRNA was reduced and not other related *SCL* transcripts the Northern blots were re-hybridized with probes of the closest-related family members (*SCL1*, *SCL5* and *PAT1*). The expression levels of the other *SCL* genes were not affected (data not shown).

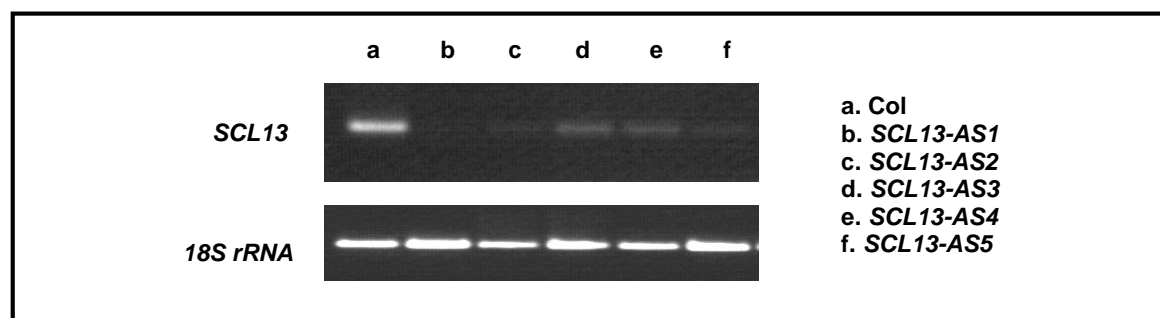


Figure 18. Transgenic *SCL13* antisense lines show a reduction in the endogenous *SCL13* mRNA. RT-PCR for *SCL13* expression levels was performed on total RNA from 4-day-old plants grown under continuous R light ($0.5 \mu\text{mol m}^{-2} \text{s}^{-1}$). The expression levels in five *SCL13* antisense lines are shown in comparison to Col-WT. Control PCR using primers amplifying the *18S rRNA* gene showed that equal amounts of reverse transcribed RNA were used.

4.3. Physiological characterization of SCL1, SCL5, SCL21 and PAT1

4.3.1. Hypocotyl elongation under different light conditions

The regulation of hypocotyl elongation by light during seedling de-etiolation is an example of the complex interplay among the photoreceptors. A frequently used assay to characterize *Arabidopsis thaliana* mutants involved in light signal transduction pathways is the growth of seedlings under different light conditions and subsequent measurement of hypocotyl elongation. As *phyA* is the major photoreceptor/effector for most far-red light responses, the elongation of the hypocotyl is inhibited by light and in case of FR light this is exclusively a *phyA*-mediated response. Thus, a *phyA* photoreceptor mutant (*phyA*) is completely blind to FR light, resulting in long hypocotyls under these conditions (Whitelam *et al.* 1993, Shinomura *et al.* 2000). To establish whether the loss of the *SCL1*, *SCL5*, *SCL21* and *PAT1* genes are specific for *phyA* signalling, we analyzed the lines under different light conditions, such as continuous red (R), far-red (FR) and blue (B) light and darkness (D). Briefly, seeds were surface-sterilized and sown on Petri dishes containing Murashige and Skoog basal medium (MS), 0.8% (w/v) agar and no sucrose. Plates were stored at 4°C for 4 days for vernalization and germination was induced by 2 h of W light followed by 22 h of D at 21°C. After this treatment plates were transferred into the appropriate light conditions for 4 days. Hypocotyl lengths of at least three independent experiments were measured using the NIH Image Software (ImageJ, National Institutes of Health, Bethesda, MO) and the data were statistically analyzed.

In all lines, in which *PAT1*, *SCL21*, *SCL5* and *SCL1* gene expression is reduced or abolished a reduced inhibition of hypocotyl compared to WT was detected (Fig. 19). This was also true for antisense lines of *SCL21* and *PAT1* (data not shown). Under R and B light the seedlings are similar to WT ($P > 0.05$), suggesting that this is indeed a FR light specific phenotype. When grown under D the lines were indistinguishable from WT, indicating that the effects of the mutations are light-dependent. The effect under FR light was not as strong as in the *phyA* mutant. But the fact that all differently generated lines, insertion, antisense and RNAi lines, exhibit a similar and statistically significant difference to the WT ($P < 0.05$) makes us confident that *SCL1*, *SCL5*, *SCL21* and *PAT1* are involved in *phyA*-dependent signalling responses. As these loss-of-function lines show a decreased responsiveness to FR light, all proteins should act as positive regulators.

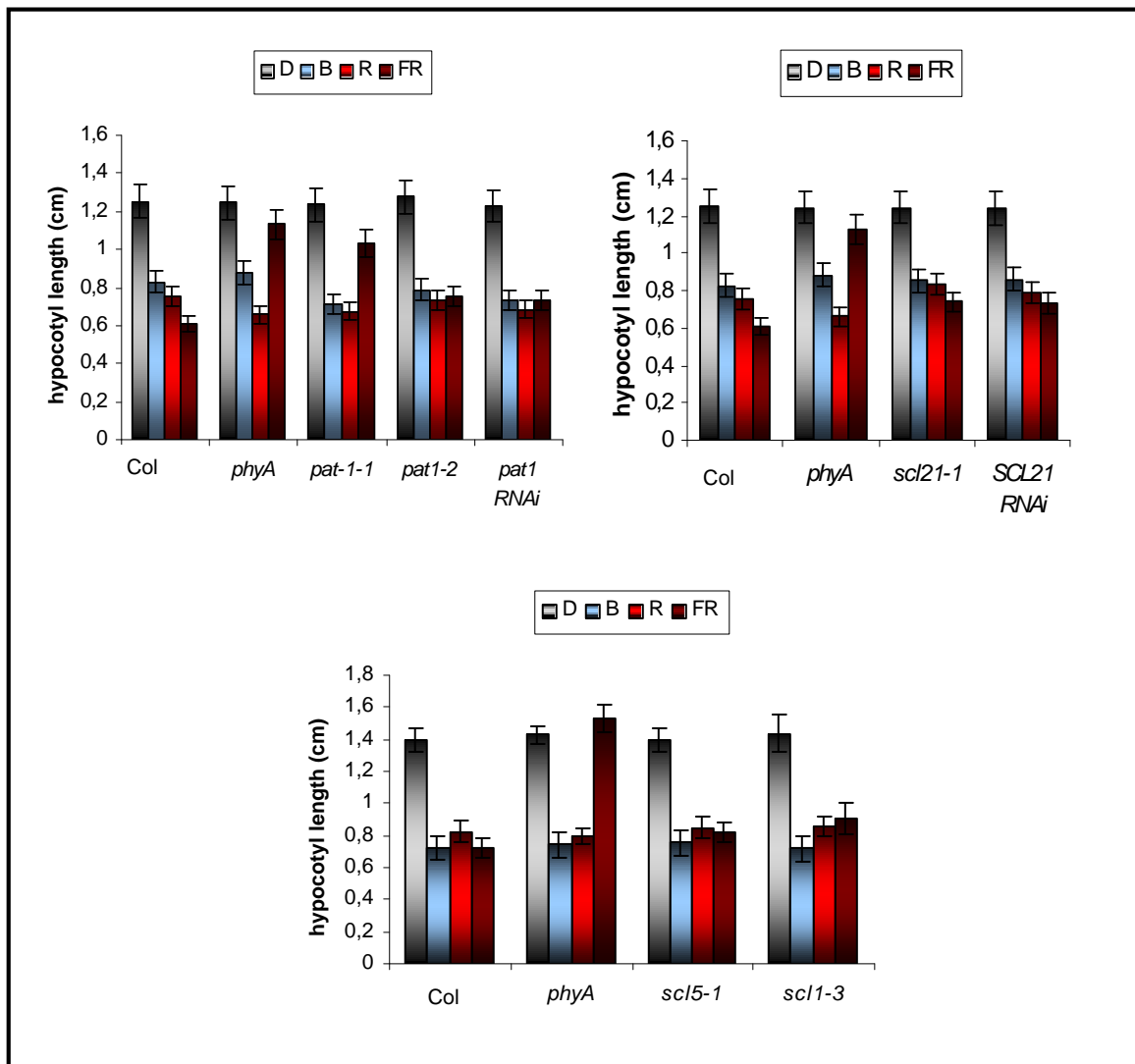


Figure 19. Physiological analysis of the *PAT1*, *SCL21*, *SCL5* and *SCL1* loss-of-function lines under different light conditions. Hypocotyl length of 4-day-old seedlings grown in darkness (D), or under continuous far-red (FR; $0.5 \mu\text{mol m}^{-2} \text{s}^{-1}$), red (R; $1 \mu\text{mol m}^{-2} \text{s}^{-1}$) and blue (B; $8 \mu\text{mol m}^{-2} \text{s}^{-1}$) light. Errors bars indicate standard deviation.

4.3.2. Response to different FR light fluences

As the inhibition of hypocotyl elongation is fluence rate response dependent (Kendrick and Kronenberg 1994), the hypocotyl length of the different lines were analyzed under different intensities of FR light to quantitatively characterize the sensitivity toward FR light. The hypocotyl elongation of the different lines was measured and statistically analyzed (Fig. 20). In a *phyA* mutant the hypocotyl elongation is not inhibited even with higher fluences, whereas the hypocotyl length of wild-type seedlings is drastically reduced. The *scl21*, *pat1*, *scl5* and *scl1* loss-of-function lines have a slight, but statistically significant longer hypocotyl than WT ($P < 0.05$). The loss of inhibition of hypocotyl elongation was stronger at lower fluences but still evident under higher fluences.

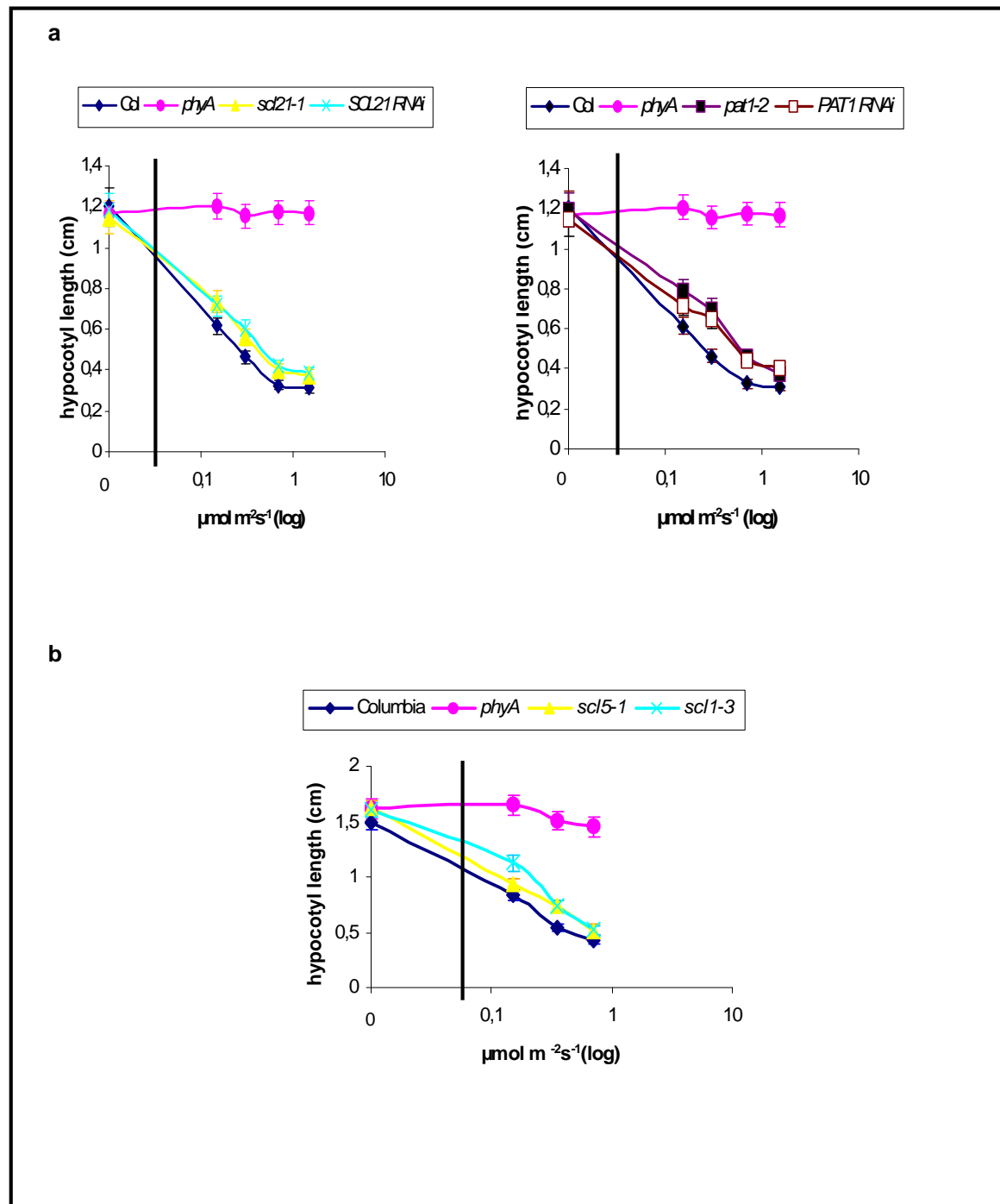


Figure 20. (a) Fluence rate response curve for hypocotyl elongation under FR light of WT (Col), *phyA*, *scl21-1*, *pat1-2* and representative *SCL21* and *PAT1-RNAi* lines. **(b)** Fluence rate response curve for hypocotyl elongation under far-red light of WT (Col), *phyA*, *scl5-1* and *scl1-3* lines. Error bars indicate standard deviation.

4.3.3. Hook opening and cotyledon unfolding

After seed germination, *Arabidopsis* seedlings follow one of two developmental patterns. In D, seedlings follow skotomorphogenic or etiolated development leading to long hypocotyls and closed, unexpanded cotyledons protected by an apical hook. In contrast, growth in the light results in photomorphogenic or de-etiolated development characterized by short hypocotyls and

open, expanded cotyledons that are capable of photosynthesis. The regulation of de-etiolation involves a complex interplay of all photoreceptors (Wang and Deng 2003, Chen *et al.* 2004).

FR-dependent apical hook opening, cotyledon unfolding and expansion were also examined in this study for the different loss-of-function and RNAi lines. FR light is sufficient to trigger this response in wild-type seedlings. As can be seen in the Fig. 21, in contrast to *phyA*, all lines were able to unfold the cotyledons and expand them. This shows that the effect of these proteins is stronger on hypocotyl elongation than on cotyledon development.

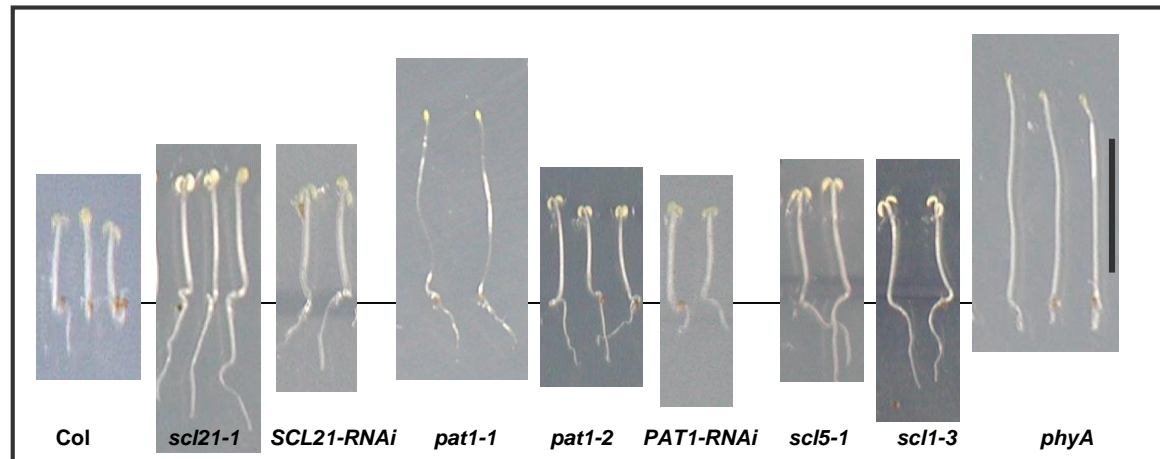


Figure 21. Phenotype of *scl21-1*, *SCL21-RNAi*, *pat1-1*, *pat1-2*, *PAT1-RNAi*, *scl5-1* and *scl1-3* after 4 days of FR light. Seedlings grown on MS medium, without sucrose and 0.8% (w/v) agar plates under FR light ($0.7 \mu\text{mol m}^{-2} \text{s}^{-1}$) for 4 days. Loss-of-function and RNAi lines are compared to WT (Col) and *phyA*. Bar at right is 1.0 cm.

4.4. Physiological characterization of *SCL13* antisense lines

4.4.1. Inhibition of hypocotyl elongation under R light conditions is specifically impaired in *SCL13* antisense lines

The regulation of hypocotyl elongation by light during seedling de-etiolation is an example of the complex interplay among the photoreceptors. In W or R light, *phyB* plays a major role, but even *phyB* null mutants do not have a hypocotyl as long as that of dark-grown plants. A high-resolution kinetic analysis of the growth of *Arabidopsis* seedlings has uncovered that the R light inhibition of hypocotyl elongation is controlled by a sequential and coordinated action of *phyA* and *phyB*. *phyA* contributes to the initial hypocotyl growth inhibition (first 3 h of irradiation), while *phyB* functions in the later phase (Parks and Spalding 1999).

Two independent antisense lines, *SCL13-AS1* and *SCL13-AS2*, which showed the strongest reduction in *SCL13* expression (Fig. 18), were used for physiological analysis. The hypocotyl elongation of transgenic *SCL13* antisense lines was analyzed under all major light regimes. In contrast to the other lines defective in proteins of the PAT1 branch, we found a reduced inhibition of hypocotyl elongation when transgenic seedlings were grown under continuous R light for

4 days compared to WT and not under FR light. These differences were statistically significant for both lines ($P < 0.01$). This result suggests the involvement of SCL13 in the phytochrome B, C, D or E signalling pathways. In addition, a marginally elongated hypocotyl could be observed under FR light conditions, which proved not to be statistically significant at the 95% confidence level. When grown under B or W light seedlings of the antisense lines were indistinguishable from WT, indicating that SCL13 is specific for R light signalling and not a general regulator of light responsiveness. The antisense lines also had normal growth responses in D establishing that the phenotype is light-dependent (Fig. 22).

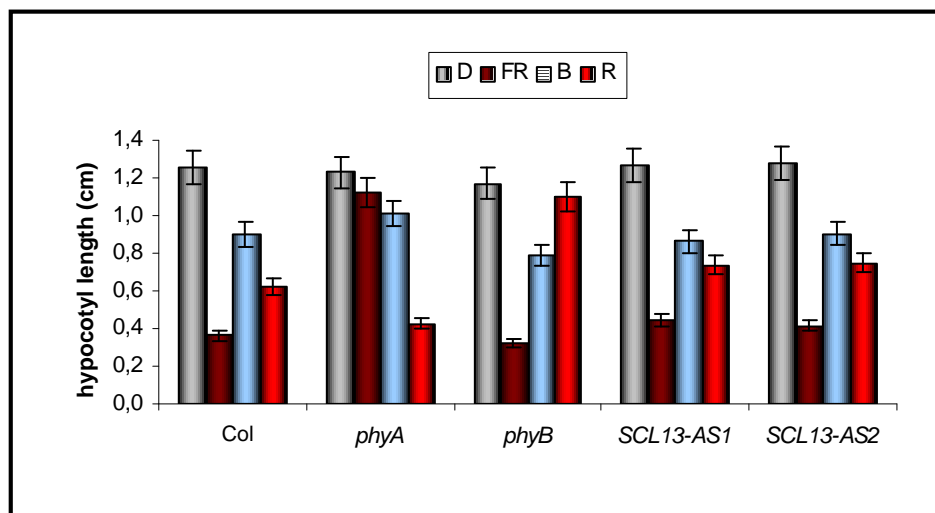


Figure 22. Hypocotyl length of 4-day-old seedlings grown in darkness (D), or under continuous far-red (FR; $0.5 \mu\text{mol m}^{-2} \text{s}^{-1}$), red (R; $1 \mu\text{mol m}^{-2} \text{s}^{-1}$) and blue (B; $5 \mu\text{mol m}^{-2} \text{s}^{-1}$) light. Error bars indicate standard deviation.

4.4.2. Response to different R light fluences

Fluence rate response curves with different intensities of R light were used to quantitatively characterize the sensitivity towards R light. The hypocotyl length of the different lines were analyzed under different fluences of R light and measured from at least three independent experiments using the NIH Image Software and the data were statistically analyzed (T-test). The results confirmed that *SCL13* antisense lines are taller than wild-type seedlings at all R light fluence rates tested, therefore showing reduced sensitivity to R light, but not as strongly as in a *phyB* mutant (Fig. 23). The hypocotyl length of the *SCL13-AS3* line, which exhibits a higher residual accumulation for *SCL13* mRNA as *SCL13-AS1* and 2 (Fig. 23), is more sensitive to R light under higher fluence rates. Therefore, we were able to correlate the reduction of *SCL13* mRNA with the severity of the phenotype. These findings indicate that SCL13 plays a role in seedling de-etiolation processes under prolonged R light.

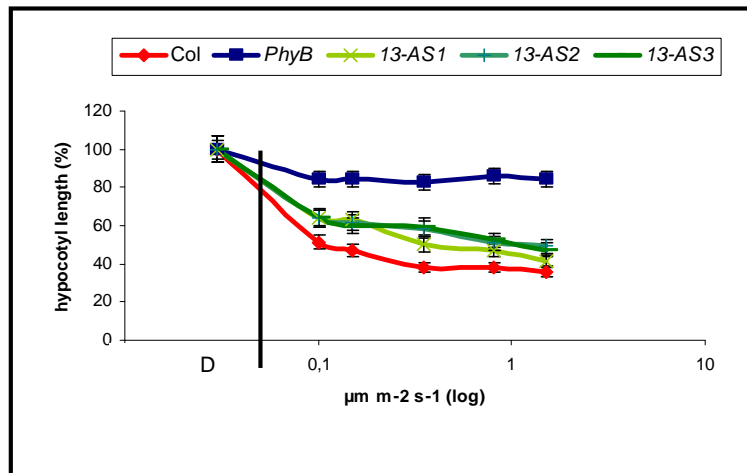


Figure 23. Fluence rate response curve for hypocotyl elongation under R light of WT(Col), *phyB* null mutant and *SCL13-AS1*, 2 and 3. Hypocotyl length in D was considered 100%. Error bars indicate standard deviation.

4.5. Expression pattern of all genes of the PAT1 branch

4.5.1. Role of the Intron in the 5'-UTR

All genes encoding proteins for the PAT1 branch contain an intron upstream of the ATG in the 5'-untranslated region (5'-UTR). As the 5'-UTR of the *SCL13* transcript includes a 750 nt-long intron we wanted to investigate a possible role of this intron for expression. For *SCL13 promoter-GUS* fusions, two DNA fragments containing the 5' upstream sequences were used. The 5'-end of both fragments was located at 2,514 bp upstream of ATG start codon. One fragment had its 3'-end located at the beginning of the 5'-UTR, 882 bp upstream of the ATG start codon leading to the promoter fragment lacking the 5'-UTR and intron therein, whereas the 3' end of the other fragment was located 117 bp downstream of the ATG generating the *SCL13 promoter-5'-UTR* construct. The 5'-end of the third construct, which contained only the 5'-UTR with the intron sequence began at the predicted transcription start site, 908 bp upstream of the ATG and the 3'-end was located 117 bp downstream of the ATG.

The 5'-UTR including the intron on its own was not able to induce any GUS activity, suggesting that no alternative transcription start sites are available within this region. The promoter construct that lacked the 5'-UTR and the intron generated the same spatial distribution of *GUS* expression, as the *SCL13 promoter-5'-UTR* construct although at a weaker level. This indicates that enhancing elements could be located within the 5'-UTR or the intron. The following panel (Fig. 24a) shows the expression of a *SCL13 promoter-5'-UTR-GUS* fusion in transgenic lines. This expression showed that younger leaves exhibited stronger GUS staining compared to adult leaves. GUS activity was strongest in cotyledons and roots.

When seedlings carrying the *SCL13 promoter-5'-UTR-GUS* construct were grown under different light qualities the overall GUS activity did not change, but its distribution varied. No GUS activity

was detected in the hypocotyl under W light conditions, but when seedlings were grown under D or R light some GUS staining in the hypocotyl and in the roots can be detected (Fig. 24b).

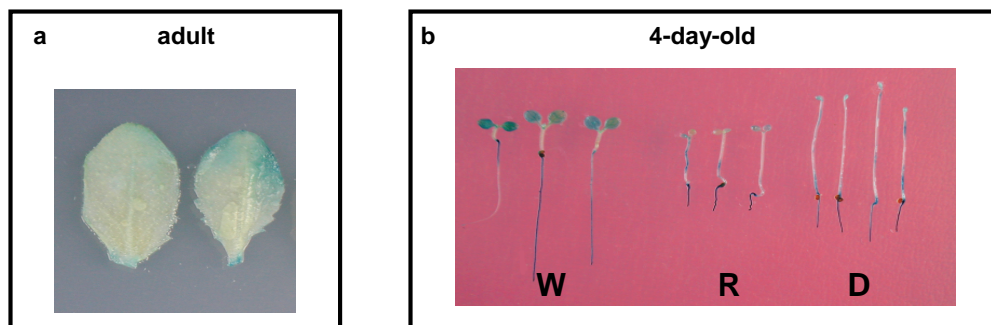


Figure 24. Expression analysis of *SCL13*. (a) GUS activity in *Arabidopsis* transformed with a *SCL13 promoter-5'-UTR-GUS* construct observed in leaves of 20-day-old plants grown under greenhouse conditions. (b) GUS activity in *Arabidopsis* transformed with a *SCL13 promoter-5'-UTR-GUS* construct observed in 4-day-old seedlings under continuous white (W), red (R) light or darkness (D).

4.5.2. Analysis of the *SCL1*, *SCL21* and *SCL13* promoter activities with the β -glucuronidase (*GUS*) reporter gene

To examine the expression pattern at the cellular level, histochemical staining using β -glucuronidase (*GUS*) can be used. The promoter fragments of the genes of interest were fused in front of the *GUS* reporter gene and plants (*Col*) were transformed with these constructs. A 1,385 bp long fragment upstream of the ATG start codon was used for *SCL1* and a 1,946 bp long for *SCL21*. These constructs were cloned into the Gateway-adapted binary vector pKGWFS7 (Karimi *et al.* 2002). Wild-type plants were transformed with these constructs and at least 10 independent lines were obtained for each construct. Eight of them were examined at the F2 generation.

We performed *GUS* assays comparing the expression of the *SCL21 promoter-GUS* fusion construct in *Arabidopsis* (*Col*) between adult plants and 4-week-old *Arabidopsis* seedlings. After incubation in X-GLUC solution for 12 h, we observed *GUS* activity in adult plants as well as in 4-week-old seedlings although the *GUS* expression in adult plants was at a very weak level (data not shown). The strength of the staining in 4-week-old seedlings differed between the transformed plants but not the distribution. WT did not show any staining and was used as a control for these assays. *GUS* activity was strongest in the apical meristem and in the root apex (Fig. 25). The expression observed for *SCL21 promoter-GUS* fusion constructs confirms the data derived from microarray analysis, suggesting that the expression of *SCL21* is very weak in adult plants.

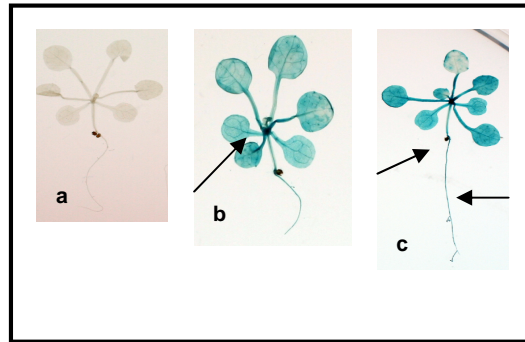


Figure 25. Expression of the *SCL21 promoter-GUS* construct in 4-week-old seedlings. (a) Col-WT as a control. (b, c) *in vivo* GUS staining in *Arabidopsis* transformed with *SCL21 promoter-GUS* construct observed in 4-week-old seedlings. Arrows indicate the strongest GUS activity.

We also compared the expression of a *SCL21 promoter-GUS* fusion construct in transformed *Arabidopsis* seedlings grown under different light conditions. The seedlings were grown in darkness (D) and then transferred for 6 h in far-red (FR 6h) or white light (WL 6h), or they were grown for 24 h in white light (WL 24h) (Fig. 26). After incubation in X-GLUC solution for 12 h, we observed GUS activity (cotyledons) in all seedlings tested, although the *GUS* expression in seedlings grown in FR or WL for 6 h and in those grown in WL for 24 h were weaker compared to the level in dark-grown seedlings. When the seedlings were grown in D, GUS activity was observed in the apical hooks and root apex similar to the results observed in 4-week-old seedlings (Fig. 25).

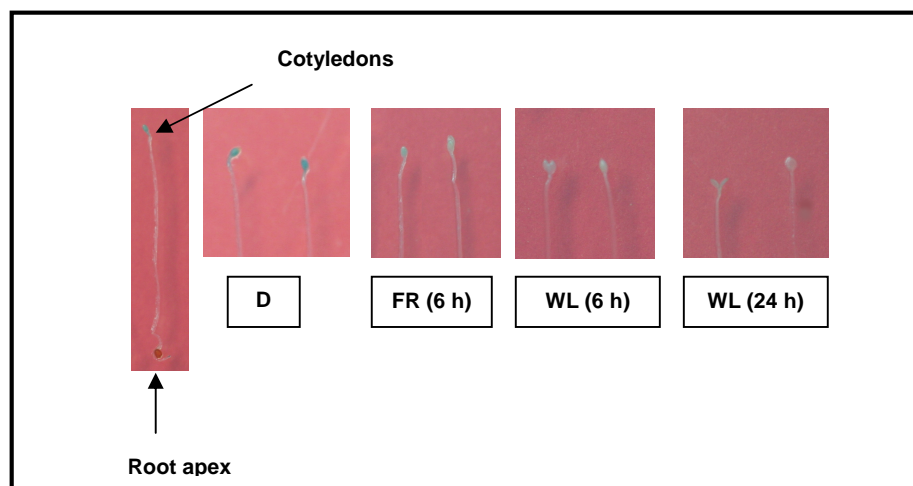


Figure 26. *In vivo* GUS staining in *Arabidopsis* transformed seedlings with *SCL21 promoter-GUS* construct. Seedlings were grown in dark (D), far-red 6h (FR 6h), white 6h (WL 6h) and white light 24h (WL 24h). Strongest GUS activity is indicated by arrows.

The *SCL1 promoter-GUS* fusion constructs showed blue staining in the leaves after incubation in X-GLUC solution for 12 h (Fig. 27). The strength of the staining differed between different transformed lines but not the distribution. The majority of the examined plants showed completely stained leaves and an intensive staining was observed in those parts of the leaf that had lesions

either from parasites or from cutting the tissue for the assay, suggesting that perhaps SCL1 is involved in wounding processes (Fig. 27).

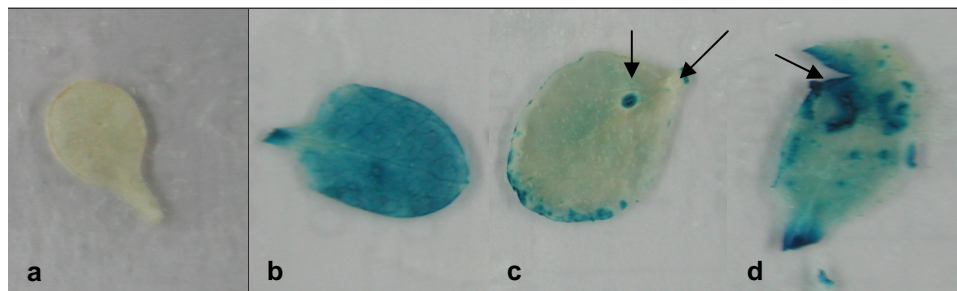


Figure 27. Expression of the *SCL1* promoter-*GUS* construct. (a) Leaf of untransformed plants as a control. **(b, c and d)** *In vivo* GUS staining in leaves. Arrows indicate lesions.

4.5.3. Expression pattern of all genes coding for proteins of the PAT1 branch

To test for the expression pattern of *SCL21* and *PAT1* in different tissues and conditions a digital Northern analysis was performed using data generated by microarrays, especially by AtGenExpress (Schmid *et al.* 2005). These data indicate that expression of *SCL21* is very weak, much weaker than *PAT1*, and barely detectable. Digital Northern analysis, where expression levels in different developmental stages and tissues were compared, revealed only detectable levels of *SCL21* in maturing seeds compared to seedlings and adult plants (Fig. 28). *SCL21* is induced especially beginning with seed stage 8, in which the embryo is in the walking stick stage. This suggests a role during germination and in the first days of a plant's life. *PAT1*, on the other hand, is expressed to a higher level in all tissues. In seedlings, it is detectable predominantly in the hypocotyl and in adult tissue mainly in the mature flower (in stamen and petals) and in the cauline and senescent leaves (Fig. 29).

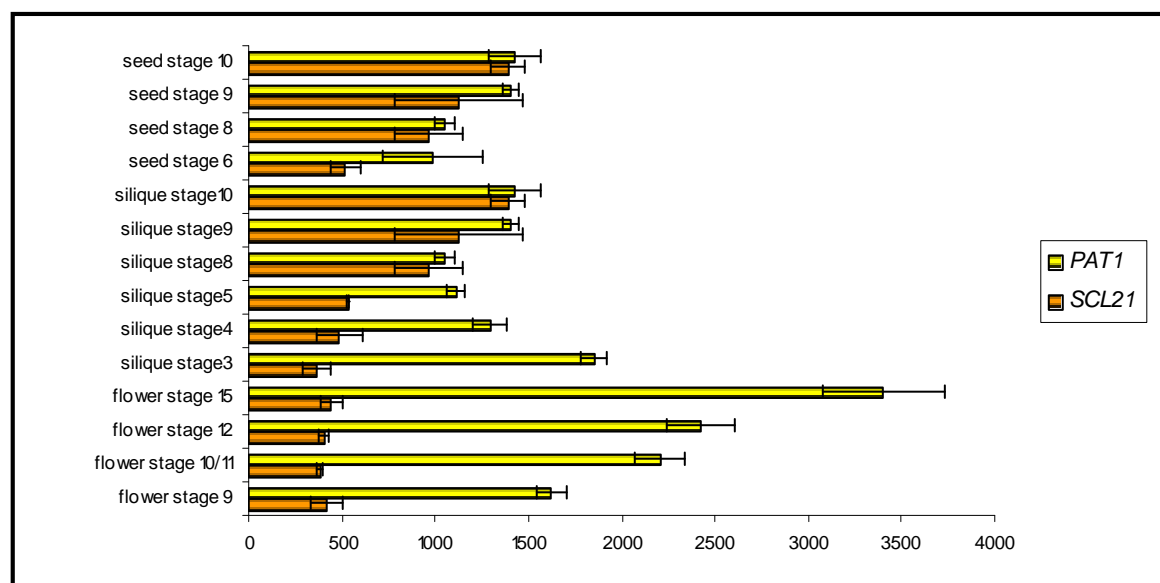


Figure 28. Expression levels of *SCL21* and *PAT1* in different tissues. Expression of *SCL21* and *PAT1* in different stages of flower, siliques and seed development. Developmental stages are described in Schmid *et al.* 2005. Data are derived from the AtGenExpress 22k microarray expression profiling experiments. Mean values of replicas were generated. Error bars indicate standard deviation between the replicas.

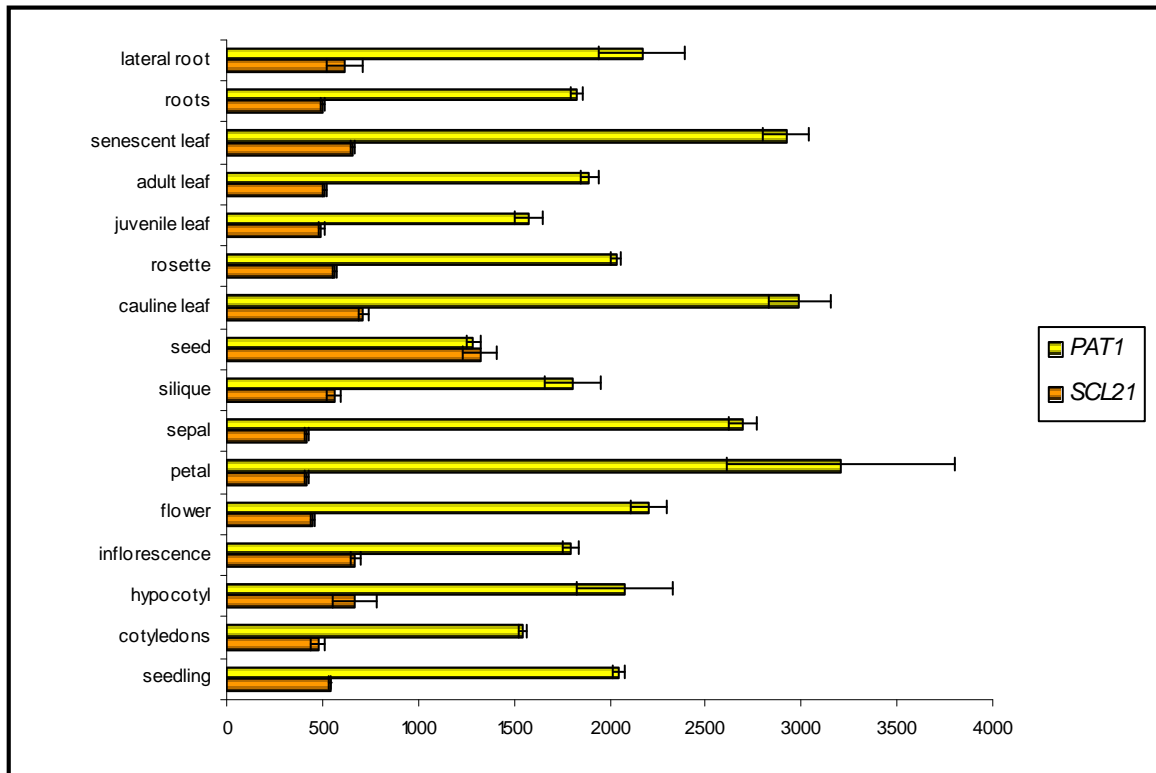


Figure 29. Expression levels of *SCL21* and *PAT1* in different tissues (Schmid *et al.* 2005). Data are derived from the AtGenExpress 22K microarray expression profiling experiments. Error bars indicate standard deviation.

Data derived from microarrays suggested that *SCL21*, in contrast to *PAT1*, is negatively regulated by light (Fig. 30, light treatments as described under http://arabidopsis.org/servlets/TairObject?type=expression_set&id=1007966126, data provided by Kretsch *et al.*, unpublished). All light conditions, B, R, W and FR had a similar down regulating effect on *SCL21* gene expression after 4 h, less so after 45 min. FR light reduces the *SCL21* gene expression but no difference in the *PAT1* gene expression level could be detected.

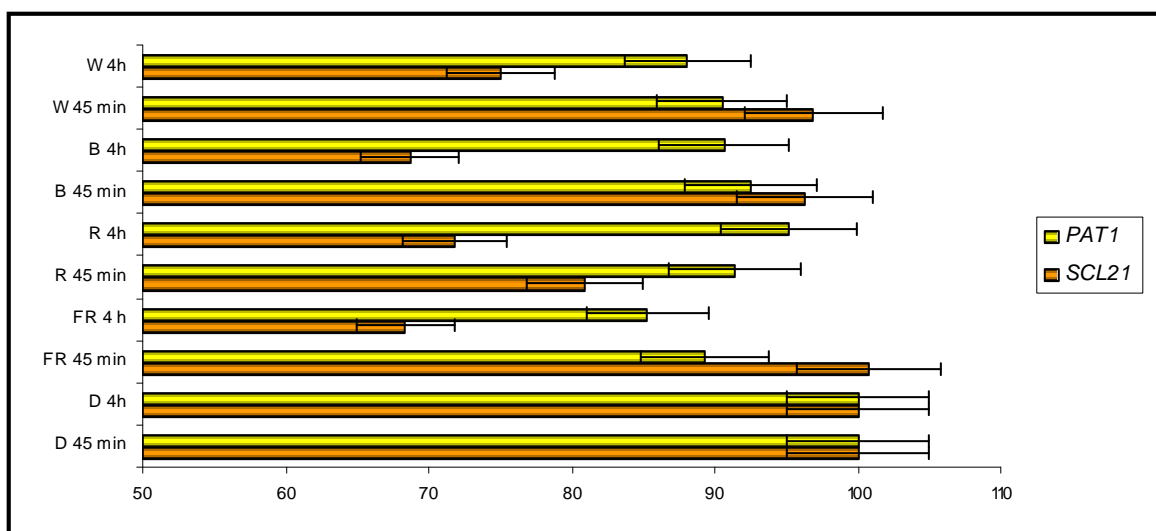


Figure 30. Expression of *SCL21* and *PAT1* after 45 min. and 4 h of continuous white (W), red (R), blue (B) and far-red (FR) light compared to the expression in dark (D). For better comparison the D value was set at 100%. Error bars indicate standard deviation.

For *SCL1* and *SCL5* we also performed a digital Northern to answer the question how strongly these two genes are expressed in different organs and tissues. These data indicate that the expression of *SCL1* and *SCL5* are very similar in adult plants. Analyses, which compared the expression levels in different developmental stages and tissues, revealed different levels of *SCL1* and *SCL5* in maturing seeds. Both genes are induced in seed stage 6, the torpedo stage, although the expression level of *SCL1* is weaker than *SCL5* (Fig. 31). In seedlings, the expression of *SCL1* and *SCL5* is detectable predominantly in the hypocotyl and in the cotyledons. In adult tissues, the expression of *SCL1* is detectable mainly in the mature flower (sepal), in the adult leaf (senescent leaf) and in the roots (lateral roots). On the other hand, the expression of *SCL5* in adult tissues is mainly detectable in the mature flower (petal), in the adult leaf (cauline and senescent leaves) and in the roots (Fig. 32).

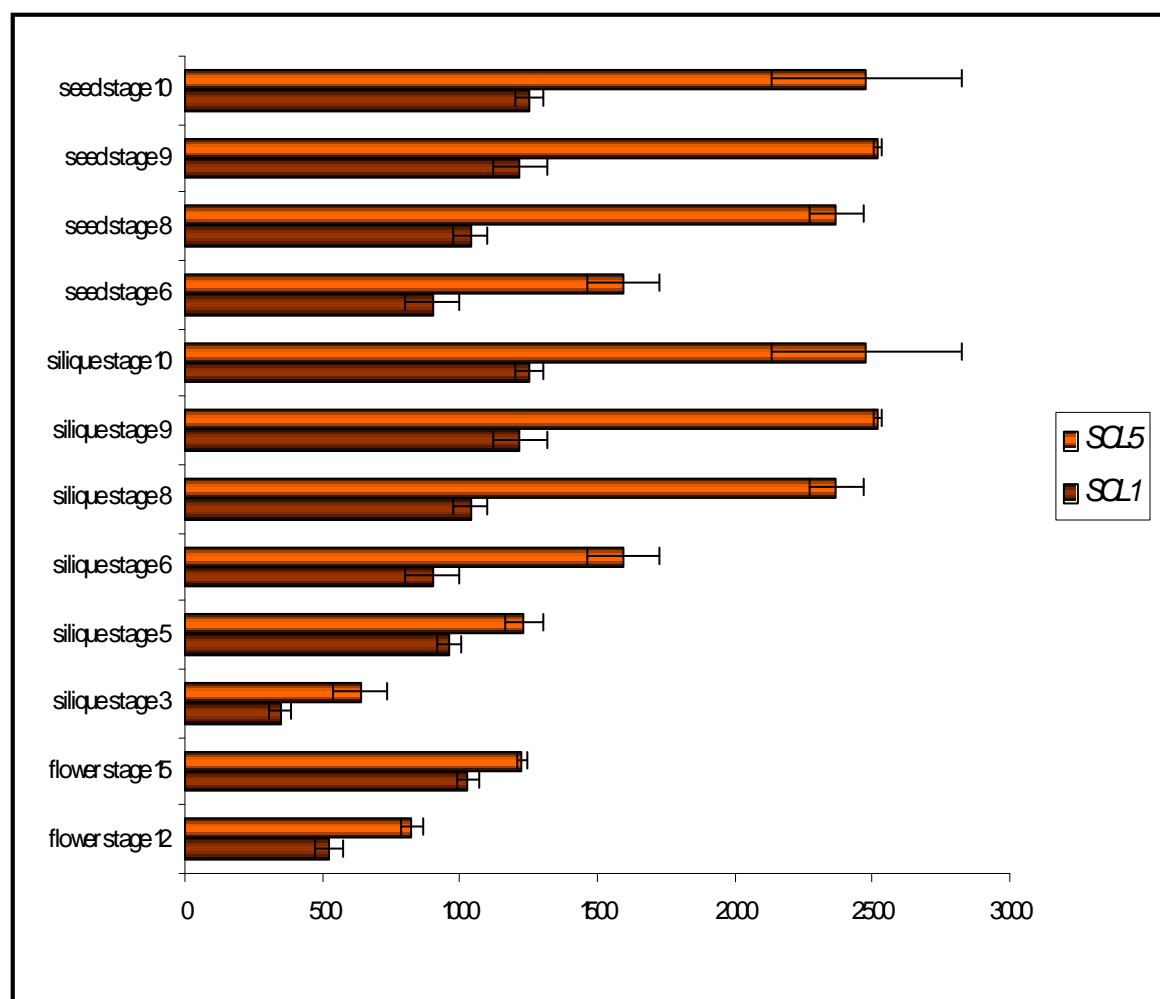


Figure 31. Expression levels of *SCL1* and *SCL5* in different tissues. Expression of *SCL1* and *SCL5* in different stages of flower, siliques and during seed development. Developmental stages are described in Schmid *et al.* 2005. Data are derived from the AtGenExpress 22K microarray expression profiling experiments. Mean values of replicas were generated. Error bars indicate standard deviation between the replicas.

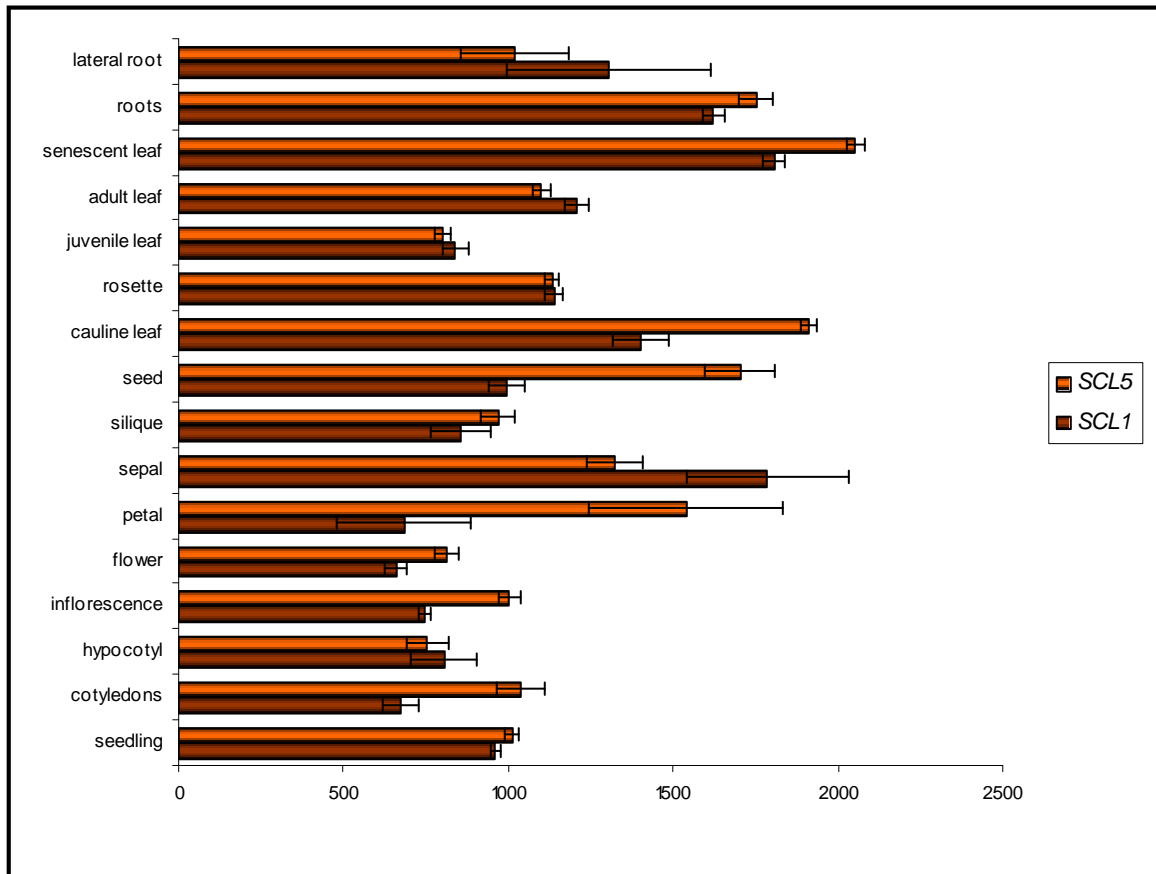


Figure 32. Expression levels of *SCL1* and *SCL5* in different adult tissues (Schmid *et al.* 2005). Data are derived from the AtGenExpress 22K microarray expression profiling experiments. Error bars indicate standard deviation.

Evaluation of microarray data detected no changes in *SCL1* and *SCL5* expression under different light conditions compared to D suggesting that *SCL1* and *SCL5* are not induced or repressed under R or FR light (Fig. 33).

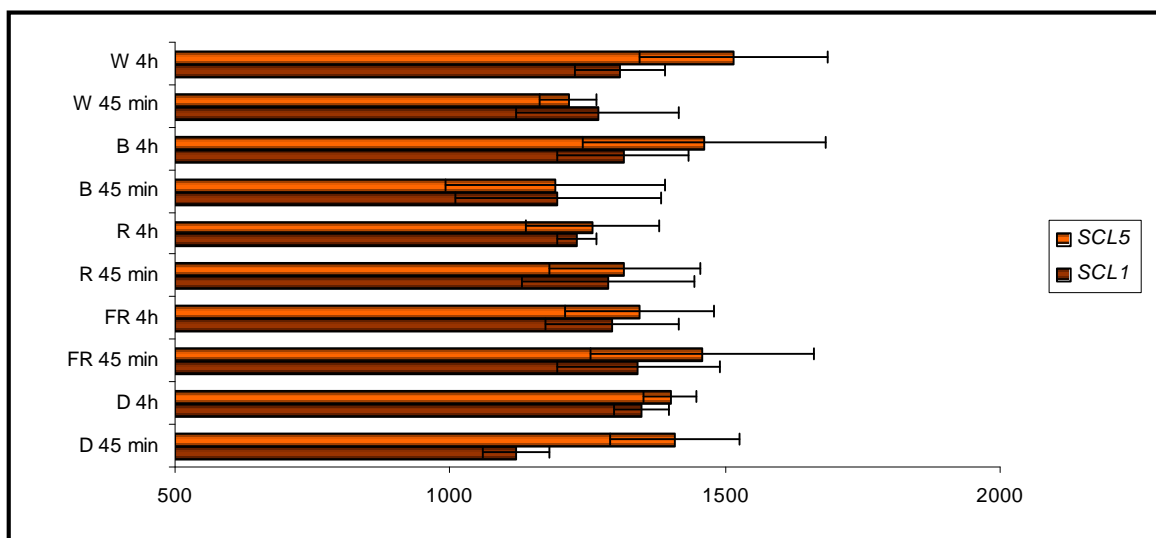


Figure 33. Expression of *SCL1* and *SCL5* after 45 min. or 4 h of continuous white (W), red (R), blue (B) and far-red (FR) light. Error bars indicate standard deviation.

As we could show that *SCL13* is involved in R light signal transduction we were interested whether this is also reflected in the expression pattern. In 7d-old seedlings *SCL13* expression is highest in the green tissues (cotyledons and young leaves), whereas in the shoot apex and hypocotyl less expression can be detected. Additionally, *SCL13* is also expressed in roots (Fig. 34). In adult plants, 21-day-old or older, high *SCL13* transcript levels can be observed in leaves, with higher levels in younger rosette leaves. Within a leaf, the distal region shows higher *SCL13* mRNA levels than the proximal region or the petiole (Fig. 35). In addition, expression is elevated in senescing leaves. As in young seedlings, less *SCL13* mRNA can be detected in shoots, stem and apical meristems even after transition to flowering. Furthermore, high *SCL13* mRNA levels can be observed in petals and sepals of flowers, which were tested at different developmental stages (Fig. 35). In later stages, such as siliques and seed formation, no elevated levels could be seen. This indicates that *SCL13* plays a role not only in the seedling stage but also throughout the lifetime of *Arabidopsis*. This notion is confirmed by our observation that the *SCL13* antisense lines flower earlier than WT (data not shown). The expression of a *SCL13 promoter-5'-UTR-GUS* fusion in transgenic lines confirmed the data derived from microarray analysis, as younger leaves showed stronger GUS staining compared to adult leaves (Fig. 24). As in the microarray, GUS activity was strongest in cotyledons and in roots. This also correlates with the function of *SCL13* in the signalling pathway of the light-stable phytochromes.

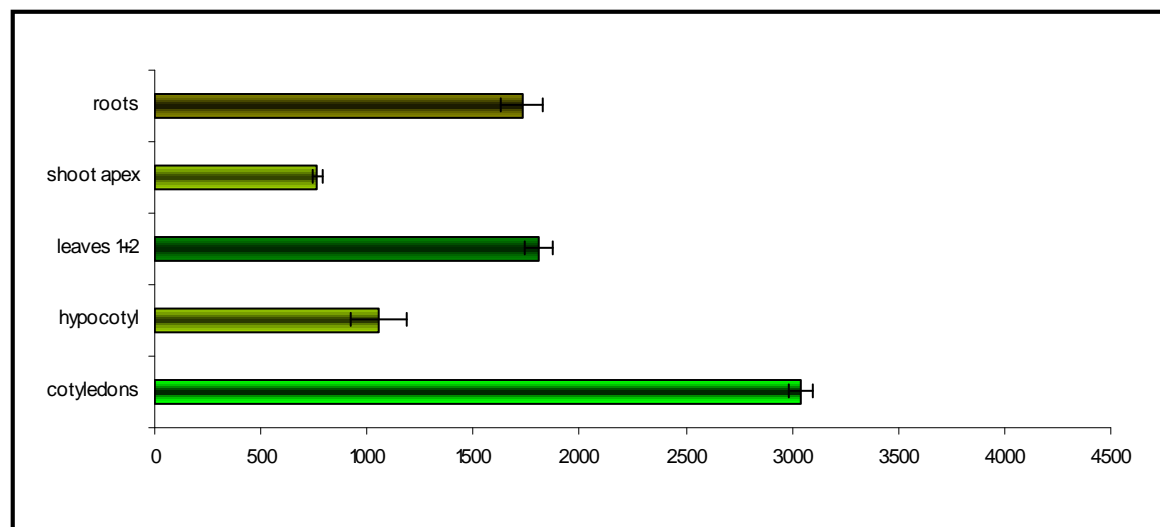


Figure 34. Expression profiling of *SCL13*. Expression of *SCL13* in different tissues of 7-day-old seedlings (Schmid *et al.* 2005). Data are derived from the AtGenExpress 24k microarray expression profiling experiments. Mean values of replicas were generated. Error bars indicate standard deviation.

Evaluation of microarray data and semiquantitative RT-PCR experiments detected no changes in *SCL13* expression under different light conditions compared to D suggesting that *SCL13* is not induced or repressed under R or FR light (Fig. 36). Only pulses of UV-B light induced *SCL13* expression, but this is probably due to a stress response since *SCL13* is also induced by some other stresses, such as osmotic or salt stress or after treatment with methyl jasmonate (data not shown).

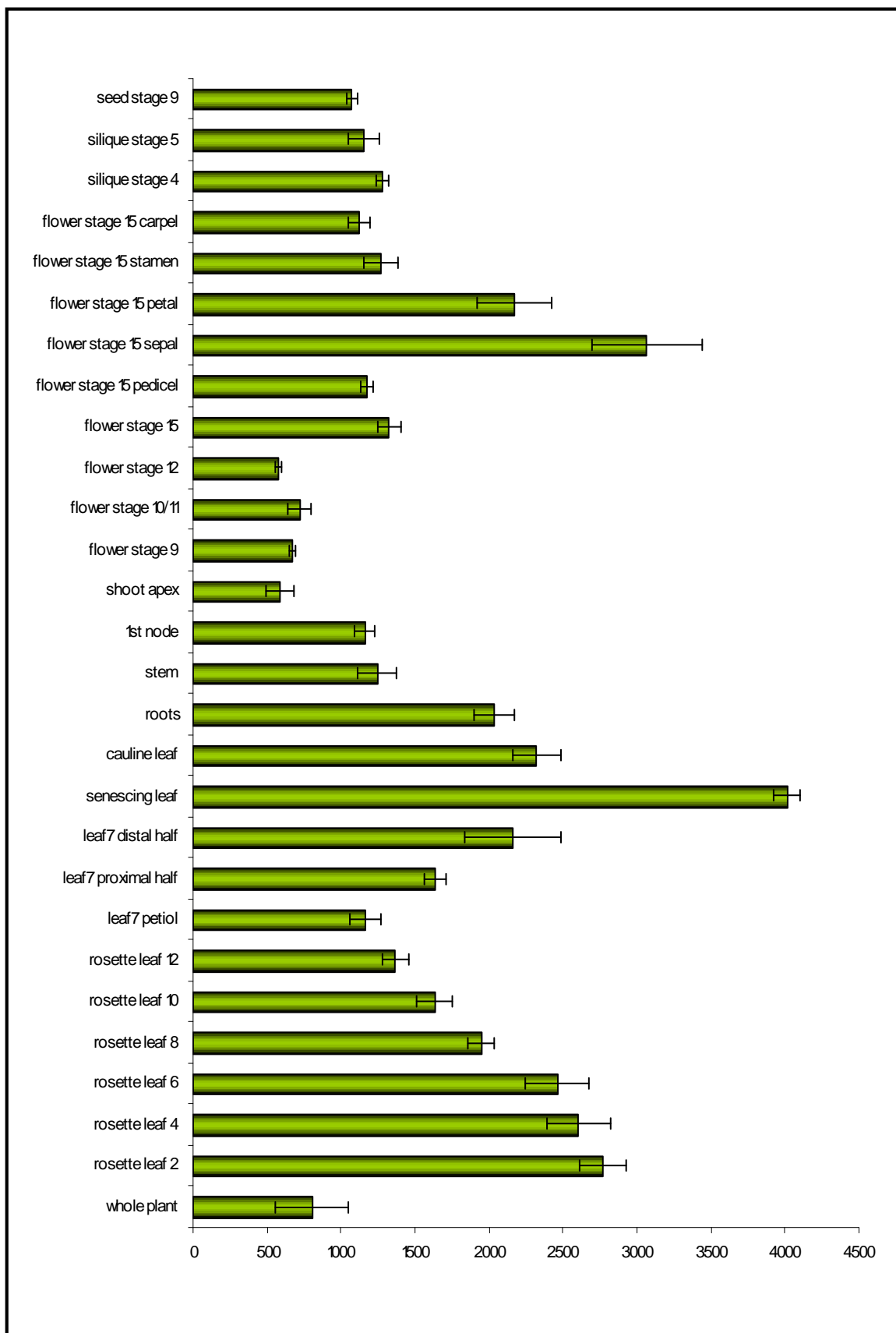


Figure 35. Expression of *SCL13* in different tissues of adult plants. Developmental stages are described in Schmid *et al.* 2005. Error bars indicate standard deviation.

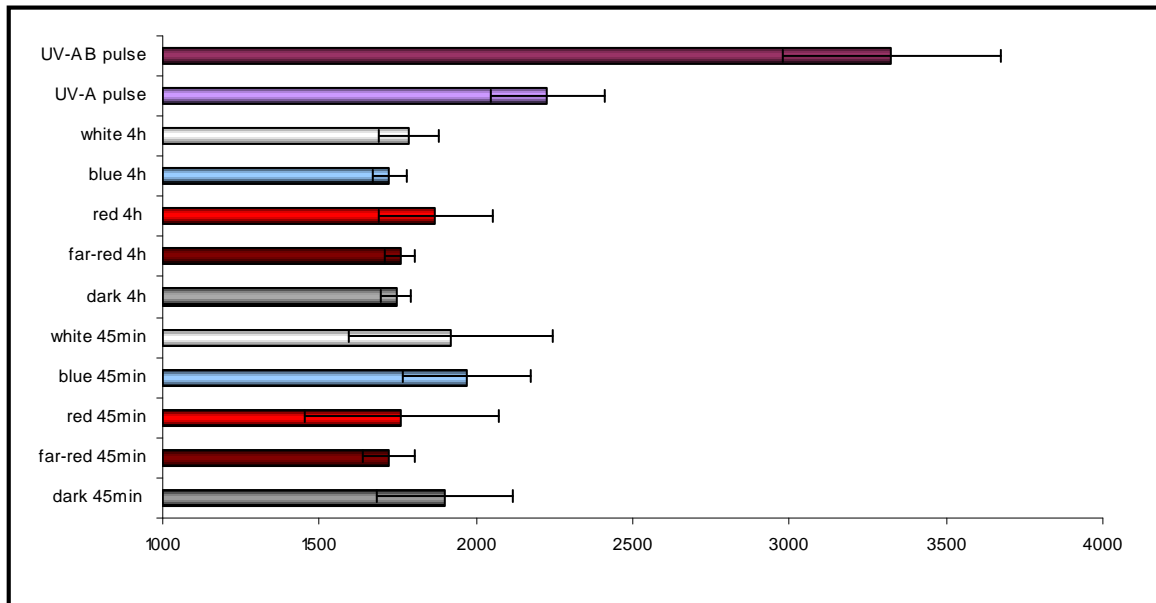


Figure 36. Expression of SCL13 after 45 min or 4 h of continuous W, R, B and FR light compared to the expression in dark and after a pulse of UV-AB or UV-A light in seedlings. Light treatments are described under http://arabidopsis.org/servlets/TairObject?type=expression_set&id=1007966126, data provided by Kretsch *et al.*, unpublished).

4.6. Analysis of the subcellular localization by expressing GFP fusions

4.6.1. Analysis of the subcellular localization by fluorescence microscopy

To investigate the subcellular localization of PAT1, SCL21, SCL13, SCL1 and SCL5 we fused the gene encoding the green fluorescent protein (GFP) to the 3'-terminus of the different GRAS genes. The fusion genes were placed under the control of a *35S-CaMV* promoter and the constructs transiently expressed in onion epidermal cells by particle bombardment. To visualize GFP fluorescence, cells were examined using an Axioskop microscope (Carl Zeiss, Jena, Germany).

As shown in Fig. 37, the resulting SCL21-GFP, SCL13-GFP, SCL1-GFP and SCL5-GFP proteins were localized throughout the cytoplasm and the nucleus, very similar to PAT1 and GFP. To verify the position of the nucleus we used the DAPI stain (data not shown). The distribution was not changed under different light conditions. These results indicate that the proteins could act in the cytoplasm or in the nucleus.

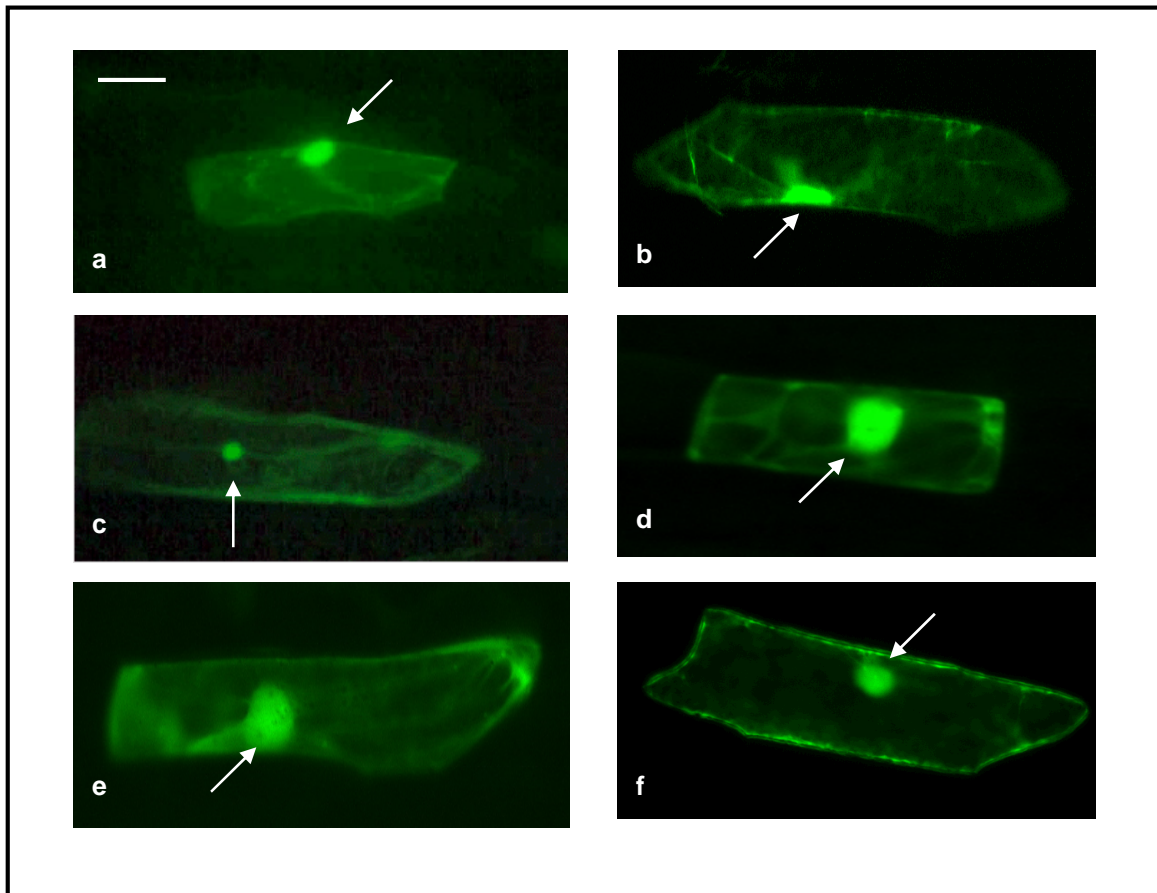


Figure 37. GFP fluorescence in transiently transformed onion epidermis cells. (a) PAT1-GFP fusion, (b) SCL21-GFP fusion, (c) SCL13-GFP fusion, (d) SCL1-GFP fusion (e) SCL5-GFP fusion and (f) GFP as a control. Arrows indicate the nucleus. Bar = 50 μ m.

For SCL21-GFP we noted that besides cells in which the fluorescence was distributed between nucleus and cytoplasm (Fig. 38a), about 30% of the cells expressing the constructs showed staining only in the cytoplasm (Fig. 38b). For this experiment the constructs were transiently expressed in leek epidermal cells transformed by particle bombardment.

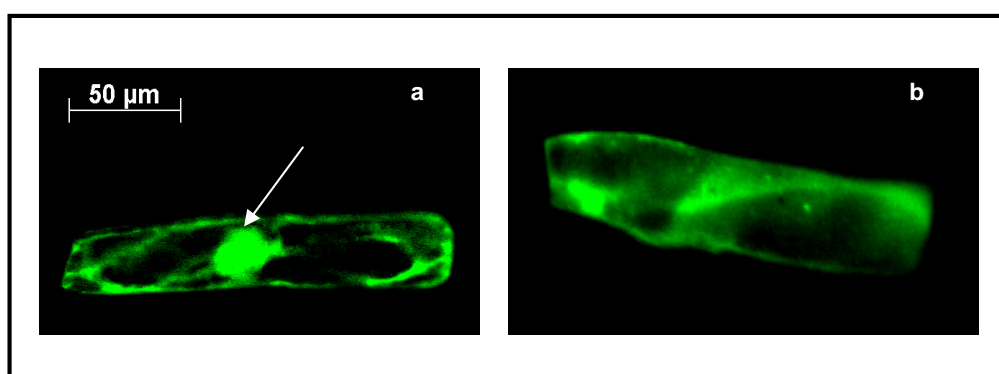


Figure 38. SCL21-GFP fluorescence in transiently transformed leek epidermis cells. (a) the SCL21-GFP fusion is visible in the nucleus and in the cytoplasm and (b) the SCL21-GFP fusion is visible only in the cytoplasm. Arrow indicate the nucleus.

4.7. Detailed physiological analysis of the function of SCL21 and PAT1 in Phytochrome A signalling

4.7.1. Block of greening after FR irradiation

One effect of phytochrome A on chlorophyll accumulation is known as the “far-red block of greening” (Barnes *et al.* 1996, Van Tuinen *et al.* 1996). When seedlings grown for several days under FR light are transferred to W light they fail to synthesize chlorophyll. Etiolated seedlings accumulate high levels of protochlorophyllide and the PORA protein mediates rapid conversion of protochlorophyllide into chlorophyll once the plant emerges into the light. Light, including FR light, downregulates *PORA* expression (Sperling *et al.* 1997). However, the activation of *pora* is a light-dependent step that is not activated by FR light, so that seedlings grown in FR light de-etiolate partially but stay yellowish. When such seedlings are transferred into W light they have little *pora* and cannot accumulate chlorophyll rapidly enough (Sperling *et al.* 1997). This effect is known as the “Far-red killing effect”. As the *phyA* mutant does not sense the FR light it responds like a dark grown seedling maintaining the ability to green in subsequent W light exposition.

The loss-of-function lines of *PAT1*, *SCL21* and the *PAT1* and *SCL21-RNAi* lines were tested to see whether they are more resistant than the WT to this “Far-red killing effect” (Fig. 39). For *pat1-1* it has been previously shown that this mutant can green after FR light in a similar way as the *phyA* mutant. Briefly, after seedlings were grown 4 days in FR light they were transferred to W light for 2 days and then chlorophyll accumulation was measured compared to seedlings grown 4 days in dark and 2 days in W light. A total of 25 seedlings were harvested for these measurements and the experiment was repeated three times. It was observed that, in contrast to *pat1-1*, the loss-of-function lines of *SCL21* and the *SCL21* and *PAT1-RNAi* lines display no or perhaps only a slightly decreased sensitivity to the phyA-dependent block of greening in W light after continuous FR light, very similar to the WT.

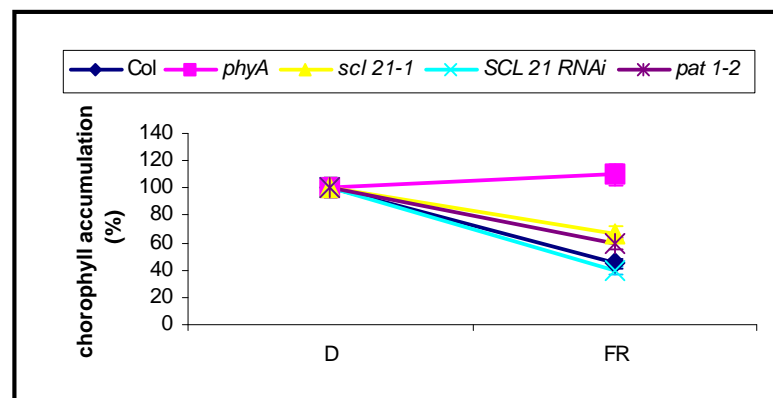


Figure 39. Chlorophyll accumulation in the mutants and RNAi lines. Chlorophyll content (mg/seedling) of seedlings grown 4 d in far-red (FR) and an additional 2 d in white light, compared to seedlings grown 4 d in dark (D) and 2 d in white light. The value of the chlorophyll level in the seedlings pre-grown in the D was set 100 % for better comparison.

4.7.2. Germination efficiency

The light-dependent germination of *Arabidopsis* seeds is mediated entirely by phytochrome (Casal and Yanovsky 1998). Previous reports indicated that phyA and phyB play key roles in regulating seed germination under different light conditions (Shinomura *et al.* 1994,1996, Botto *et al.* 1996, Poppe and Schäfer 1997). In *Arabidopsis*, R/FR reversible, Low Fluence Response (LFR) germination is largely mediated through phyB. Germination is also induced by low quantities of R or FR light, the so called “Very Low Fluence Response” (VLFR), or by continuous FR light, the “High Irradiance Response” (HIR), both mediated through phyA (Casal 2000, Schäfer and Nagy 2006). Mutants lacking this photoreceptor cannot germinate in FR light.

In this study we tested whether phytochromes regulate seed germination through PAT1 and SCL21. Irradiation with FR light for 10 min after 48 h of imbibition was used to determine the involvement of these proteins in this phyA-dependent response. Irradiation for 10 min with R light after 3 h of imbibition as well as W light and D controls were performed to obtain information, whether other light conditions also influence the germination processes. As a certain percentage of seeds is not capable of germination (“dead seeds”) and another percentage germinates even without stimulation by light pulse, the germination rate was corrected by these factors.

The Fig. 40 shows that all *sc121* lines as well as the *pat1* lines tested exhibit between a 30 and 15% reduction in the efficiency to germinate under FR light compared to WT. The capacity to germinate after a R light pulse three hours after imbibition, a well characterized phyB response, was not impaired (data not shown).

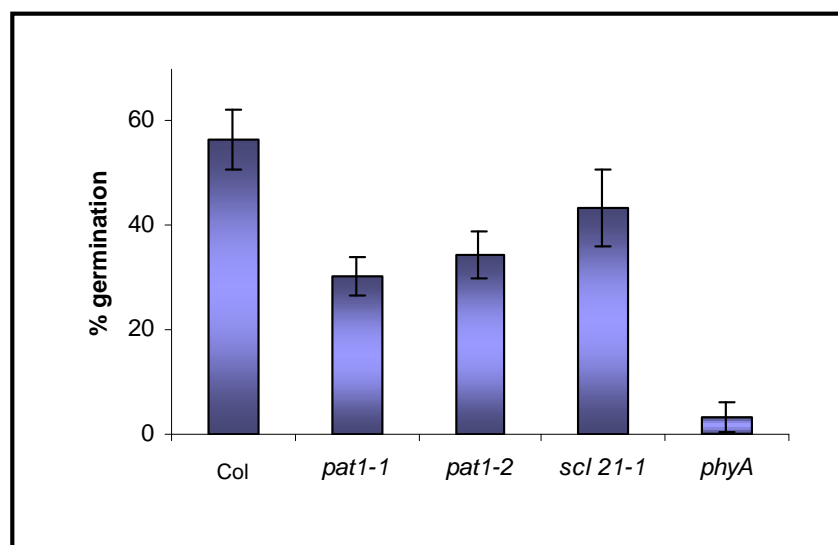


Figure 40. Germination assays of WT (Col), *pat1-1*, *pat1-2*, *scl21-1* and *phyA* mutants. Seeds were treated with a far-red light pulse directly after sterilization. Treated seeds were irradiated with a 10 min. FR light pulse ($1 \mu\text{mol m}^{-2} \text{s}^{-1}$) after 48 h of imbibition. Germination was assessed after 7 days in D.

The results obtained from germination assays suggests that VLFR, at least those important for germination, are only partially transduced via PAT1 and SCL21, indicating that these proteins are predominantly involved in HIR.

4.7.3. Expression of light regulated genes in *SCL21* and *PAT1*

To relate our analysis of gene expression in *SCL21* loss-of-function and in *PAT1-RNAi* lines to the phyA-signal transduction pathways, we have focused on the phyA-mediated induction of genes encoding the chlorophyll *a/b* binding protein (*CAB*), the chalcone synthase (*CHS*) and the xyloglucan endotransglycosylase-related protein (*XTR7*). *CAB* and *CHS* gene expression are reduced under FR light conditions in the phyA mutant and dependent on a functional phyA-signalling pathway under FR light conditions (Barnes *et al.* 1996). Both genes are regulated by cGMP- and calcium-dependent signal transduction pathways, respectively (Barnes *et al.* 1995, Bowler and Chua 1994, Millar *et al.* 1995). *XTR7*, which is involved in cell elongation, is negatively regulated by phyA in FR light (Kuno and Furuya 2000).

Pat1-1 has been shown to be essential for appropriate expression of this subset of phyA-regulated genes (Bolle *et al.* 2000). Total RNA was harvested from 4-day-old seedlings (WT, *phyA*, *scL21-1* and *PAT1-RNAi*) grown in darkness, without exposure to FR (D) or after 3 h (FR-3) or 6 h (FR-6) irradiation with FRc ($1\mu\text{mol m}^{-2} \text{s}^{-1}$). Duplicate samples for each treatment were prepared from seedlings grown under similar conditions. RNA was denatured through incubation with 30% glyoxal, electrophoretically separated in 1.2% agarose gels in MOPS buffer and transferred onto a Hybond-N nylon membrane in 20x SSC buffer. Each lane contained 5 μg of total RNA. RNA was fixed to the membrane by UV crosslinking and the membrane was immediately stained with Methylene Blue to visualize *rRNA* bands, used as a loading control, and documented using a digital camera (Fig. 41b). The same blot was probed successively for transcripts encoding *CAB*, *CHS* and *XTR7*.

Figure 41 indicates that there are no major differences in the expression patterns of WT and the mutant lines. After 3 h in far-red light (FR-3), the induction of *CAB* and *CHS* transcripts and the decrease in *XTR7* are similar between the WT and the mutant lines. However, after 3 h in far-red light (FR-3), no induction of *CAB*, *CHS* and no decrease of *XTR7* can be observed in a *phyA* mutant.

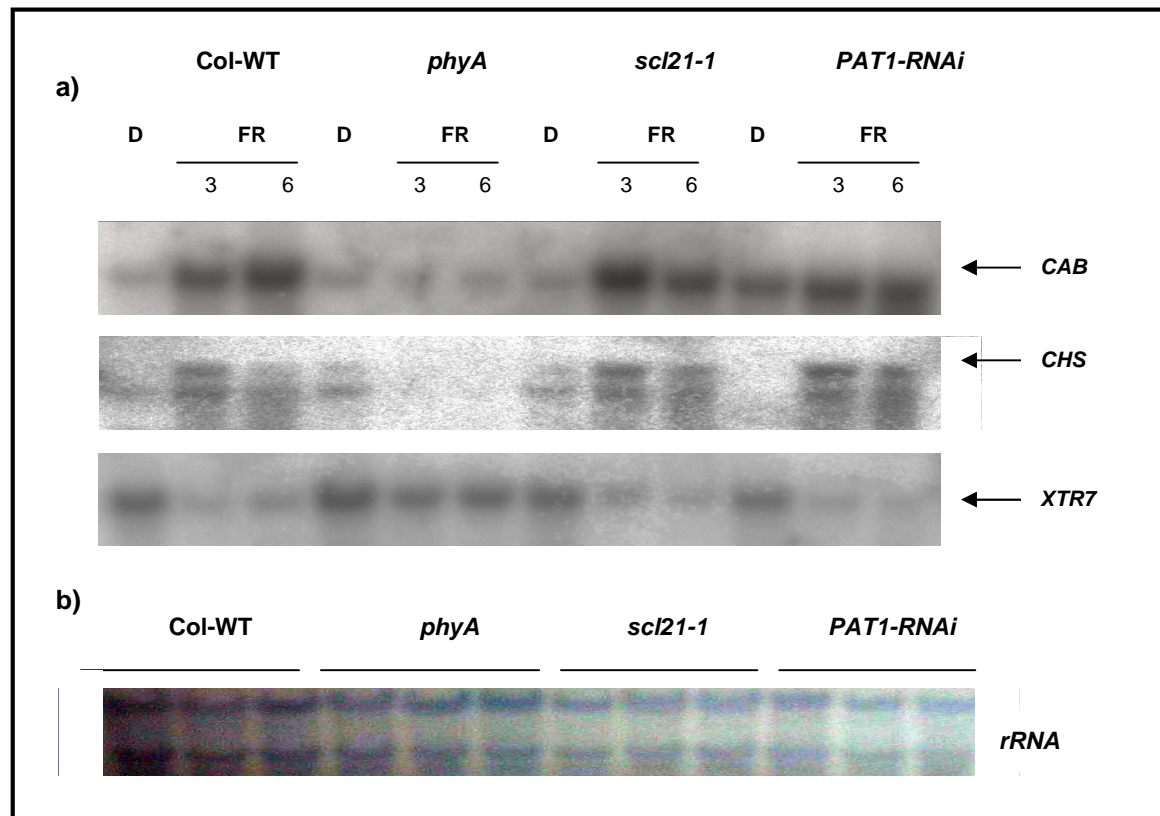


Figure 41. Expression of light regulated genes (*CAB*, *CHS*, *XTR7*) in Col-WT, *phyA*, *scl21-1* and *PAT1-RNAi*. (a) 4-day-old etiolated seedlings (D) were compared with those that received an additional 3 or 6 h of far-red light (FR). (b) Equal loading of 5 μ g of RNA was verified by staining the membrane with Methylene Blue (*rRNA*).

4.7.4. Regulation of the expression of *SCL21* by light

A semiquantitative RT-PCR (Fig. 42) was performed to detect *SCL21* in 4-day-old seedlings that were grown either without exposure to FR light (D) or after 3 h (3) or 6 h (6) irradiation with continuous far-red light (FRc; $1 \mu\text{mol m}^{-2} \text{s}^{-1}$). This confirmed the microarray data and showed that FR light reduces the *SCL21* gene expression but no difference in the *PAT1* gene expression level could be detected. Furthermore, we could demonstrate that the expression level under FR light was controlled by *phyA*, since no reduction of the *SCL21* gene expression level was observed in the *phyA* mutant. Hence, under FR light conditions *phyA* regulates the expression of *SCL21* negatively. The downregulation of *SCL21* is also abolished in *pat1-1* and *pat1-RNAi* mutants, suggesting that *SCL21* gene expression is regulated by *phyA* through *PAT1*. Gene expression of *PAT1*, on the other hand is not regulated by *SCL21*. To control that equal amounts of cDNA were used in the semiquantitative RT-PCR an actin probe was amplified.

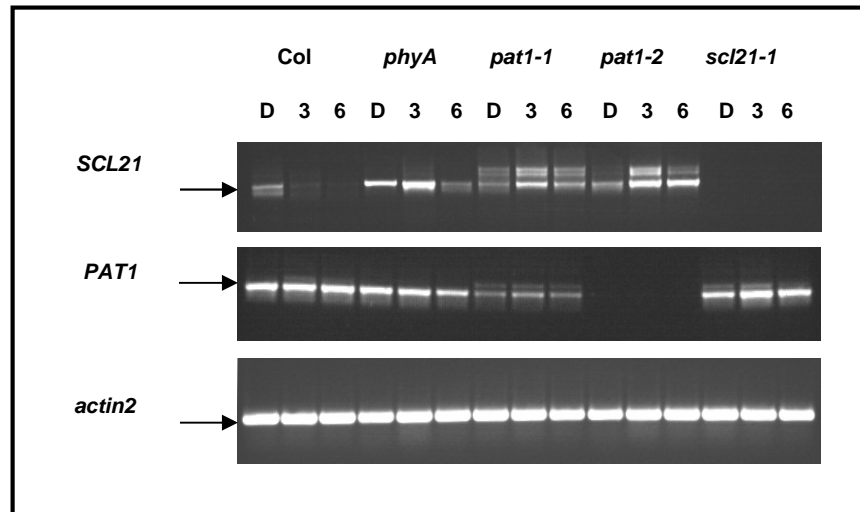


Figure 42. Semiquantitative RT-PCR analysis of *SCL21* and *PAT1* gene expression. Total RNA was harvested from 4-day-old seedlings Col-WT, *pat1-1*, *pat1-2*, *scl21-1* and *phyA* grown in darkness (D) or after 3 h (3) or 6 h (6) irradiation with FRC. 2 μ g of the respective cDNA were used. No expression of the respective genes could be detected in *pat1-2* and *scl21-1*. In *pat1-1* a PCR product can be detected as the 5' part of the mRNA served as template, which is still present in the *pat1-1* mutant. As a control a primer pair amplifying the *actin2* gene was employed.

To test if the negative regulation of *SCL21* gene expression is FR light specific another experiment was performed to detect *SCL21* gene expression in 4-day-old seedlings that were grown under different light conditions: in D, under R ($1 \mu\text{mol m}^{-2} \text{s}^{-1}$), B ($1 \mu\text{mol m}^{-2} \text{s}^{-1}$) and FR ($1 \mu\text{mol m}^{-2} \text{s}^{-1}$) light. In Fig. 43 it can be seen that the *SCL21* gene expression was observed in wild-type seedlings grown in D slightly reduced and under R light conditions, but in wild-type seedlings grown under B and FR light the *SCL21* gene expression was strongly reduced. In a *PAT1-RNAi* mutant and *pat1-1*, the *SCL21* gene expression was still strongly reduced in B light, but not under FR-light. As a cDNA control a primer pair amplifying the *actin2* gene was used. These results indicate that not only FR light reduces the *SCL21* gene expression level, as in the results obtained above (Fig. 42), but B and to a lesser extent R light as well. But only the FR light reduction is PAT1-dependent.

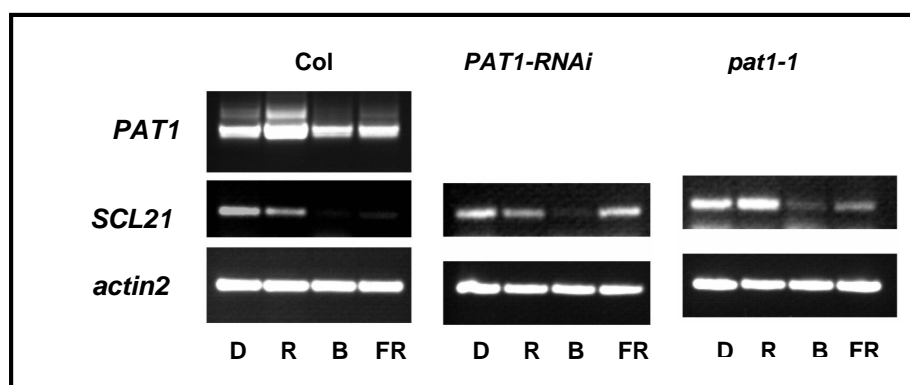


Figure 43. Semiquantitative RT-PCR analysis of *SCL21* gene expression. Total RNA was harvested from 4-day-old seedlings Col-WT, *PAT1-RNAi* and *pat1-1* grown in darkness (D) or after red (R), blue (B) and far-red (FR) light irradiations. As a cDNA control *actin2* gene was used.

4.8. Expression of the genes on the protein level

4.8.1. Confirmation of the loss of SCL21 and PAT1 in the knock-out lines

We have been able to show that the mRNA level of *SCL21* and *PAT1* in the loss-of-function mutants was drastically reduced. In order to be sure that no protein was present in these lines we performed a Western blot with a total protein extraction from WT and the mutant plants. We therefore generated antibodies against PAT1 and SCL21. A previous attempt to generate antibodies against overexpressed PAT1 had failed, therefore we used peptides for antibody production. Peptides were selected from unique domains with a high potential of surface area.

Figure 44 shows a Western blot with protein extracts from leaves of the same lines used for RT-PCR analysis (Fig. 42), namely WT (Col), *PAT1-RNAi*, *pat1-2* and *pat1-1*, incubated with the anti-PAT1 antibody as a primary antibody. Fifty μg of total protein extract was loaded per lane. The anti- PAT1 antibody detected specific bands in the WT extract corresponding to the apparent molecular weight of PAT1 (55 kDa). These bands could not be detected in extracts from the mutant lines. Thus the protein is missing or strongly reduced in the mutants, confirming that this gene are knocked-out in the mutants or strongly reduced in the RNAi lines. Furthermore, with the anti-PAT1 antibody we were able to detect a smaller protein in the *pat1-1* mutant. This is supporting the data gained from Northern analysis, where a truncated mRNA could be detected in the *pat1-1* mutant (Bolle *et al.* 2000). It also suggests that the truncated protein is more stable than the full-length protein as it is more abundant compared to WT. Similar experiments with the *scL21-1* and *SCL21-RNAi* lines gave similar results (data not shown). These experiments also showed that the antibodies are specific for the respective proteins and could be used for further analyses.

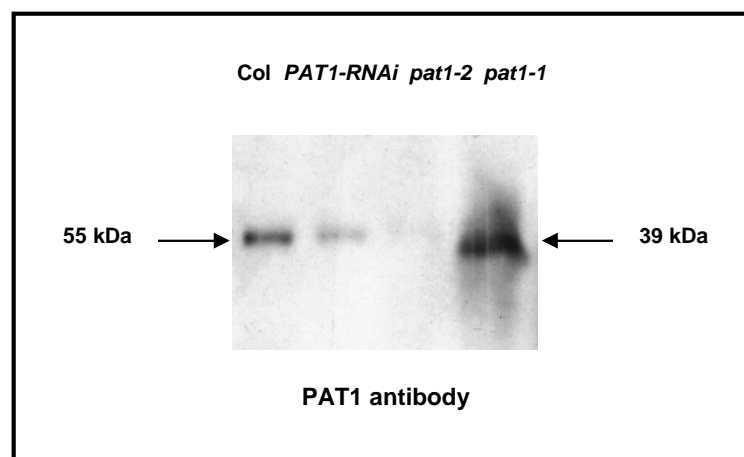


Figure 44. Western blot analysis from leaves of WT (Col) and mutant lines. Anti-PAT1 used as a primary antibody. Equal loading was checked by a parallel gel with Coomassie staining.

4.8.2. Expression of SCL21 and PAT1 at the protein level

The results shown above indicated that at least *SCL21* is regulated at the transcriptional level by light, therefore, it was examined whether the light-regulated reduction of the mRNA level also leads to a reduction of the SCL21 protein levels. Figure 45 shows a Western blot with protein extracts from 4-day-old wild-type seedlings grown in D, without exposure to FR or after irradiation with FRc light ($1 \mu\text{mol m}^{-2} \text{s}^{-1}$) for 3 h (FR-3) or 6 h (FR-6), incubated with the anti-SCL21 (SCL21 Ab) or anti-PAT1 (PAT1 Ab) antibody as the primary antibodies. Detection was performed as in Fig. 44 (Section 3.13.). Western analysis showed that the protein level of SCL21 is induced under FR light compared to D. Also the level of PAT1 seems to increase after three hours of FR light. These data stand in contrast to the expression experiments.

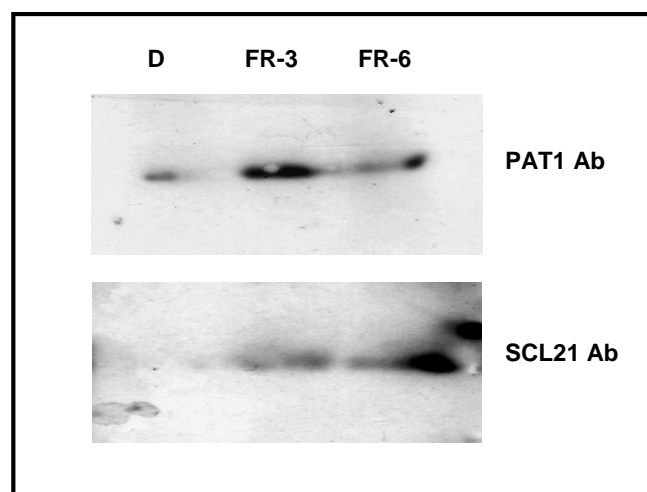


Figure 45. Western blot analysis from 4-day-old WT (*Col*) seedlings grown in darkness (D) or in far-red light (FRc; $1 \mu\text{mol m}^{-2} \text{s}^{-1}$) for 3 h or 6 h, incubated with the anti-SCL21 (SCL21 Ab) or anti-PAT1 (PAT1 Ab) antibody as a primary antibodies.

4.9. Yeast Two-Hybrid analysis

The sequence similarity and the similar function between SCL21 and PAT1 prompted us to examine whether these two proteins interact physically. This was tested with the yeast Two-Hybrid system.

4.9.1. SCL21 activates transcription in yeast

The full-length *SCL21* and *PAT1* cDNAs were fused to sequences encoding the *GAL4* DNA binding domain. These fusion constructs were introduced into yeast and tested for their ability to promote expression of the *HIS3* reporter gene, whose expression is driven by *GAL4*-binding upstream activator sequences (UAS). The interaction was quantified by testing the growth response on different concentration of 3-Amino-1,2,4,-Triazole (3AT). This test was performed

without an additional interacting partner. Only proteins that possess an activation domain can induce transcription of the reporter gene of this one-hybrid assay.

Both, SCL21 and PAT1 were able to transactivate. SCL21 was still able to confer transactivation on plates containing 50 - 75 mM 3AT, whereas PAT1 was only able to grow on plates containing 25 mM 3AT. This indicated that both proteins have a transactivational activity when fused to the yeast GAL4-DNA-binding domain, SCL21 more effectively. When the N-terminus of SCL21 (123 bp= 41 AA) was deleted the remaining protein was no longer able to confer a high level of transcriptional activity, suggesting that the capacity to activate transcription in yeast resides at least partially within the N-terminal 41 amino acid residues of SCL21 (Fig. 46).

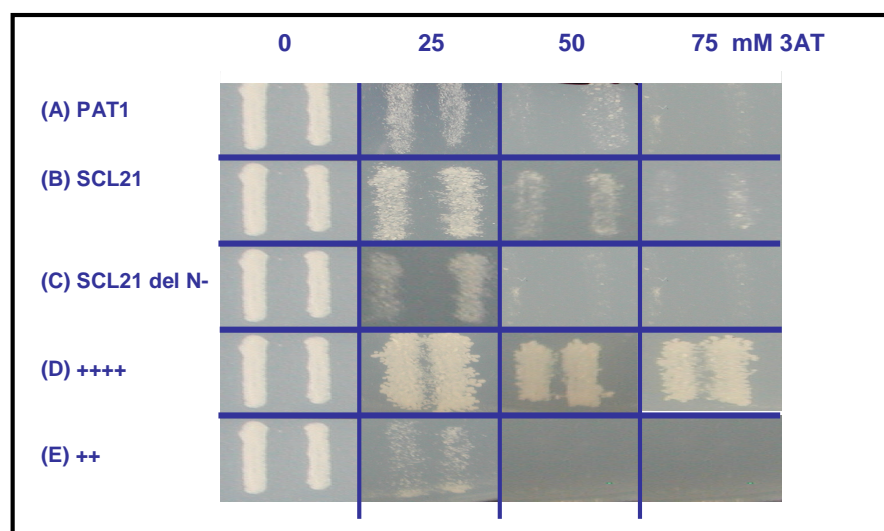


Figure 46. SCL21 and PAT1 can transactivate in a yeast one hybrid assay. A GAL4 DNA binding domain was fused to full length PAT1 (A), full-length SCL21 (B) and a N-terminal deletion of SCL21 (C) and expressed in yeast carrying GAL4-responsive upstream activator sequences upstream of the *HIS3* reporter gene. This leads to the ability to grow on media without histidine. Furthermore, growth on different amounts of 3AT reflects the strength of transactivation. Growth without and with 3AT is shown and compared to a strong (D) and a weak activator (E).

In Two-Hybrid assays we were not able to detect any homodimerization of SCL21 and PAT1, but also no interaction between SCL21 and PAT1 above background. Unfortunately, as both proteins transactivate we cannot exclude that interaction takes place, albeit at lower strength.

4.10. SEUSS-LIKE (SL)1, a putative interactor of PAT1 and SCL21

Seuss-like (SL)1 (At5g62090) has been identified as a putative interactor of PAT1 in a yeast Two-Hybrid screen (C. Bolle, personal communication). It is a member of a small protein family. SEUSS has been identified as an important factor for transcriptional repression. To determine whether *Seuss-like1* is involved in similar processes as PAT1 we employed reverse genetics to generate loss-of-function lines. Two insertion lines could be identified: *SLA* (SALK-collection number N585761) and the *SLB* (SALK-collection number N589954). Homozygous lines were

identified and characterized at the molecular level. These loss-of-function lines were then used for physiological analysis to establish whether they are also involved in the phyA-signalling pathway.

4.10.1. Physiological analysis of the *seuss-like (sl)1* mutants

Homozygous lines lacking *SL1* were tested first under FR light conditions and those with elongated hypocotyls compared to WT (Col), were analyzed in detail. As can be seen in Fig. 47, all insertion lines showed an elongated hypocotyl under FR light, with *sla2-4* and the *slb6-5* being the longest. The progeny of these putative mutants was tested under different light conditions, continuous B, R and FR light and D to establish whether the loss of the *SL1* gene led to a phenotype specific for phyA-signalling. Briefly, seeds were surface-sterilized and sown on MS medium plates with 0.8% (w/v) agar and no sucrose. Plates were stored at 4°C for 4 days and germination was induced by 2 h of W light followed by 22 h of D at 21°C. After this treatment plates were transferred to appropriate light conditions for 4 days. Hypocotyl lengths were measured and statistically analyzed.

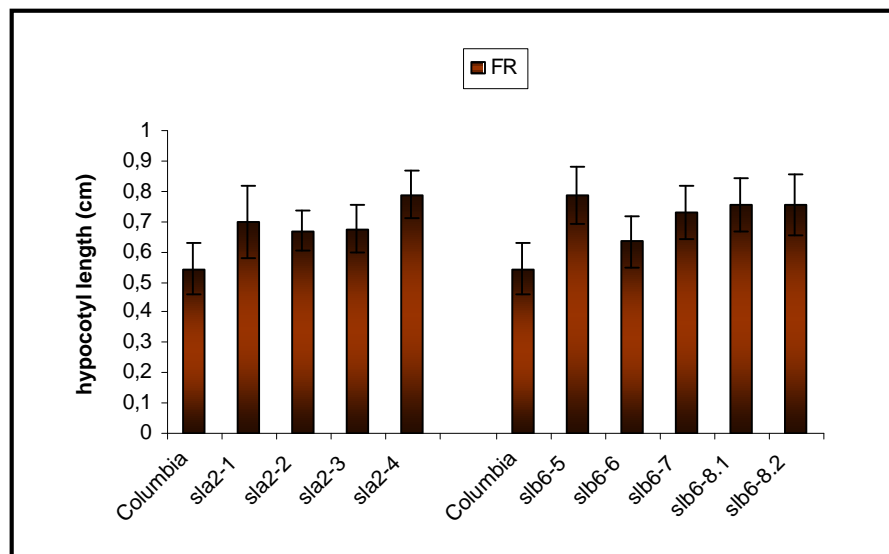


Figure 47. Hypocotyl elongation under far-red light of WT (Col) and different, independent *SLA* and *SLB* loss-of-function lines. 4-day-old seedlings grown under continuous FR light ($0.75 \mu\text{mol m}^{-2} \text{s}^{-1}$) for 4 days. Error bars indicate standard deviation.

The *sla2-4* and *slb6-5* lines show a marginally reduced inhibition of hypocotyl elongation under FR light compared to WT (Col; Fig. 48). Under R and B light the seedlings are similar to WT, suggesting that this is indeed a FR light specific phenotype. When grown under D the lines were indistinguishable from WT, suggesting that the effects of the mutations are light-dependent. These results suggest that *SL1* is also involved in phyA-dependent signalling responses. The reason for the weak phenotype could lie in the fact that *SL1* has a close homolog in the *Arabidopsis* genome and that therefore only the double mutant will show a more prominent phenotype.

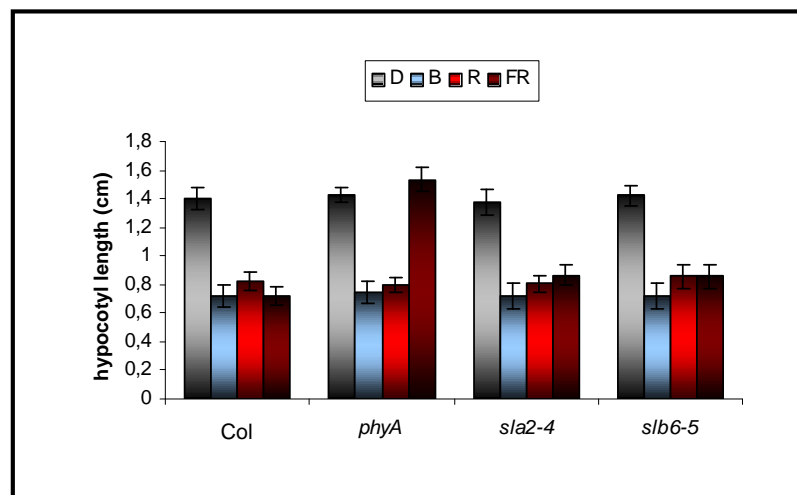


Figure 48. Physiological analysis of SLA and SLB loss-of-function lines. Hypocotyl length of 4-day-old seedlings grown in darkness (D), or under continuous far-red (FR; $0.5 \mu\text{mol m}^{-2} \text{s}^{-1}$), red (R; $1 \mu\text{mol m}^{-2} \text{s}^{-1}$) and blue (B; $8 \mu\text{mol m}^{-2} \text{s}^{-1}$) light. Error bars indicate standard deviation.

4.10.2. Response to different FR light fluences

Fluences rate response curves with different intensities of FR light were used to characterize the sensitivity of these mutants (*sla/slb*) towards FR light. The hypocotyl lengths of these two lines were measured and statistically analyzed. The *sla* and *slb* loss-of-function lines have a slightly longer hypocotyl than WT (Col) (Fig. 49) very similar to the *scl21/pat1-2* mutants.

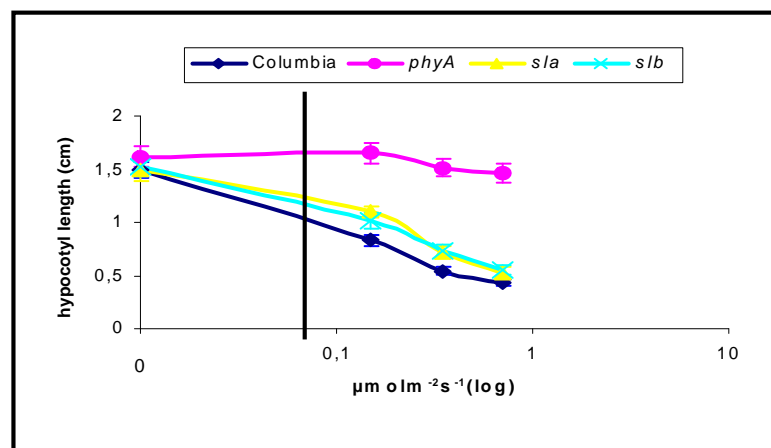


Figure 49. Fluence rate response curve for hypocotyl elongation under far-red light of Col-WT, *phyA*, *sla* and *slb* lines. Error bars indicate standard deviation.

4.10.3. SEUSS-Like1 can transactivate in yeast Two-Hybrid assay

Similar to SCL21 and PAT1 the full-length Seuss-like1 and the SL1₉₀₀ can confer transactivation when tested in a yeast one-hybrid assay (Fig. 50A). For this experiment we fused the full-length *SL1* cDNA and a 5'-deleted fragment (1 - 296 AA; SL₉₀₀) to sequences encoding the *GAL4* DNA binding domain. These fusion constructs were introduced into yeast and tested for their ability to

promote expression of the *HIS3* reporter gene and for their ability to interact. The interaction was quantified by testing the growth response on different concentration of 3AT.

That SL1₉₀₀ was still able to confer strong transactivation on plates containing 50 mM 3AT suggests that the domain necessary for transactivation is not located in the N-terminal part of the protein. Furthermore, homodimerization between SL1₉₀₀ and SL1 were tested. Yeast growth was detected on plates containing 25 mM 3AT, but as the transactivating SL1₉₀₀ construct is able to grow on 50 mM 3AT we cannot conclude that SL₉₀₀ has homodimerization ability.

4.10.4. Interaction between SEUSS-Like1 and the GRAS proteins, PAT1 and SCL21

The SEUSS-LIKE (SL)1 protein was analyzed in this study also for Two-Hybrid analysis because previous protein-protein assays with a cDNA library have revealed these proteins as putative interactors with PAT1. We used the yeast Two-Hybrid system in order to confirm whether Seuss-like1 interacts physically with PAT1 and SCL21. The full-length *SL1* cDNA and a 5'-deleted fragment (1 - 296 AA; SL₉₀₀) were fused to sequences encoding the *GAL4* DNA binding domain. PAT1 and SCL21, on the other hand, were fused to an activation domain. These fusion constructs were introduced pairwise into yeast and again tested for their ability to grow on different concentration of 3AT.

The assays show that a weak interaction with PAT1 was detected on plates containing 25 mM 3AT and slightly stronger interaction with SCL21 as yeast growth was still detectable on plates containing 50 mM 3AT (Fig. 50). As for the interaction between SL1 and SL1₉₀₀ we are not able to determine without doubt whether SL₉₀₀ can interact physically with both proteins because of the transactivation ability of SL1. Nevertheless, it is interesting to note that the yeast growth on 50 mM 3AT is diminished in the two-hybrid assays compared to the transactivation assays. This indicates that the postulated interaction actually represses activation.

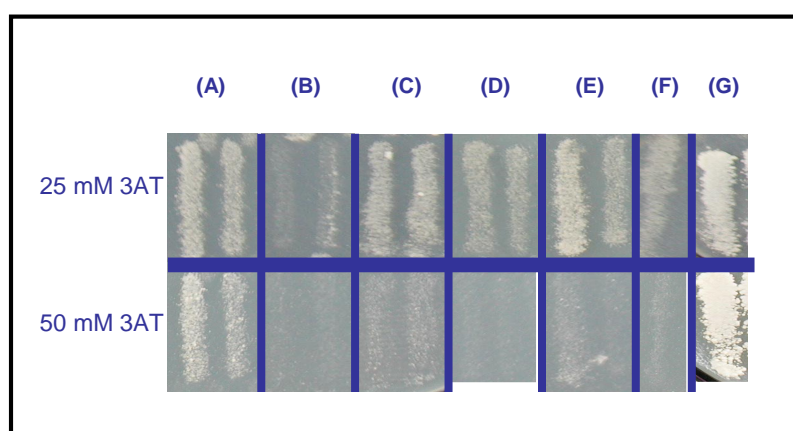


Figure 50. SL₉₀₀ can transactivate and dimerize in yeast. GAL4-DNA binding fusions with SL₉₀₀ with the different genes **(A)** = SL₉₀₀-pEXP, **(B)** = SL₉₀₀-PAT1, **(C)** = SL₉₀₀-SCL21, **(D)** = SL₉₀₀-SL, **(E)** = SL₉₀₀-SL₉₀₀. Growth on different amounts of 3AT reflects the strength of the transactivation and is compared to a strong **(G)** and a weak activator **(F)**.

5. DISCUSSION

The aim of this study was to determine whether GRAS proteins different from PAT1 are involved in light signal transduction and what role these proteins play in this signal transduction. Loss-of-function mutants of SCL1, 5, 13, 21 and PAT1 were characterized physiologically by observing light specific responses in order to evaluate the possible functions of the different proteins. Expression analysis and localization studies were utilized to address cell biological roles of these GRAS proteins. Furthermore, their biochemical role was studied by evaluating transactivation capacity, dimerization and interaction with other proteins.

5.1. All members of the PAT1 sub-branch of the GRAS protein family are involved in light signalling

To that end for all members of the PAT1 sub-branch of the GRAS protein family, SCL1, 5, 13, 21 and PAT1 homozygous loss-of-function lines were generated with the help of reverse genetics utilizing T-DNA insertion lines or with the help of RNAi- and antisense-techniques.

The best-studied effect of light signal transduction is the de-etiolation process (Sullivan and Deng 2003, Chen *et al.* 2004). During de-etiolation hypocotyl elongation of seedlings is inhibited, cotyledons unfold and green and gene expression is changed. Especially the inhibition of hypocotyl elongation can be attributed to specific photoreceptors by using different light conditions. Under FR light only phyA is responsible for initiating the signalling cascade, whereas under R light the predominant photoreceptor is phyB. Under B light the cryptochromes are most important for inhibition of hypocotyl elongation. Nevertheless, cross-talk between the different signalling pathways is well documented (Casal 1996, Canton *et al.* 1999, Casal *et al.* 2000, Hennig *et al.* 2001).

In a first approach, seedlings of all transgenic lines were subjected to different light regimes. The results led to the conclusion that SCL1, 5, 21 and PAT1 act as positive components of the phyA-dependent signalling pathway. Three independently generated types of function lines, insertion, RNAi and antisense lines, demonstrated very similar phenotypes: a decreased inhibition of hypocotyl elongation under FR light conditions, but not under any other light conditions such as W, B and R light or D. The difference to WT is not drastic, but statistically significant, suggesting that these proteins are important regulators of phyA signalling. The alternative that the FR light specific phenotype is an indirect consequence of a reduction in the photoreceptor phyA itself appears unlikely as the effect is not as severe as that of the *phyA* mutant.

The fifth member of the PAT1 sub-branch, SCL13, functions as a positive regulatory component of the R light signalling pathway, predominantly dependent on phyB. The reduction of

SCL13 mRNA in antisense lines specifically decreased the inhibition of hypocotyl elongation under R light conditions. The observation that the antisense lines had mainly wild-type phenotype under other wavelengths (FR, B, W) and in D established that the phenotype is light dependent and specific for R light. Furthermore, the observed phenotype is not a general effect of cell elongation under low fluences of light as the effect could be observed also under non-saturating conditions of R, but not of FR light.

From the phenotypes observed and analyzed from the loss-of-function, insertion, RNAi and antisense lines we conclude that *SCL1*, 5, 21 and *PAT1* act as positive regulators of FR light signal transduction whereas *SCL13* acts as a positive regulator of R light signal transduction. This corresponds also with the fact that *SCL13* is phylogenetically more distant to *PAT1* than for example *SCL21*.

5.1.1. Detailed physiological analysis of the *phyA* responses in the mutant lines

As *phyA* is the only photoreceptor in FR light, mutants with defects in *phyA* show the most drastic phenotype. Under continuous FR light, the *phyA* mutants are characterized by an elongated hypocotyl, closed, unexpanded cotyledons protected by an apical hook, and their ability to green in W light after growing for several days under continuous FR light (Barnes *et al.* 1996, Van Tuinen *et al.* 1996).

The absence of any effects of the *scl21* and *pat1* mutations on FR light regulated hook opening, cotyledon expansion, greening in W light after a prolonged FR treatment (FR dependent block of greening) and FR light induced germination, indicates that the *SCL21* and *PAT1* loci modulate a distinct subset of *phyA*-regulated responses mainly affecting hypocotyl elongation. Most mutants deficient in positively acting intermediates in *phyA* signalling are affected in hypocotyl elongation (Hudson *et al.* 1999, Bolle *et al.* 2000, Fairchild *et al.* 2000, Fankhauser and Chory 2000, Soh *et al.* 2000, Ballesteros *et al.* 2001, Wang and Deng 2002, Wang *et al.* 2002). Hypocotyl elongation under continuous FR light has been characterized as a high irradiance response (HIR), and we could not show that mutants in *SCL21* and *PAT1*, including the semi-dominant mutation *pat1-1*, had any defects in very low fluence responses (VLFR), indicating that only the HIR are channelled through these proteins.

The most important steps during germination are the elongation of the seedling and the change from using energy stored in the seed to using light energy. Elongation is accomplished especially through longitudinal cell expansion. One of the important enzymes which are needed for cell expansion is *XTR7*, a xyloglucan endotransglycosylase (Xu *et al.* 1996). Once the hypocotyl senses light with its photoreceptors, the elongation is inhibited. Gene expression of *XTR7* is high in the D and negatively regulated by light, the reduction under FR light signal is dependent on *phyA*. We have compared expression levels of several phytochrome-responsive genes (*CHS* coding for the chalcone synthetase and *CAB2* coding for the light harvesting complex

apoprotein 2) including *XTR7* between *scf21-1*, *pat1-RNAi* and the WT under FR light. Results from these assays indicate that there are no major differences in the expression patterns of Col and the mutant lines for the expression of *CAB* and *CHS* genes, but we observed that *SCL21* and *PAT1* affect the expression of *XTR7*. This correlates with the fact that mutants lacking these genes have an elongated hypocotyl compared to WT. For *pat1-1* it has been shown that in this mutant *CAB* and *CHS* expression levels in FR light are reduced or abolished (Bolle *et al.* 2000).

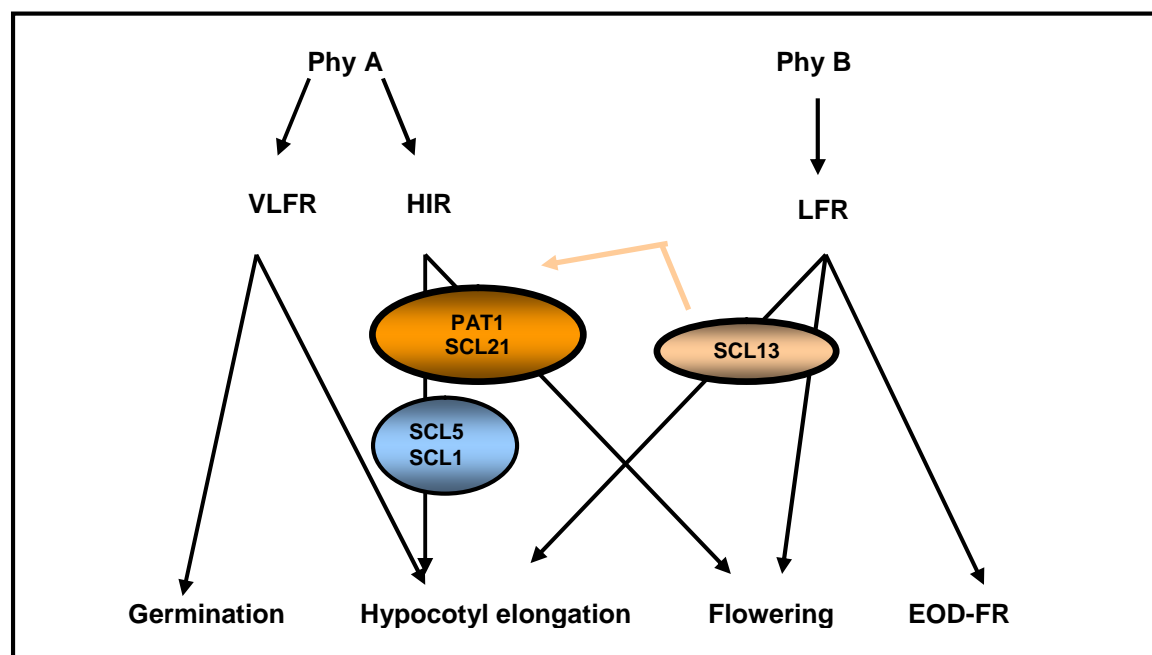


Figure 51. Schematic presentation of the physiological responses of *SCL1*, *SCL5*, *SCL13*, *SCL21* and *PAT1*.

5.1.2. Detailed analysis of the R light responses in *SCL13* antisense lines

Three phytochromes have been shown in *Arabidopsis thaliana* to be involved in R light signalling besides phyB, notably phyC, D and E. The mutants with defects in phyB have an elongated hypocotyl and smaller cotyledons under continuous R and W light, and they are slightly pale because of reduced chlorophyll accumulation. They also have elongated petioles, flower earlier and do no longer respond to an EOD (end-of-day)-FR pulse. In contrast, we could not detect any changes in the many well-described phyB-dependent responses such as germination under R light, cotyledon expansion, EOD-FR response, petiole elongation, chlorophyll accumulation and gene expression in our *SCL13* antisense lines. The main phenotype that could be observed was the sensitivity of the hypocotyl elongation towards R light, and the earlier onset of flowering under short- and long-day conditions. *SCL13* is the only protein to our knowledge in which the loss-of-function specifically affects hypocotyl length and not cotyledon expansion.

Not many intermediates in phyB signalling have been identified so far. One reason may be that functional redundancy renders it difficult to identify mutants impaired in R light signalling. Most of the proteins that have been identified as intermediates of the phyB signal transduction are

transcription factors, especially basic helix-loop-helix proteins (bHLH) that are localized in the nucleus such as PIF3, 4, PIL1, 6, GI, ELF3 and ELF4 (Ni *et al.* 1998, Liu *et al.* 2001, Fowler *et al.* 1999, Huq *et al.* 2000, Doyle *et al.* 2002, Khanna *et al.* 2003). However, *SRR1* codes for a nuclear/cytoplasmic protein (Staiger *et al.* 2003) and *RED1* encodes a cytoplasmic cytochrome P450 (Hoecker *et al.* 2004). This suggests that the R light signal transduction is at least modulated in the cytoplasm.

5.1.3. Interaction between phyA and phyB signal transduction cascades

Previous reports have established a complex pattern of cross-talks between phyA and phyB (and other photoreceptors) in the photoregulation of complex developmental processes (Casal 1996, Canton and Quail 1999, Casal *et al.* 2000, Hennig *et al.* 1999, 2001). PhyA has a synergistic effect with phyB under HIR conditions, whereas under VLFR the effect is inhibitory (Neff and Chory 1998, Hennig *et al.* 1999). Activation of phyB signalling appears to be unnecessary for this modulation of phyA-mediated HIR, because FR light, which does not induce signalling via phyB, is sufficient for the effect. Furthermore a point mutation in phyB (*phyB4*) can still inhibit the phyA-dependent HIR, whereas it is unable to induce a signalling cascade. It was speculated that phyA and phyB might compete for the same signalling partner in the cytoplasm leading to a negative interaction (Hennig *et al.* 2001).

For *SCL13* we crossed the antisense lines into *phyA* and *phyB* null mutants to analyze whether phyA and phyB are required for the phenotype of these lines. The results show that the *SCL13-AS-phyA* line is still less sensitive to R light compared with *phyA*, suggesting that phyA is not required or plays a minor role in the *SCL13* antisense phenotype under R light. The hypocotyl elongation of the *SCL13-AS-phyB* double mutant was statistically indistinguishable from the *phyB* null mutant when grown under R light conditions ($P > 0.05$). These data indicate that hypocotyl responsiveness to continuous R light is fully dependent on phyB. Under FR light conditions, the *SCL13-AS-phyB* lines showed an increase in hypocotyl elongation compared to WT ($P < 0.05$). This suggests that in the absence of phyB, *SCL13* can act downstream of phyA or at least modulate phyA signals. In a *SCL13* antisense line in a *phyA* background the *phyA* phenotype dominated under FR light. This shows that *SCL13* is not necessary for phyA signalling, whereas it can modulate hypocotyl length under FR light in a phyB-independent way, because phyB is not activated by FR light. Together, these data indicate that *SCL13* is able to antagonize phyA function in continuous FR light.

5.2. Subcellular localization studies suggest that SCL1, 5, 13, 21 and PAT1 could play a biological role in the cytoplasm and nucleus

All PAT1-related proteins lack distinguishable nuclear localization (NLS) and nuclear exclusion (NES) motives. Therefore, GFP-fusions were generated and transiently expressed in onion-epidermis cells. GFP-mediated fluorescence of a *SCL1*, 5, 13 and *SCL21*-GFP fusions

were observed in the same compartments as PAT1, nucleus and cytoplasm. This localization seems not to be affected by different light conditions including D. Therefore, it is up to speculation, whether the proteins are distributed evenly in cytoplasm and nucleus or if they cycle between the nucleus and the cytoplasm, one of the compartments harbouring the active form the other the inactive one. Nevertheless, the results indicate that these proteins could act in the nucleus or in the cytoplasm.

Other GRAS proteins have been shown to localize exclusively in the nucleus such as SCR, SHR and SCL8 (Rothmeier and Bolle, unpublished results). This indicates that the active form is needed in the nucleus.

For SCL13 we therefore generated lines expressing SCL13-NES/NLS fusions to determine in which compartment SCL13 is biologically active. A conserved NLS was fused to the N-terminus of the SCL13 protein. This leads to an exclusive nuclear localization of the protein suggesting that the SCL13 protein is not actively exported from the nucleus. If the NLS was substituted for a nuclear exclusion signal (NES) the protein localized predominantly in the cytoplasm. The fact that lines overexpressing an NLS-SCL13-GFP-GUS fusion protein in the nucleus as well as lines overexpressing the cytosolic form of SCL13 have a hypersensitive reaction under R light in their hypocotyl elongation suggests that SCL13 can perform its role in both compartments.

The weaker GUS activity observed in SCL13-NLS overexpressing lines could be due to a faster turnover of the protein in the nucleus. Furthermore, the results underline the findings that SCL13 is important for the R light signalling as no hypersensitive effect could be measured under D and FR light conditions.

The question of localization of the proteins is crucial as phytochrome itself is transported from the cytoplasm to the nucleus under activating conditions (Sakamoto and Nagatani 1996, Kircher *et al.* 1999). Furthermore, several signalling intermediates, such as SPA1 (nuclear WD-repeat protein, Hoecker *et al.* 1999), FAR1 (nuclear protein, Hudson *et al.* 1999), HFR1 (also known as REP1) a member of the basic helix-loop-helix (bHLH) family of DNA-binding proteins (Fairchild *et al.* 2000, Soh *et al.* 2000) and the phyA/phyB interacting protein PIF3 (Ni *et al.* 1998, 1999), are localized in the nucleus. Conversely, cytoplasmic localization of the phyA/phyB-interacting proteins PSK1 and NDPK2, and the involvement of putative heterotrimeric GTP-binding proteins, Ca²⁺/CaM and cGMP in phyA signalling suggest that important early signalling events occur in the cytoplasm (Wu *et al.* 1996, Barnes *et al.* 1995, Guo *et al.* 2001, Wang *et al.* 2007).

The constitutive expression of *SCL13* indicates that SCL13 has already to be present under non-induced conditions so that a quick response can take place after illumination and activation of the phytochrome. SCL13 could interact with phyB to transport the latter to the nucleus upon illumination. Another possibility is that SCL13 is a signalling intermediate, which amplifies the R

light signal either in the cytoplasm or in the nucleus. Further experiments will be necessary to determine how SCL13 executes its function.

Comparable experiments have been initiated with SCL21 and PAT1. Besides the fusions with either a NES or a NLS sequence, these proteins were also fused to a glucocorticoid-receptor. The fusion protein is retained in the cytoplasm, upon induction with dexamethasone, the fusion protein is split and the released protein can move to the nucleus. With these experiments we will be able to determine whether SCL21 and PAT1 are involved in the cytoplasmic stages of phyA-signalling, with the targeting of the Pfr form of phyA to the nucleus or with the signalling within the nucleus.

5.3. Tissue-specific expression of the *PAT1*-related genes

Experiments with transgenic lines carrying the *SCL13 promoter-5'-UTR-GUS* fusion, which contained 2,514 bp of the promoter region upstream of the transcription start site, showed that the overall GUS activity is similar under different light conditions, but that the tissue-specific expression varied. When seedlings grown in W light GUS activity was mainly restricted to cotyledons and root, whereas hardly any activity was detectable in hypocotyls. By contrast, seedlings grown in D or in R light, which had elongated hypocotyls compared to WT, showed also GUS staining in hypocotyls (Fig. 27). It looks as if *SCL13* is predominantly expressed in the active elongation zones of the hypocotyl.

The *SCL13* mRNA is not regulated in a light-dependent fashion, at least under the conditions used in the microarray experiments. Microarray analysis revealed that *SCL13* mRNA is induced in all green tissues and in the root. This implies a function of the protein during the entire life cycle of a plant - similar to phyB (Sharrock and Clack 2002).

Differences between microarray data and GUS expression patterns could arise from the fact that GUS assays were performed on 4-day-old seedlings rather than on 7-day-old seedlings used for the microarray assays or from differences in fluence rates.

Microarray analysis revealed that *SCL1* and *SCL5* are also induced in maturing seeds and seedlings, although the expression is higher in maturing seeds compared to seedlings. The expression pattern for *SCL1* is at a weaker level than for *SCL5*. In seedlings the expression pattern is induced in hypocotyl and cotyledons. In the maturing seed the expression is induced in seed stage 6 (90 days after flowering, torpedo stage). In addition, the results obtained from GUS expression patterns and microarray analysis suggest that *SCL1* is also induced by wounding processes.

Expression patterns from SCL21 determined by promoter GUS assays showed that GUS activity is strongest in cotyledons, apical hook and root apex confirming data derived from the microarray

analysis. As the latter data suggested, and confirmed by our Northern analysis (data not shown) the expression of *SCL21* is very weak, specially in adult plants. The fact that *SCL21* is expressed at higher levels in maturing seeds compared to seedlings indicates that *SCL21* is necessary in the first moments of the germinating seedling.

5.4. *SCL21* gene expression is negatively regulated by phyA

Whereas *PAT1* gene expression is not affected by FR light, the level of *SCL21* is reduced by FR light in a *phyA*-dependent manner; this reduction is not observed in a *phyA* mutant. Furthermore, the expression is also not reduced in the *pat1-1* und *pat1-2* mutants, indicating that *PAT1* acts upstream of *SCL21* gene expression. The fact that *SCL21* gene expression is reduced under those conditions, in which we postulate its function, is paradoxical at first. On the other hand, *PAT1* is more abundant at the transcriptional level and protein level, determined by Western analysis. The data obtained from GUS assays and microarray analysis suggest that *SCL21* first helps the seedling to perceive the FR light *via phyA* signal transduction, whereas *PAT1* is important in slightly later stages.

Few other genes or proteins involved in FR light signal transduction such as *FHY1* have been shown to react in a similar way (Desnos *et al.* 2001, Zeidler *et al.* 2001). Most probably their proteins are involved in the first steps after the transition from D to light and it is important that after the signal has been perceived it is then desensitized. This pattern does not hold for all genes of FR light components, because others transcripts (e.g. *PAT1*, *FAR1*) are unaffected by light or actually increased by FR light (e.g. *SPA1*, *HFR1*) (Hudson *et al.* 1999, Bolle *et al.* 2000, Fairchild *et al.* 2000, Duek and Fankhauser 2003, Laubinger *et al.* 2004, Hoecker *et al.* 1998).

However, additional photoreceptors are also involved in the downregulation of *SCL21* transcript levels, since *SCL21* is also reduced in R, B and W light. This may reflect a point of interaction between the signal-transduction pathways associated with these different photoreceptors and the PHYA signal-transduction pathway.

5.5. Role of introns in the 5'-untranslated region of the genes

All genes encoding proteins for the *PAT1* branch contain a 400 to 700 bp long intron upstream of the ATG in the 5'-untranslated region (5'-UTR). By contrast, the coding region is not interrupted by any intron, a feature common to most GRAS protein encoding genes in *Arabidopsis*. We wanted to investigate the possible role of this intron for expression pattern and exemplarily, we analyzed the *SCL13* and *SCL1* promoter in more detail .

As the 5'-UTR of the *SCL13* transcript includes a 750 nt-long intron, a possible role of this intron for expression was investigated. The 5'-UTR including the intron on its own was not able to induce any GUS activity. A promoter construct that lacked the 5'-UTR and the intron generated

the same spatial distribution of *GUS* expression, although at a weaker level, indicating that enhancing elements could be located within the 5'-UTR or the intron.

In a similar way, for *SCL1* we performed experiments with transgenic lines containing 1,380 bp upstream of the transcription site (promoter), the 5'-UTR and the intron within (*SCL1 promoter-GUS* construct) and lines containing 800 bp of the promoter lacking the intron in the 5'-UTR (*SCL1 Intron-GUS* construct). Transgenic plants carrying the *SCL1 promoter-GUS* construct showed *GUS* activity that could be detected in the leaves. In contrast, but analogous to the *SCL13* lines, the transgenic lines carrying the *SCL1-Intron-GUS* construct were not able to induce any *GUS* activity (data not shown) suggesting that no alternative transcription start sites are available within the intron sequence.

5.6. Protein stability

The semi-dominant *pat1-1* mutation has a much stronger phenotype compared to the loss-of-function mutant *pat1-2*. Nevertheless, the responses observed are very similar, just at a more moderate level. We had assumed that in the *pat1-1* mutant the protein is still expressed, albeit in a C-terminally deleted version (Bolle *et al.* 2000). Here we could detect a truncated protein serologically and confirm this hypothesis. The deletion of the C-terminal could shift the protein to act in a negative fashion either by changing protein stability or the way it interacts with its protein partners. As the protein amount of PAT1 in the *pat1-1* mutant is higher as in wild-type control we favour the hypothesis that the C-terminal deletion increases the protein stability. Overexpression of a 3'-deleted *PAT1* gene mimics in part the *pat1-1* phenotype (Bolle *et al.* 2000). Yet, a similar deletion with *SCL21* did not lead to any elongated hypocotyls under FR light (or any other visible phenotypes) supporting the idea that both proteins have different roles in the phyA signalling pathway. Overexpression of the full length *SCL21* and *PAT1* genes does not result in any change of phenotype suggesting that the protein level is rigidly controlled (data not shown).

5.7. Seuss-Like 1, a putative interaction partner of PAT1 and SCL21

Yeast two-hybrid screens had revealed SEUSS-LIKE protein 1 as a possible interactor of PAT1. Furthermore, we were able to detect weak interaction with PAT1 and a slightly stronger interaction with SCL21 in the yeast Two-Hybrid assays and this interaction has since been strengthened by experiments with the Split-YFP assay (Zintl and Bolle, unpublished results). *SEUSS* (*SEU*) encodes a plant protein with two glutamine-rich (Q-rich, 15% Q overall) domains and a highly conserved central domain that shares sequence identity to the dimerization domain of the LIM domain-binding (Ldb) family of transcriptional coregulators in animals such as the Ldb1 in mouse and Chip in *Drosophila* (Franks *et al.* 2002, van Meyel *et al.* 2003, Jurata and Gill 1997). Ldb protein family members regulate transcription via direct physical interactions with DNA-binding transcription factors such as the LIM-homeodomain proteins (Agulnick *et al.* 1996,

Bach *et al.* 1997, Jurata and Gill 1997). A second domain of the Ldb proteins, the LIM Interaction Domain (LID), mediates the interaction between Ldb proteins and the LIM homeodomain proteins. SEU does not have any function in repressing transcription and, on the contrary, may have an intrinsic activation potential as revealed in yeast Two-Hybrid assays (Sridhar *et al.* 2004).

SEU therefore defines a class of plant-specific transcription factors and is a member of a small gene family in *Arabidopsis thaliana* (*SEUSS-LIKE* genes, Franks *et al.* 2002). Between 21% and 81% amino acid sequence identity was found within the conserved central domain when compared with other *SEUSS-LIKE* plant proteins and animal Ldb proteins. While the Ldb proteins are similar to SEU only in the conserved central domain, the *SEUSS-LIKE* proteins from plants are similar to SEU in the entire protein. The *Arabidopsis thaliana* genome encodes two *SEUSS-LIKE* genes, *SL1* (*At5g62090.1*) and *SL2* (*At5g62090.2*); both are 55% identical to SEU in the putative dimerization domain and 33% identical over the entire protein.

With the exception of *SEU*, the molecular function of other family members of these *SEUSS-LIKE* genes is largely unknown. *SEU* has been isolated as a factor which is important for flower development (Franks *et al.* 2002). Morphological, physiological and genetic evidence implicate *SEU* in auxin-regulated growth and development. *Seu* exerts a pleiotropic phenotype that includes reductions in several classic auxin responses such as apical dominance, lateral root initiation, sensitivity to exogenous auxin and activation of the DR5 auxin response reporter. Auxin is required in the root for organization of the meristem, gravitropic response, primary root elongation and initiation of lateral roots (Sabatini *et al.* 1999, Moore 2002, Casimiro *et al.* 2003). Furthermore, a role for auxin in light signalling has been described (Morelli and Ruberti 2002; Halliday and Fankhauser 2003) but there is no proof that auxin is directly integrated with GRAS protein function.

Our results from the physiological analysis of the *seuss-like (sl)1* mutants suggest that *SL1* can function as a positive component of the phyA-dependent signalling pathway as the *sl1* mutant lines show a decreased inhibition of hypocotyl elongation under FR light but not under any other light conditions (W, R and B light or D). The difference to WT is not very drastic but statistically significant.

Interesting would be further physiological experiments to test whether *SL1* is also involved in auxin signalling or to test if there is an integration auxin with *SL1* protein function.

5.8. SCL21 and PAT1 as potential factors involved in activation of transcription

One-hybrid analysis showed that both proteins *PAT1* and *SCL21* can function as transactivation factors in yeast, albeit *SCL21* to a much better degree as *PAT1*. Deletion of the N-terminus of *SCL21* demonstrated that that region plays an important role in transactivation. These results are

similar to *in vitro* results of other GRAS proteins such as OsGAI/SLR1, LeLs, and LISCR (Ogawa *et al.* 2000, Itoh *et al.* 2002, Morohashi *et al.* 2003). Evidence that GRAS proteins could be involved in transcriptional regulation is derived from studies on an SCL gene of lily, LISCL (*Lilium longiflorum* scarecrow-like; Morohashi *et al.* 2003). Transcriptional activation experiments demonstrate that the N-terminus of LISCL fused to a GAL4-DNA binding domain can function as a transactivator in yeast and in plant cells. Detailed analysis of essential motifs for the transactivation is not available, however.

Although dimerization has been implied in the function of GRAS proteins (Pysh *et al.* 1999) we can neither detect homo- or heterodimers between SCL21 and PAT1. This result could be compromised as the experiments in the yeast Two-Hybrid system are difficult to interpret due by the fact that the proteins can transactivate. PAT1 and SCL21 could also be acting in a hierarchical order comparable to the GRAS proteins SCR and SHR. It has been shown that SHR acts upstream of SCR as it controls its expression (Nakajima *et al.* 2001). Indeed we can demonstrate that *SCL21* gene expression is dependent on the presence of PAT1. Both SCL21 and PAT1 have been shown to be able to transactivate, albeit at different levels. Also SCL13 was found to display some transactivation capacity in yeast One-Hybrid assays (Rothmeier and Bolle, unpublished data). Nevertheless, for many of the GRAS proteins it has yet to be determined whether they play a role in transcriptional activation. As PAT1 and SCL13 are also localized in the cytoplasm, this would mean that in order to activate the transcription machinery they have to migrate to the nucleus. Both PAT1 and SCL13 possess no conserved NLS, future research should focus on the mechanisms by which these proteins are transferred into the nucleus for light signalling.

5.9. Are GRAS proteins transcription factors?

GRAS genes are proposed to be transcription factors. However, no direct DNA binding ability of any GRAS protein has been demonstrated. Future research will be required to determine whether transcriptional activation is a hallmark of this protein family and if GRAS proteins can directly interact with DNA.

A typical plant transcription factor contains a DNA-binding region, an oligomerization site, a transcription regulation domain, and a nuclear localization signal (Liu *et al.* 1999). It has been speculated that the LHRI-VHIID-LHRII region may function as a DNA binding and oligomerization domain, analogous to the bZIP protein-DNA interaction, with LHRI and LHRII mediating protein-protein interactions and the VHIID mediating protein-DNA interactions (Pysh *et al.* 1999). The C-terminal region with their conserved PFYRE and SAW motifs may act as a regulatory domain (Itoh *et al.* 2002).

It is intriguing to think that the GRAS proteins could act as transcriptional co-activators, perhaps together with other co-transactivators such as the SEU-like proteins, thereby integrating different signals.

5.10. GRAS proteins and light signalling

GRAS proteins have been shown to be involved in many different developmental processes (Bolle 2004). Here we could demonstrate that all members of the PAT1- subbranch play roles in light signal transduction.

GRAS proteins are highly conserved in their C-terminus, whereas their N-terminus is more variable, suggesting that the N-terminus is responsible for the specificity of the different signalling cascades. Whereas many GRAS proteins contain stretches of homopolymeric amino acid residues such as serine, proline or threonine, PAT1 and SCL21 do not contain these. The N-terminal domain of SCL21 is less than half the size of PAT1 and besides a conserved motif at its very C-terminal part no homologies can be recognized. In contrast to PAT1, SCL21 contains more acidic residues, especially in the motif "ELSMWPDDAKD". These acidic amino acids could be attributed to the transcriptional activity of SCL21, but this remains to be confirmed.

SCL1 and 5 are also conserved in the only N-terminal domain, especially the "EAISSRRDL"-motif, which is homologous between PAT and SCL21. As all these proteins are involved in the phyA-dependent signal transduction, the "EAISSRRDL" motif could play a crucial role in this, as it is the only conserved motif between all proteins involved in phyA signalling.

It is interesting to note that no SCL21 homologs could be isolated in any other organisms, whereas homologs to PAT1 could be determined. Especially from the EST libraries of *Solanum tuberosum* and *Nicotiana benthamiana* two sequences could be isolated that show a high degree of homology to PAT1. In SCL13, this motif is not maintained (Torres Galea *et al.* 2005). During evolution GRAS proteins seem to have acquired different N-terminal domains, which then convey the specificity to processes. Nevertheless, further analysis is necessary to validate the importance of these motifs in GRAS proteins.

The detection of ESTs with sequence similarity to GRAS proteins in bryophytes indicates that the GRAS gene family arose before the appearance of land plants over 400 million years ago (Nishiyama *et al.* 2003). Molecular and phylogenetic analysis of GRAS genes from lower plants, such as ferns, bryophytes, and green algae, will help to resolve the evolutionary history of the GRAS gene family. The phylogenetic and comparative analysis of the GRAS gene family in *Arabidopsis thaliana* and *Oryza sativa* will provide a first step towards a functional characterization of the GRAS gene family in future. Better knowledge of the mechanisms of the action of GRAS proteins and of the biochemical function in individual pathways they act in will serve to understand how the proteins are adapted to carry out plant-specific processes.

6. SUMMARY

In this study, loss-of-function, antisense and RNAi lines of one sub-branch of the GRAS protein family, the PAT1 branch, were characterized. The GRAS protein family is a recently discovered family of plant-specific proteins. Although plants contain a remarkable number of GRAS proteins, they are not present in any other organisms, suggesting a specialized role in plant development and signalling. Several *Arabidopsis* proteins cluster to the PAT1 branch of the GRAS protein family, namely SCL21, SCL5, SCL13 and SCL1.

Homozygous insertion lines of *SCL1*, *SCL5*, *SCL21* and *PAT1* were selected and confirmed by PCR. Furthermore, RNAi lines for *PAT1* and *SCL21* were generated. The reduction of the RNA levels in all lines used were confirmed by a semiquantitative RT-PCR and, in the case of *SCL21* and *PAT1*, the loss of the protein was confirmed by Western analysis. Several light responses such as hypocotyl elongation, hook opening, cotyledon unfolding, germination and chlorophyll accumulation were analyzed. From the five members of the PAT1 branch, *PAT1*, *SCL21*, *SCL1* and *SCL5* seem to be involved in phytochrome A signalling. All three different types of lines, insertion, antisense and RNAi lines, show a reduced inhibition of the hypocotyl under far-red light conditions compared to WT but not under other light conditions, and this suggests strongly that they are specifically involved in phyA-dependent signalling responses. Examination of the apical hook opening, cotyledon unfolding and expansion uncovers that the effect of these proteins is stronger on hypocotyl elongation than on cotyledon development. The loss-of-function lines of *SCL21* and the *SCL21*- and *PAT1*-RNAi lines, in contrast to *pat1-1*, display some sensitivity to the phyA-dependent block of greening. No strong defect in very low fluence responses such as germination could be found, which suggests that these proteins are positive regulators of high irradiance responses (HIR). *SCL13* antisense lines, in contrast to the other members of the PAT1 branch, showed a reduced inhibition of hypocotyl elongation when were grown under continuous red light. This suggests the involvement of SCL13 in the phytochrome B, C, D or E signalling pathways.

Developmental and tissue specific expression patterns were analyzed using transgenic promoter-GUS plants. The *SCL21* promoter induced GUS expression in the cotyledons and in the root apex. Expression of a *SCL13 promoter-5'-UTR-GUS* fusion in transgenic lines showed that younger leaves showed stronger GUS staining compared to adult leaves. In contrast, the analysis of the *SCL1* promoter activity by *in vivo* GUS expression led to staining in those parts of the leaf that had lesions from parasites, suggesting that SCL1 may be also involved in wounding processes. In transient assays, the SCL1-, SCL5-, SCL13-, SCL21- and PAT1-GFP fusion proteins were detected in cytoplasm and nucleus. It is conceivable that these proteins might have a function in the latter compartments.

Genetic and molecular approaches were used additionally, to characterize the biological function of the members of the PAT1 branch, specific of SCL21 and PAT1. Under far-red (FR) light the

SCL21 transcript itself is downregulated in a phytochrome A- and PAT1-dependent manner. Both PAT1 and SCL21 are positive factors specific for the phytochrome A signal transduction pathway. Because of sequence similarities between SCL21 and PAT1, yeast Two-Hybrid assays were performed to evaluate whether these proteins interact. Furthermore, One-Hybrid assays showed that SCL21 and PAT1 can transactivate in the yeast system, SCL21 more efficiently.

SEUSS-Like1 was isolated as a protein that can interact with PAT1 in the yeast Two-Hybrid assay. Therefore, with the aid of reverse genetics mutants were characterized in the *Seuss-like (s)1* locus. The lines were characterized physiologically in the same way as the loss-of-function lines of PAT1 branch proteins. The physiological analysis showed us that the *Seuss-like1* gene is also involved in phytochrome A signalling responses. Two-Hybrid analyses were also performed with the SEUSS-LIKE1 protein demonstrating that it could interact with the SCL21 as well as the PAT1 protein.

7. REFERENCES

- Agulnick, A. D., Taira, M., Breen, J. J., Tanaka, T., Dawid, I. B. and Westphal, H. (1996) Interactions of the LIM-domain-binding factor Ldb1 with LIM homeodomain proteins. *Nature* **384**, 270-2.
- Ahmad, M. and Cashmore, A. R. (1997) The blue-light receptor cryptochrome 1 shows functional dependence on phytochrome A or phytochrome B in *Arabidopsis thaliana*. *Plant J* **11**, 421-7.
- Andel, F. 3rd, Lagarias, J.C. and Mathies, R.A. (1996) Resonance raman analysis of chromophore structure in the lumi-R photoproduct of phytochrome. *Biochemistry* **35**, 15997-6008.
- Ang, L.H. and Deng, X.W. (1994) Regulatory hierarchy of photomorphogenic loci: allele specific and light-dependent interaction between HY5 and COP1 loci. *Plant Cell* **6**, 613-28.
- Aukerman, M.J., Hirschfeld, M., Wester, L., Weaver, M., Clack, T., Amasino, R.M. and Sharrock, R.A. (1997) A deletion in the PHYD gene of the *Arabidopsis* Wassilewskija ecotype defines a role for phytochrome D in red/far-red light sensing. *Plant Cell* **9**, 1317-26.
- Bach, I., Carriere, C., Ostendorff, H. P., Andersen, B. and Rosenfeld, M.G. (1997) A family of LIM domain-associated cofactors confer transcriptional synergism between LIM and Otx homeodomain proteins. *Genes Dev* **11**, 1370-80.
- Ballaré C.L. (1999) Keeping up with the neighbours: phytochrome sensing and other signalling mechanisms. *Trends in Plant Science* **4**, 97-102.
- Ballaré, C. L., Scope, A. L., Sanchez, R. A., Casal, J. J. and Ghera, C. M. (1987) Early detection of neighbour plants by phytochrome perception of spectral changes in reflected sunlight. *Plant Cell Env* **10**, 551-7.
- Ballesteros, M., Bolle, C., Lois, L.M., Moore, J.M., Vielle-Calzada, J.-P., Grossniklaus, U., Chua, N.-H. (2001) LAF1, a MYB transcription activator for phytochrome A signalling. *Genes Dev* **15**, 2613-25.
- Barnes, S.A., Quaggio, R.B., Whitelam, G.C. and Chua, N.H. (1997) *fhy1* defines a branch point in phytochrome A signal transduction pathways for gene expression. *Plant J* **10**, 1155-61.
- Barnes, S.A., Nishizawa, N.K., Quaggio, R.B., Whitelam, G.C. and Chua, N.H. (1996) Far-red light blocks greening of *Arabidopsis* seedlings via a phytochrome A-mediated change in plastid development. *Plant Cell* **8**, 601-15.
- Barnes, S.A., Quaggio, R.B. and Chua, N.H. (1995) Phytochrome signal-transduction: characterization of pathways and isolation of mutants. *Philos Trans R Soc Lond B Biol Sci* **350**, 67-74.
- Benvenuto, G., Formiggini, F., Laflamme, P., Malakhov, M. and Bowler, C. (2002) The photomorphogenesis regulator DET1 binds the aminoterminal tail of histone H2B in a nucleosome context. *Curr Biol* **12**, 1529-34.
- Bolle, C. (2004) The role of GRAS proteins in plant signal transduction and development. *Planta* **218**, 683-92.
- Bolle, C., Koncz, C. and Chua, N.H. (2000) PAT1, a new member of the GRAS family, is involved in phytochrome A signal transduction. *Genes Dev* **14**, 1269-78.
- Borthwick, H.A., Hendricks, S.B., Parker, M.W., Toole, E.H. and Toole, V.K. (1952) A Reversible Photoreaction Controlling Seed Germination. *Proc Natl Acad Sci USA* **38**, 662-6.
- Botto, J.F., Sanchez, R.A., Whitelam, G.C. and Casal, J.J. (1996) Phytochrome A Mediates the Promotion of Seed Germination by Very Low Fluences of Light and Canopy Shade Light in *Arabidopsis*. *Plant Physiol* **110**, 439-44.
- Bowler, C. and Chua, N.H. (1994) Emerging themes of plant signal transduction. *Plant Cell* **6**, 1529-41.
- Bowler, C., Neuhaus, G., Yamagata, H. and Chua, N.H. (1994) Cyclic GMP and calcium mediate phytochrome phototransduction. *Cell* **77**, 73-81.

- Bowler, C., Yamagata, H., Neuhaus, G. and Chua, N.H. (1994) Phytochrome signal transduction pathways are regulated by reciprocal control mechanisms. *Genes Dev* **8**, 2188-202.
- Brantl, S. (2002) Antisense-RNA regulation and RNA interference. *Biochim et Biophys Acta* **1575**, 15-25.
- Briggs, W.R. and Olney, M.A. (2001) Photoreceptors in plant photomorphogenesis to date. Five phytochromes, two cryptochromes, one phototropin, and one superchrome. *Plant Physiol* **125**, 85-8.
- Butler, W.L., Norris, K.H., Seigelman, H.W. and Hendricks, S.B. (1959) Detection, assay, and preliminary purification of the pigment controlling photoresponsive development of plants. *Proc Natl Acad Sci USA* **45**, 1703-08.
- Canton, F.R. and Quail, P.H. (1999) Both phyA and phyB mediated light-imposed repression of PHYA gene expression in Arabidopsis. *Plant Physiol* **121**, 1207-16.
- Casal, J.J., Yanovsky, M.J. and Luppi, J.P. (2000) Two photobiological pathways of phytochrome A activity, only one of which shows dominant negative suppression by phytochrome B. *Photochem Photobiol* **71**, 481-6.
- Casal, J.J. (2000) Phytochromes, cryptochromes, phototropin: photoreceptor interactions in plants. *Photochem Photobiol* **71**, 1-11.
- Casal, J.J., Cerdan, P.D., Staneloni, R.J. and Cattaneo, L. (1998) Different phototransduction kinetics of phytochrome A and phytochrome B in Arabidopsis thaliana. *Plant Physiol* **116**, 1533-8.
- Casal, J.J. and Mazzella, M.A. (1998) Conditional synergism between cryptochrome 1 and phytochrome B is shown by the analysis of phyA, phyB, and hy4 simple, double, and triple mutants in Arabidopsis. *Plant Physiol* **118**, 19-25.
- Casal, J.J., Sanchez, R.A. and Yanovsky, M.J. (1997) The function of phytochrome A. *Plant, Cell & Environment* **20**, 813-19.
- Casal, J.J. (1996) Phytochrome A enhances the promotion of hypocotyl growth caused by reductions in levels of phytochrome B in its far-red-light-absorbing form in light-grown Arabidopsis thaliana. *Plant Physiol* **112**, 965-73.
- Casimiro, I., Beeckman, T., Graham, N., Bhalerao, R., Zhang, H., Casero, P., Sandberg, G. and Bennett Malcolm, J. (2003) Dissecting Arabidopsis lateral root development. *Trends Plant Sci* **8**, 165-71.
- Chen, M., Chory, J. and Fankhauser, C. (2004) Light signal transduction in higher plants. *Annu Rev Genet* **38**, 87-117.
- Choi, G., Yi, H., Lee, J., Kwon, Y.K., Soh, M.S., Shin, B., Luka, Z., Hahn, T.R. and Song, P.S. (1999) Phytochrome signalling is mediated through nucleoside diphosphate kinase 2. *Nature* **401**, 610-3.
- Chory, J., Chatterjee, M., Cook, R.K., Elich, T., Fankhauser, C., Li, J., Nagpal, P., Neff, M., Pepper, A., Poole, D., Reed, J. and Vitart, V. (1996) From seed germination to flowering, light controls plant development via the pigment phytochrome. *Proc Natl Acad Sci USA* **93**, 12066-71.
- Christie, J.M. (2006) Phototropin Blue-Light Receptors. *Annu Rev Plant Biol* **26**.
- Christie, J.M., Reymond, P., Powell, G.K., Bernasconi, P., Raibekas, A.A., Liscum, E. and Briggs, W.R. (1998) Arabidopsis NPH1: a flavoprotein with the properties of a photoreceptor for phototropism. *Science* **282**, 1698-701.
- Church, G.M. and Gilbert, W. (1984) Genomic sequencing. *Proc. Natl. Acad. Sci. USA* **81**, 1991-95.
- Clack, T., Mathews, S. and Sharrock, R.A. (1994) The phytochrome apoprotein family in Arabidopsis is encoded by five genes: the sequences and expression of PHYD and PHYE. *Plant Mol Biol* **25**, 413-27.
- Clapham, D.H., Kolukisaoglu, H.U., Larsson, C.T., Qamaruddin, M., Ekberg, I., Wiegman, C., Eirund, C., Schneider-Poetsch, H.A.W. and Von Arnold, S. (1999) Phytochrome types in Picea and Pinus. Expression patterns of PHYA-related types. *Plant Mol Biol* **40**, 669-78.

- Clough, R.C., Jordan-Beebe, E.T., Lohman, K.N., Marita, J.M., Walker, J.M., Gatz, C. and Vierstra, R.D. (1999) Sequences within both the N- and C-terminal domains of phytochrome A are required for PFR ubiquitination and degradation. *Plant J* **17**, 155-67.
- Clough, S.J. and Bent, A.F. (1998) Floral dip: a simplified method for *Agrobacterium*-mediated transformation of *Arabidopsis thaliana*. *Plant J* **16**, 735-43.
- Day, R.B., Shibuya, N. and Minami, E. (2003) Identification and characterization of two new members of the GRAS gene family in rice responsive to N-acetylchitooligosaccharide elicitor. *Biochim Biophys Acta* **1625**, 261-8.
- Deng, X.W. and Quail, P.H. (1999) Signalling in light-controlled development. *Semin Cell Dev Biol* **10**, 121-9.
- Desnos, T., Puente, P., Whitelam, G.C. and Harberd, N.P. (2001) FHY1: a phytochrome A-specific signal transducer. *Genes Dev* **15**: 2980-90.
- Devlin, P.F. and Kay, S.A. (2000) Cryptochromes are required for phytochrome signalling to the circadian clock but not for rhythmicity. *Plant Cell* **12**, 2499-510.
- Devlin, P.F., Patel, S.R. and Whitelam, G.C. (1998) Phytochrome E influences internode elongation and flowering time in *Arabidopsis*. *Plant Cell* **10**, 1479-87.
- Devlin, P.F., Halliday, K.J., Harberd, N.P. and Whitelam, G.C. (1996) The rosette habit of *Arabidopsis thaliana* is dependent upon phytochrome action: novel phytochromes control internode elongation and flowering time. *Plant J* **10**, 1127-34.
- Devlin, P.F., Rood, S.B., Somers, D.E., Quail, P.H. and Whitelam, G.C. (1992) Photophysiology of the Elongated Internode (ein) Mutant of *Brassica rapa*: ein Mutant Lacks a Detectable Phytochrome B-Like Polypeptide. *Plant Physiol* **100**, 1442-7.
- Di Laurenzio, L., Wysocka-Diller, J., Malamy, J.E., Pysh, L., Helariutta, Y., Freshour, G., Hahn, M.G., Feldmann, K.A. and Benfey, P.N. (1996) The SCARECROW gene regulates an asymmetric cell division that is essential for generating the radial organization of the *Arabidopsis* root. *Cell* **86**, 423-33.
- Doyle, M.R., Davis, S.J., Bastow, R.M., Mc Watters, H.G., Kozma-Bognar, L., Nagy, F., Millar, A.J. and Amasino, R.M. (2002) The ELF4 gene controls circadian rhythms and flowering time in *Arabidopsis thaliana*. *Nature* **419**, 74-7.
- Doyle, J.J. and Doyle J.L.. (1990). Isolation of plant DNA from fresh tissue. *Focus* **12**:13-15.
- Duek, P.D. and Fankhauser, C. (2005) bHLH class transcription factors take centre stage in phytochrome signalling. *Trends Plant Sci* **10**, 51-4
- Duek, P. and Fankhauser, C. (2003) HFR1, a putative bHLH transcription factor, mediates both phytochrome A and cryptochrome signalling. *Plant J* **34**, 827-36.
- Esch, H., Hartmann, E., Cove, D., Wava, M. and Lamparter, D. (1999) Phytochrome-controlled phototropism of protonemata of the moss *ceratodon purpureus*: physiology of the wild type and class 2 ptr-mutants. *Planta* **209**, 290-8.
- Fairchild, C.D., Schumaker, M.A. and Quail, P.H. (2000) HFR1 encodes an atypical bHLH protein that acts in phytochrome A signal transduction. *Genes Dev* **14**, 2377-91.
- Fankhauser, C. (2001) The phytochromes, a family of red/far-red absorbing photoreceptors. *J Biol Chem* **276**, 11453-6.
- Fankhauser, C., and Chory, J. (2000) RSF1, an *Arabidopsis* locus implicated in phytochrome A signalling. *Plant Physiol* **124**, 39-45.
- Fankhauser, C. (2000) Phytochromes as light-modulated protein kinases. *Semin Cell Dev Biol* **11**, 467-73.

- Fankhauser, C., Yeh, K.C., Lagarias, J.C., Zhang, H., Elich, T.D. and Chory, J. (1999) PKS1, a substrate phosphorylated by phytochrome that modulates light signalling in Arabidopsis. *Science* **284**, 1539-41.
- Fankhauser, C. and Chory, J. (1997) Light control of plant development. *Annu Rev Cell Dev Biol* **13**, 203-29.
- Feinberg, A.P. and Vogelstein, B. (1983) A technique for radiolabeling DNA restriction endonuclease fragments to high specific activity. *Anal Biochem* **132**, 6-13.
- Force, A., Lynch, M., Pickett, F.B., Amores, A., Yan, Y. and Postlethwait, J. (1999) Preservation of duplicate genes by complementary, degenerative mutations. *Genetics* **151**, 1531-45.
- Fowler, S., Lee, K., Onouchi, H., Samach, A., Richardson, K., Morris, B., Coupland, G. and Putterill, J. (1999) GIGANTEA: a circadian clock-controlled gene that regulates photoperiodic flowering in Arabidopsis and encodes a protein with several possible membrane-spanning domains. *EMBO J* **18**, 4679-88.
- Franklin, K.A., Larner, V.S. and Whitelam, G.C. (2005) The signal transducing photoreceptors of plants. *Int J Dev Biol* **49**, 653-64.
- Franklin, K.A. and Whitelam, G.C. (2005) Phytochromes and shade-avoidance responses in plants. *Ann Bot (Lond)* **96**, 169-75.
- Franklin, K.A. and Whitelam, G.C. (2004) Light signals, phytochromes and cross-talk with other environmental cues. *J Exp Bot* **55**, 271-6.
- Franklin, K.A., Davis, S.J., Stoddart, W.M., Vierstra, R.D. and Whitelam, G.C. (2003) Mutant analyses define multiple roles for phytochrome C in Arabidopsis photomorphogenesis. *Plant Cell* **15**, 1981-9.
- Franklin, K.A., Praekelt, U., Stoddart, W.M., Billingham, O.E., Halliday, K.J. and Whitelam, G.C. (2003) Phytochromes B, D, and E act redundantly to control multiple physiological responses in Arabidopsis. *Plant Physiol* **131**, 1340-6.
- Franks, R. G., Wang, C., Levin, J. Z. and Liu, Z. (2002) SEUSS, a member of a novel family of plant regulatory proteins, represses floral homeotic gene expression with LEUNIG. *Development* **129**, 253-63.
- Fukaki, H., Wysocka-Diller, J., Kato, T., Fujisawa, H., Benfey, P.N. and Tasaka, M. (1998) Genetic evidence that the endodermis is essential for shoot gravitropism in Arabidopsis thaliana. *Plant J* **14**, 425-30.
- Furuya, M., and Song, P.-S. (1994) Assembly and properties of holophytochrome. *Photomorphogenesis in Plants* (R. E. Kendrick and G. H. M. Kronenberg, Eds.), 105-40.
- Furuya, M. (1993) Phytochromes: their molecular species, gene family and functions. *Annu. Rev. Plant Physiol. Plant Mol. Biol.* **44**, 617-45.
- Gilbert, I. R., Seavers, G. P., Jarvis, P. G. and Smith, H. (1995) Photomorphogenesis and canopy dynamics. Phytochrome-mediated proximity perception accounts for the growth dynamics of canopies of *Populus trichocarpa* X *deltoides* 'Beaupré'. *Plant Cell Env* **18**, 475-97.
- Greb, T., Clarenz, O., Schafer, E., Muller, D., Herrero, R., Schmitz, G. and Theres, K. (2003) Molecular analysis of the LATERAL SUPPRESSOR gene in Arabidopsis reveals a conserved control mechanism for axillary meristem formation. *Genes Dev* **17**, 1175-87.
- Guo, H., Mockler, T., Duong, H. and Lin, C. (2001) SUB1, an Arabidopsis Ca²⁺-binding protein involved in cryptochrome and phytochrome coaction. *Science* **19**, 487-90.
- Halliday, K.J. and Fankhauser, C. (2003) Phytochrome-hormonal signalling networks. *New Phytol* **157**, 449-59.
- Haupt, W. and Häder, D.P. (1994) Photomovement. *Photomorphogenesis in Plants*, 702-32.

- Heery, D.M., Kalkhoven, E., Hoare, S. and Parker, M.G. (1997) A signature motif in transcriptional co-activators mediates binding to nuclear receptors. *Nature* **387**, 733-6.
- Heckmann, A.B., Lombardo, F., Miwa, H., Perry, J.A., Bunnewell, S., Parniske, M., Wang, T.L. and Downie, J.A. (2006) Lotus japonicus nodulation requires two GRAS domain regulators, one of which is functionally conserved in a non-legume. *Plant Physiol* **142**, 1739-50.
- Helariutta, Y., Fukaki, H., Wysocka-Diller, J., Nakajima, K., Jung, J., Sena, G., Hauser, M.T. and Benfey, P.N. (2000) The SHORT-ROOT gene controls radial patterning of the Arabidopsis root through radial signalling. *Cell* **101**, 555-67.
- Hennig, L., Stoddart, W.M., Dieterle, M., Whitelam, G.C. and Schafer, E. (2002) Phytochrome E controls light-induced germination of Arabidopsis. *Plant Physiol* **128**, 194-200.
- Hennig, L., Poppe, C., Sweere, U., Martin, A. and Schäfer, E. (2001) Negative interference of endogenous phytochrome B with phytochrome A function in Arabidopsis. *Plant Physiol* **125**, 1036-44.
- Hennig, L., Buche, C., Eichenberg, K. and Schafer, E. (1999) Dynamic properties of endogenous phytochrome A in Arabidopsis seedlings. *Plant Physiol* **121**, 571-7.
- Hennig, L., Funk, M., Whitelam, G.C. and Schafer, E. (1999) Functional interaction of cryptochrome 1 and phytochrome D. *Plant J* **20**, 289-94.
- Hennig, L., Poppe, C., Unger, S. and Schafer, E. (1999) Control of hypocotyl elongation in Arabidopsis thaliana by photoreceptor interaction. *Planta* **208**, 257-63.
- Hirschfeld, M., Tepperman, J.M., Clack, T., Quail, P.H. and Sharrock, R.A. (1998) Coordination of phytochrome levels in phyB mutants of Arabidopsis as revealed by apoprotein-specific monoclonal antibodies. *Genetics* **149**, 523-35.
- Hoecker, U., Toledo-Ortiz, G., Bender, J. and Quail, P.H. (2004) The photomorphogenesis-related mutant red1 is defective in CYP83B1, a red light-induced gene encoding a cytochrome P450 required for normal auxin homeostasis. *Planta* **219**, 195-200.
- Hoecker, U., Tepperman, J.M. and Quail, P.H. (1999) SPA1, a WD-repeat protein specific to phytochrome A signal transduction. *Science* **284**, 496-99.
- Hoecker, U., Xu, Y. and Quail, P. (1998) SPA1: A new genetic locus involved in phytochrome A-specific signal transduction. *Plant Cell* **10**, 19-33.
- Hudson, M., Ringli, C., Boylan, M.T. and Quail, P.H. (1999) The FAR1 locus encodes a novel nuclear protein specific to phytochrome A signalling. *Genes Dev* **13**, 2017-27.
- Hudson, M., Robson, P.R., Kraepiel, Y., Caboche, M. and Smith, H. (1997) Nicotiana plumbaginifolia hlg mutants have a mutation in a PHYB-type phytochrome gene: they have elongated hypocotyls in red light, but are not elongated as adult plants. *Plant J* **12**, 1091-101.
- Hughes, J. and Lamparter, T. (1999) Prokaryotes and phytochrome. The connection to chromophores and signalling. *Plant Physiol* **121**, 1059-68.
- Hughes, J., Lamparter, T., Mittmann, F. and Hartmann, E. (1997) A prokaryotic phytochrome. *Nature*, 386-663.
- Huq, E., Tepperman, J.M. and Quail, P.H. (2000) GIGANTEA is a nuclear protein involved in phytochrome signalling in Arabidopsis. *Proc Natl Acad Sci U S A* **97**, 9789-94.
- Ikeda, A., Ueguchi-Tanaka, M., Sonoda, Y., Kitano, H., Koshioka, M., Futsuhara, Y., Matsuoka, M. and Yamaguchi, J. (2001) slender rice, a constitutive gibberellin response mutant, is caused by a null mutation of the SLR1 gene, an ortholog of the height-regulating gene GAI/RGA/RHT/D8. *Plant Cell* **13**, 999-1010.
- Itoh, H., Ueguchi-Tanaka, M., Sato, Y., Ashikari, M. and Matsuoka, M. (2002) The gibberellin signalling pathway is regulated by the appearance and disappearance of SLENDER RICE1 in nuclei. *Plant Cell* **14**, 57-70.

- Jurata, L. W. and Gill, G. N. (1997) Functional analysis of the nuclear LIM domain interactor NLI. *Mol Cell Biol* **17**, 5688-98.
- Kalo, P., Gleason, C., Edwards, A., Marsh, J., Mitra, R.M., Hirsch, S., Jakab, J., Sims, S., Long, S.R., Rogers, J., Kiss, G.B., Downie, J.A. and Oldroyd, G.E. (2005) Nodulation signalling in legumes requires NSP2, a member of the GRAS family of transcriptional regulators. *Science* **308**, 1786-89.
- Karimi, M., Inze, D. and Depicker, A. (2002) GATEWAY vectors for Agrobacterium-mediated plant transformation. *Trends Plant Sci* **7**, 193-5.
- Kehoe, D.M. and Grossman, R. (1996) Similarity of a chromatic adaptation sensor to phytochrome and ethylene receptors. *Science* **273**, 1409-12.
- Kendrick, R.E., Peters, J.L., Kerckhoffs, L.H., van Tuinen, A. and Koornneef, M. (1994) Photomorphogenic mutants of tomato. *Biochem Soc Symp* **60**, 249-56.
- Kendrick, R.E. and Kronenberg, G.H.M. (1994) Photomorphogenesis in plants. *Kluwer Academic, Dordrecht*.
- Khanna, R., Kikis, E.A. and Quail, P.H. (2003) EARLY FLOWERING 4 functions in phytochrome B-regulated seedling de-etiolation. *Plant Physiol* **133**, 1530-8.
- Kim, J.I., Shen, Y., Han, Y.J., Park, J.E., Kirchenbauer, D., Soh, M.S., Nagy, F., Schafer, E. and Song, P.S. (2004) Phytochrome phosphorylation modulates light signalling by influencing the protein-protein interaction. *Plant Cell* **16**, 2629-40.
- Kim, J.I., Kozhukh, G.V. and Song, P.S. (2002) Phytochrome-mediated signal transduction pathways in plants. *Biochem Biophys Res Commun* **298**, 457-63.
- Kircher, S., Kozma-Bognar, L., Kim, L., Adam, E., Harter, K., Schafer, E. and Nagy, F. (1999) Light quality-dependent nuclear import of the plant photoreceptors phytochrome A and B. *Plant Cell* **11**, 1445-56.
- Koncz, C., Martini, N., Szabados, L., Hrouda, M., Bachmair and Schell, J. (1994) Specialized vectors for gene tagging and expression studies. In: *Plant Molecular Biology Manual*. Vol. B2 (Gelvin, S.B. and Schilperoort, R.A., eds). Dordrecht: Kluwer Academic Publishers, 1-22.
- Koornneef, M., Rolff, E. and Spruitt, C.J.P. (1980) Genetic control of light-inhibited hypocotyl elongation in *Arabidopsis thaliana*. *Zeitschrift für pflanzenphysiologie* **100**, 147-60.
- Kost, B., Spielhofer, P. and Chua, N.H. (1998) A GFP-mouse talin fusion protein labels plant actin filaments in vivo and visualizes the actin cytoskeleton in growing pollen tubes. *Plant J* **16**, 393-401.
- Kuno, N. and Furuya, M. (2000) Phytochrome regulation of nuclear gene expression in plants. *Semin Cell Dev Biol* **11**, 485-93.
- Lagarias, J.C. and Rapoport, H. (1980) Chromopeptides from phytochrome. The structure and linkage of the Pr form of the phytochrome chromophore. *J Am Chem Soc* **102**, 4821-8.
- Lapko, V.N., Jiang, X.Y., Smith, D.L. and Song, P.S. (1999) Mass spectrometric characterization of oat phytochrome A: isoforms and posttranslational modifications. *Protein Sci* **8**, 1032-44.
- Lapko, V.N., Jiang, X.Y., Smith, D.L. and Song, P.S. (1997) Posttranslational modification of oat phytochrome A: phosphorylation of a specific serine in a multiple serine cluster. *Biochemistry* **36**, 10595-9.
- Lariguet, P. and Fankhauser, C. (2004) Hypocotyl growth orientation in blue light is determined by phytochrome A inhibition of gravitropism and phototropin promotion of phototropism. *Plant J* **40**, 826-34.
- Laubinger, S., Fittinghoff, K. and Hoecker, U. (2004) The SPA quartet: a family of WD-Repeat proteins with a central role in suppression of photomorphogenesis in *Arabidopsis*. *Plant Cell* **16**, 2293-06.

- Liu, X.L., Covington, M.F., Fankhauser, C., Chory, J. and Wagner, D.R. (2001) ELF3 encodes a circadian clock-regulated nuclear protein that functions in an Arabidopsis PHYB signal transduction pathway. *Plant Cell* **13**, 1293-304.
- Liu, X.L., White, M.J. and Mc Rae, T.H. (1999) Transcription factors and their genes in higher plants functional domains, evolution and regulation. *Eur J Biochem* **262**, 247-57.
- Lopez-Juez, E., Nagatani, A., Tomizawa, K., Deak, M., Kern, R., Kendrick, R.E. and Furuya, M. (1992) The cucumber long hypocotyl mutant lacks a light-stable PHYB-like phytochrome. *Plant Cell* **4**, 241-51.
- Lynch, M. and Conery, J.S. (2000) The evolutionary fate and consequences of duplicate genes. *Science* **290**, 1151-55.
- Lynch, M. and Force, A. (2000) The probability of duplicate gene preservation by subfunctionalization. *Genetics* **154**, 459-73.
- Ma, L. G. *et al.* (2001) Light control of Arabidopsis development entails coordinated regulation of genome expression and cellular pathways. *Plant Cell* **13**, 2589-607.
- Mathews, S. (2006) Phytochrome-mediated development in land plants: red light sensing evolves to meet the challenges of changing light environments. *Mol Ecol* **15**, 3483-503.
- Mathews, S. and Donoghue, M.J. (1999) The root of angiosperm phylogeny inferred from duplicate phytochrome genes. *Science* **286**, 947-50.
- Mathews, S. and Sharrock, R.A. (1997) Phytochrome gene diversity. *Plant, Cell & Environment* **20**, 666-71.
- Mathews, S., Lavin, M. and Sharrock, R.A. (1995) Evolution of the phytochrome gene family and its utility for phylogenetic analyses of angiosperms. *Annals of the Missouri Botanical Garden* **82**, 296-321.
- Matsushita, T., Mochizuki, N. and Nagatani, A. (2003) Dimers of the N-terminal domain of phytochrome B are functional in the nucleus. *Nature* **424**, 571-4.
- McMaster, G.K. and Carmichael, G.G. (1977) Analysis of single and double-stranded nucleic acids on polyacrilamid and agarose gels by using glyoxal and acridine orange. *Proc Natl Acad Sci* **74**, 4835-8.
- Millar, A.J., Straume, M., Chory, J., Chua, N.H. and Kay, S.A. (1995) The regulation of circadian period by phototransduction pathways in Arabidopsis. *Science* **267**, 1163-6.
- Millar, A.J., McGrath, R.B. and Chua, N.H. (1994) Phytochrome phototransduction pathways. *Annu Rev Genet* **28**, 325-49.
- Monte, E., Alonso, J.M., Ecker, J.R., Zhang, Y., Li, X., Young, J., Austin-Phillips, S. and Quail, P.H. (2003) Isolation and characterization of phyC mutants in Arabidopsis reveals complex crosstalk between phytochrome signalling pathways. *Plant Cell* **15**, 1962-80.
- Montgomery, B.L. and Lagarias, J.C. (2002) Phytochrome ancestry: sensors of bilins and light. *Trends Plant Sci* **7**, 357-66.
- Moore, I. (2002) Gravitropism: lateral thinking in auxin transport. *Curr Biol* **12**, 452-4.
- Morohashi, K., Minami, M., Takase, H., Hotta, Y. and Hiratsuka, K. (2003) Isolation and characterization of a novel GRAS gene that regulates meiosis-associated gene expression. *J Biol Chem* **278**, 20865-73.
- Morelli, G. and Ruberti, I. (2002) Light and shade in the photocontrol of Arabidopsis growth. *Trends Plant Sci* **7**, 399-404.
- Mouradov, A., Cremer, F., and Coupland, G. (2002) Control of flowering time: interacting pathways as a basis for diversity. *Plant Cell* **14**, 111-30.
- Mustilli, A.C. and Bowler, C. (1997) Tuning in to the signals controlling photoregulated gene expression in plants. *EMBO J* **16**, 5801-6.

- Nagatani, A. (2004) Light-regulated nuclear localization of phytochromes. *Curr Opin Plant Biol* **7**, 708-11.
- Nagatani, A., Reed, J.W. and Chory, J. (1993) Isolation and Initial Characterization of Arabidopsis Mutants That Are Deficient in Phytochrome A. *Plant Physiol* **102**, 269-77.
- Nagy, F., Kircher, S. and Schafer, E. (2000) Nucleo-cytoplasmic partitioning of the plant photoreceptors phytochromes. *Semin Cell Dev Biol* **11**, 505-10.
- Nakajima, K., Sena, G., Nawy, T. and Benfey, P.N. (2001) Intercellular movement of the putative transcription factor SHR in root patterning. *Nature* **413**, 307-11.
- Neff, M.M., Fankhauser, C. and Chory, J. (2000) Light: an indicator of time and place. *Genes Dev* **14**, 257-71.
- Neff, M.M. and Chory, J. (1998) Genetic interactions between phytochrome A, phytochrome B, and cryptochrome 1 during Arabidopsis development. *Plant Physiol* **118**, 27-35.
- Neff, M.M. and Van Volkenburgh, E. (1994) Light-Stimulated Cotyledon Expansion in Arabidopsis Seedlings (The Role of Phytochrome B). *Plant Physiol* **104**, 1027-1032.
- Neuhaus, G., Bowler, C., Kern, R. and Chua, N.H. (1993) Calcium/calmodulin-dependent and -independent phytochrome signal transduction pathways. *Cell* **73**, 937-52.
- Ni, M., Tepperman, J.M. and Quail, P.H. (1998) PIF3, a phytochrome-interacting factor necessary for normal photoinduced signal transduction, is a novel basic helix-loop-helix protein. *Cell* **95**, 657-67.
- Nishiyama, T. *et al.* (2003) Comparative genomics of *Physcomitrella patens* gametophytic transcriptome and *Arabidopsis thaliana*: implication for land plants evolution. *Proc Natl Acad Sci* **100**, 8007-12.
- Nozue, K. *et al.* (1998) A phytochrome from the fern *Adiantum* with features of the putative photoreceptor NPH1. *Proc Natl Acad Sci USA* **95**, 15826-30.
- Ohno, S. (1970) Evolution by gene duplication. *Springer-Verlag*, Berlin.
- Ogawa, M., Kusano, T., Katsumi, M. and Sano, H. (2000) Rice gibberellininsensitive gene homolog, OsGAI, encodes a nuclear-localized protein capable of gene activation at transcriptional level. *Gene* **245**, 21-9.
- Oyama, T., Shimura, Y. and Okada, K. (1997) The Arabidopsis HY5 gene encodes a bZIP protein that regulates stimulus-induced development of root and hypocotyl. *Genes Dev* **11**, 2983-95.
- Park, C.M., Bhoo, S.H. and Song, P.S. (2000) Inter-domain crosstalk in the phytochrome molecules. *Semin Cell Dev Biol* **11**, 449-56.
- Park, D.H., Lim, P.O., Kim, J.S., Cho, D.S., Hong, S.H. and Nam, H.G. (2003) The Arabidopsis COG1 gene encodes a Dof domain transcription factor and negatively regulates phytochrome signalling. *Plant J* **34**, 161-71.
- Parks, B.M. and Spalding, E.P. (1999) Sequential and coordinated action of phytochromes A and B during Arabidopsis stem growth revealed by kinetic analysis. *Proc Natl Acad Sci USA* **96**, 14142-6.
- Parks, B.M., Quail, P.H. and Hangarter, R.P. (1996) Phytochrome A regulates red-light induction of phototropic enhancement in Arabidopsis. *Plant Physiol* **110**, 155-62.
- Parks, B.M. and Quail, P.H. (1993) hy8, a new class of arabidopsis long hypocotyl mutants deficient in functional phytochrome A. *Plant Cell* **5**, 39-48.
- Patschinsky, T., Hunter, T., Esch, F.S., Cooper, J.A. and Sefton, B.M. (1982) Analysis of the sequence of amino acids surrounding sites of tyrosine phosphorylation. *Proc Natl Acad Sci USA* **79**, 973-7.
- Peng, J., Richards, D.E., Moritz, T., Cano-Delgado, A. and Harberd, N.P. (1999) Extragenic suppressors of the Arabidopsis gai mutation alter the dose-response relationship of diverse gibberellin responses. *Plant Physiol* **119**, 1199-208.

- Peng, J., Carol, P., Richards, D.E., King, K.E., Cowling, R.J., Murphy, G.P. and Harberd, N.P. (1997) The Arabidopsis GAI gene defines a signalling pathway that negatively regulates gibberellin responses. *Genes Dev* **11**, 3194-205.
- Polaina, J. and Adam, A.C. (1991) A fast procedure for yeast DNA purification. *Nucleic Acids Res* **19**, 5443.
- Poppe, C. and Schäfer, E. (1997) Seed germination of Arabidopsis thaliana phyA/phyB double mutants is under phytochrome control. *Plant Physiol* **114**, 1487-92.
- Pysh, L.D., Wysocka-Diller, J.W., Camilleri, C., Bouchez, D. and Benfey, P.N. (1999) The GRAS gene family in Arabidopsis: sequence characterization and basic expression analysis of the SCARECROW-LIKE genes. *Plant J* **18**, 111-9.
- Quail, P.H. (1997) The phytochromes: a biochemical mechanism of signalling in sight? *Bioessays* **19**, 571-9.
- Quail, P.H., Boylan, M.T., Parks, B.M., Short, T.W., Xu, Y. and Wagner, D. (1995) Phytochromes: photosensory perception and signal transduction. *Science* **268**, 675-80.
- Reed, J.W., Nagatani, A., Elich, T.D., Fagan, M. and Chory, J. (1994) Phytochrome A and Phytochrome B Have Overlapping but Distinct Functions in Arabidopsis Development. *Plant Physiol* **104**, 1139-49.
- Robson, P.R. and Smith, H. (1996) Genetic and transgenic evidence that phytochromes A and B act to modulate the gravitropic orientation of Arabidopsis thaliana hypocotyls. *Plant Physiol* **110**, 211-6.
- Robson, P., Whitelam, G.C. and Smith, H. (1993) Selected Components of the Shade-Avoidance Syndrome Are Displayed in a Normal Manner in Mutants of Arabidopsis thaliana and Brassica rapa Deficient in Phytochrome B. *Plant Physiol* **102**, 1179-84.
- Rockwell, N.C. and Lagarias, J.C. (2006) The structure of phytochrome: a picture is worth a thousand spectra. *Plant Cell* **18**, 4-14.
- Rockwell, N.C., Su, Y.S. and Lagarias, J.C. (2006) Phytochrome structure and signalling mechanisms. *Annu Rev Plant Biol* **57**, 837-58.
- Roux, S.J. (1994) Signal transduction in phytochrome responses. In "Photomorphogenesis in Plants" (R. E. Kendrick and G. H. M. Kronenberg, Eds.). *Kluwer Academic Publishers*, 187-209.
- Ryu, J.S., Kim, J.I., Kunkel, T., Kim, B.C., Cho, D.S., Hong, S.H., Kim, S.H., Fernandez, A.P., Kim, Y., Alonso, J.M., Ecker, J.R., Nagy, F., Lim, P.O., Song, P.S., Schäfer, E. and Nam, H.G. (2005) Phytochrome-specific type 5 phosphatase controls light signal flux by enhancing phytochrome stability and affinity for a signal transducer. *Cell* **120**, 395-406.
- Sabatini, S., Beis, D., Wolkenfelt, H., Murfett, J., Guilfoyle, T., Malamy, J., Benfey, P., Leyser, O., Bechtold, N., Weisbeek, P. et al. (1999). An auxin-dependent distal organizer of pattern and polarity in the Arabidopsis root. *Cell* **99**, 463-72.
- Sakamoto, K. and Nagatani, A. (1996) Nuclear localization activity of phytochrome B. *Plant J* **10**, 859-68.
- Schäfer, E. and Nagy, F. (2006) Photomorphogenesis in plants and bacteria: function and signal transduction mechanisms. *Springer, Berlin Heidelberg, New York*.
- Schaffer, R., Ramsay, N., Samach, A., Corden, S., Putterill, J., Carre, I.A. and Coupland, G. (1998) The late elongated hypocotyl mutation of Arabidopsis disrupts circadian rhythms and the photoperiodic control of flowering. *The Cell* **93**, 1219-29.
- Schmid, M., Davison, T.S., Henz, S.R., Pape, U.J., Demar, M., Vingron, M., Scholkopf, B., Weigel, D. and Lohmann, J.U. (2005) A gene expression map of Arabidopsis thaliana development. *Nat Genet* **37**, 501-6.
- Schmidt, M. and Schneider-Poetsch, H.A.W. (2002) The evolution of gymnosperms redrawn by phytochrome genes: The Gnetales appear at the base of the gymnosperms. *J. Mol. Evol.* **54**, 715-24.

- Schmitt, J., McCormac, A.C. and Smith, H. (1995) A test of the adaptive plasticity hypothesis using transgenic and mutant plants disabled in phytochrome-mediated elongation responses to neighbors. *American Naturalist* **146**, 937-53.
- Schneider-Poetsch, H. A. W., Kolukisaoglu, D. H., Clapham, J., Hughes, and Lamparter, T. (1998) Non-angiosperm phy-tochromes and evolution of vascular plants. *Physiol Plant* **102**, 612-22.
- Schumacher, K., Schmitt, T., Rossberg, M., Schmitz, G. and Theres, K. (1999) The Lateral suppressor (Ls) gene of tomato encodes a new member of the VHIID protein family. *Proc Natl Acad Sci USA* **96**, 290-5.
- Seo, H.S., Watanabe, E., Tokutomi, S., Nagatani, A. and Chua, N.H. (2004) Photoreceptor ubiquitination by COP1 E3 ligase desensitizes phytochrome A signalling. *Genes Dev* **18**, 617-22.
- Shao, H.B., Liang, Z.S. and Shao, M.A. (2005) Adaptation of higher plant to stress environment and stress signal transduction. *Acta Ecol Sin* **25**, 1772-81.
- Shao, H.B. (2001) The gene expression and control of flowering time in higher plants. *Biol. Biotech.* **6**, 12-8.
- Sharrock, R.A. and Clack, T. (2002) Patterns of expression and normalized levels of the five Arabidopsis phytochromes. *Plant Physiol* **130**, 442-56.
- Sharrock, R.A. and Quail, P.H. (1989) Novel phytochrome sequences in Arabidopsis thaliana: structure, evolution, and differential expression of a plant regulatory photoreceptor family. *Genes Dev* **3**, 1745-57.
- Shinomura, T., Uchida, K. and Furuya, M. (2000) Elementary processes of photoperception by phytochrome A for high-irradiance response of hypocotyl elongation in Arabidopsis. *Plant Physiol* **122**, 147-56.
- Shinomura, T. (1997) Phytochrome regulation of seed germination. *J Plant Research* **110**, 151-61.
- Shinomura, T., Nagatani, A., Hanzawa, H., Kubota, M., Watanabe, M. and Furuya, M. (1996) Action spectra for phytochrome A- and B-specific photoinduction of seed germination in Arabidopsis thaliana. *Proc Natl Acad Sci USA* **93**, 8129-33.
- Shinomura, T., Nagatani, A., Chory, J. and Furuya, M. (1994) The Induction of Seed Germination in Arabidopsis thaliana Is Regulated Principally by Phytochrome B and Secondarily by Phytochrome A. *Plant Physiol* **104**, 363-71.
- Smit, P., Raedts, J., Portyanko, W., Debelle, F., Gough, C., Bisseling, T. and Geurts, R. (2005) NSP1 of the GRAS protein family is essential for rhizobial Nod factor-induced transcription. *Science* **17**, 1789-91.
- Smith, H. (2000) Phytochromes and light signal perception by plants- an emerging synthesis. *Nature* **407**, 585-91.
- Smith, H., Xu, Y. and Quail, P.H. (1997) Antagonistic but complementary actions of phytochromes A and B allow seedling de-etiolation. *Plant Physiol* **114**, 637-41.
- Smith, H. and Whitelam, G.C. (1997) The shade avoidance syndrome: multiple responses mediated by multiple phytochromes. *Plant, Cell and Environment* **20**, 840-4.
- Smith, H. (1995) Physiological and ecological function within the phytochrome family. *Annu. Rev. Plant Physiol. Plant Mol. Biol.* **46**, 289-315.
- Smith, H. (1982) Light quality, photoperception, and plant strategy. *Annual Review of Plant Physiology* **33**, 481-518.
- Soh, M.S., Kim, Y.-M., Han, S.-J. and Song, P.-S. (2000) REP1, a basic helix-loop-helix protein, is required for a branch pathway of phytochrome A signalling in Arabidopsis. *Plant Cell* **12**, 2061-73.
- Somers, D.E. and Quail, P.H. (1995) Temporal and spatial expression patterns of PHYA and PHYB genes in Arabidopsis. *Plant J* **7**, 413-27.

- Somers, D.E., Sharrock, R.A., Tepperman, J.M. and Quail, P.H. (1991) The hy3 Long Hypocotyl Mutant of Arabidopsis Is Deficient in Phytochrome B. *Plant Cell* **3**, 1263-74.
- Song, P.S. (1999) Inter-domain signal transmission within the phytochromes. *J Biochem Mol Biol* **32**, 215-25.
- Sperling, U., van Cleve, B., Frick, G., Apel, K. and Armstrong, G.A. (1997) Overexpression of light-dependent PORA or PORB in plants depleted of endogenous POR by far-red light enhances seedling survival in white light and protects against photooxidative damage. *Plant J* **12**, 649-58.
- Steiger, D., Allenbach, L., Salathia, N., Fiechter, V., Davis, S.J., Millar, A.J., Chory, J. and Fankhauser, C. (2003) The Arabidopsis SSR1 gene mediates phyB signalling and is required for normal circadian clock function. *Genes Dev* **17**, 256-68.
- Steindler, C., Matteucci, A., Sessa, G., Weimar, T., Ohgishi, M., Aoyama, T., Morelli, G. and Ruberti, I. (1999) Shade avoidance responses are mediated by the ATHB-2 HD-zip protein, a negative regulator of gene expression. *Development* **126**, 4235-45
- Stockhaus, J., Nagatani, A., Halfter, U., Kay, S., Furuya, M. and Chua, N.H. (1992) Serine-to-alanine substitutions at the amino-terminal region of phytochrome A result in an increase in biological activity. *Genes Dev* **6**, 2364-72.
- Sridhar, V.V., Surendrarao, A., Gonzalez, D., Conlan, R.S. and Liu, Z. (2004) Transcriptional repression of target genes by LEUNIG and SEUSS, two interacting regulatory proteins for Arabidopsis flower development. *Proc Natl Acad Sci U S A* **101**, 11494-9.
- Stuurman, J., Jaggi, F. and Kuhlemeier, C. (2002) Shoot meristem maintenance is controlled by a GRAS-gene mediated signal from differentiating cells. *Genes Dev* **16**, 2213-8.
- Sullivan, A. and Deng, X-W. (2003) From seed to seed: the role of photoreceptors in Arabidopsis development. *Developmental Biology* **260**, 289-97.
- Takano, M., Xie, X., Inagaki, N. and Shinomura, T. (2005) Distinct functions of phytochromes on the photomorphogenesis in rice. In *Light Sensing in Plants*, M. Wada, K. Shimazaki, and M. Iino, eds (Tokyo: Springer-Verlag), 111-7.
- Takano, M., Kanegae, H., Shinomura, T., Miyao, A., Hirochika, H. and Furuya, M. (2001) Isolation and characterization of rice phytochrome A mutants. *Plant Cell* **13**, 521-34.
- Tepperman, J.M., Zhu, T., Chang, H.S., Wang, X. and Quail, P.H. (2001) Multiple transcription-factor genes are early targets of phytochrome A signalling. *Proc Natl Acad Sci USA* **98**, 9437-42.
- Terzaghi, W.B. and Cashmore, A.R. (1995) Light-regulated transcription. *Annu Rev Plant Physiol. Plant Mol Biol* **46**, 445-74.
- Thümmler, F., Dufner, M., Kreisl, P. and Dittrich, P. (1992) Molecular cloning of a novel phytochrome gene of the moss *Ceratodon purpureus* which encodes a putative light-regulated protein kinase. *Plant Mol Biol* **20**, 1003-17.
- Tian, C., Wan, P., Sun, S., Li, J. and Chen, M. (2004) Genome-wide analysis of the GRAS gene family in rice and Arabidopsis. *Plant Mol Biol* **54**, 519-32.
- Toledo-Ortiz, G., Huq, E. and Quail, P.H. (2003) The Arabidopsis basic/helix-loop-helix transcription factor family. *Plant Cell* **15**, 1749-70.
- Torres-Galea, P., Huang, L.F., Chua, N.H. and Bolle, C. (2006) The GRAS protein SCL13 is a positive regulator of phytochrome-dependent red light signalling, but can also modulate phytochrome A responses. *Mol Genet Genomics* **276**, 13-30.
- Van der Krol, A.R. and Chua, N.H. (1991) The basic domain of plant B-ZIP proteins facilitates import of a reporter protein into plant nuclei. *Plant Cell* **3**, 667-75.
- Van Meyel, D. J., Thomas, J. B. and Agulnick, A. D. (2003) *Development* **130**, 1915-25.

- Van Tuinen, A., Kerckhoffs, L., Nagatani, A., Kendrick, R.E. and Koornneef, M. (1995) A Temporarily Red Light-Insensitive Mutant of Tomato Lacks a Light-Stable, B-Like Phytochrome. *Plant Physiol* **108**, 939-947.
- Van Tuinen, A., Kerckhoffs, L.H., Nagatani, A., Kendrick, R.E. and Koornneef, M. (1995) Far-red light-insensitive, phytochrome A-deficient mutants of tomato. *Mol Gen Genet* **246**, 133-41.
- Vierstra, R.D. and Davis, S.J. (2000) Bacteriophytochromes: new tools for understanding phytochrome signal transduction. *Semin Cell Dev Biol* **11**, 511-21.
- Wagner, A. (2001) Birth and death of duplicated genes in completely sequenced eukaryotes. *Trends Genet* **17**, 23-39.
- Wagner, D., Fairchild, C.D., Kuhn, R.M. and Quail, P.H. (1996) Chromophore-bearing NH₂-terminal domains of phytochromes A and B determine their photosensory specificity and differential light lability. *Proc Natl Acad Sci USA* **93**, 4011-5.
- Wagner, J.R., Brunzelle, J.S., Forest, K.T. and Vierstra R.D. (2005) A light-sensing knot revealed by the structure of the chromophore-binding domain of the phytochrome. *Nature* **438**, 325-331.
- Walsh, J. B. (1995) How often do duplicated genes evolve new functions? *Genetics* **110**, 345-64.
- Wang, H. and Deng, X.W. (2004) Phytochrome Signalling mechanism. Arabidopsis Book (C. R. Somerville and E. Meyerowitz, Eds.). American Society of Plant Biologists, Rockville, MD.
- Wang, H. and Deng, X.W. (2003) Dissecting the phytochrome A-dependent signalling network in higher plants. *Trends Plant Sci* **8**, 172-8.
- Wang, H., Ma, L., Habashi, J., Li, J., Zhao, H. and Deng, X.W. (2002) Analysis of far-red light-regulated genome expression profiles of phytochrome A pathway mutants in Arabidopsis. *Plant J* **32**, 723-33.
- Wang, H. and Deng, X.W. (2002) Arabidopsis FHY3 defines a key phytochrome A signalling component directly interacting with its homologous partner FAR1. *EMBO J.* **21**, 1339-49.
- Wang, S., Narendra, S. and Fedoroff, N. (2007) Heterotrimeric G protein signalling in the Arabidopsis unfolded protein response. *Proc Natl Acad Sci USA* **6**, 3817-22.
- Wang, Z.Y., Kenigsbuch, D., Sun, L., Harel, E., Ong, M.S. and Tobin, E.M. (1997) A Myb-related transcription factor is involved in the phytochrome regulation of an Arabidopsis Lhcb gene. *Plant Cell* **9**, 491-507.
- Ward, J.M., Cufr, C.A., Denzel, M.A. and Neff, M.M. (2005) The Dof Transcription Factor OBP3 Modulates Phytochrome and Cryptochrome Signalling in Arabidopsis. *Plant Cell* **17**, 475-85.
- Wei, N. and Deng, X.W. (2003) The COP9 signalosome. *Annu Rev Cell Dev Biol.* **19**, 261-86.
- Weller, J.L., Beauchamp, N., Kerckhoffs, L.H., Platten, J.D. and Reid, J.B. (2000) Interaction of phytochromes A and B in the control of de-etiolation and flowering in pea. *Plant J* **26**, 283-94.
- Whitelam, G. C. and Devlin, P. F. (1997) Roles of different phytochromes in Arabidopsis photomorphogenesis. *Plant Cell Environ* **20**, 752-8.
- Whitelam, G.C., Johnson, E., Peng, J., Carol, P., Anderson, M.L., Cowl, J.S. and Harberd, N.P. (1993) Phytochrome A null mutants of Arabidopsis display a wild-type phenotype in white light. *Plant Cell* **5**, 757-68.
- Wu, S.H. and Lagarias, J.C. (2000) Defining the bilin lyase domain: lessons from the extended phytochrome superfamily. *Biochemistry* **39**, 13487-95.
- Wu, Y., Hiratsuka, K., Neuhaus, K. and Chua, N.H. (1996) Calcium and cGMP target distinct phytochrome-responsive elements. *Plant J* **10**, 1149-54.
- Xu, W., Campbell, P., Vargheese, A.K. and Braam, J. (1996) The Arabidopsis XET-related gene family: environmental and hormonal regulation of expression. *Plant J.* **9**, 879-89.

- Yanagawa, Y., Sullivan, J. A., Komatsu, S., Gusmaroli, G., Suzuki, G., Yin, J., Ishibashi, T., Saijo, Y., Rubio, V., Kimura, S., Wang, J., and Deng, X. W. (2004) Arabidopsis COP10 forms a complex with DDB1 and DET1 in vivo and enhances the activity of ubiquitin conjugating enzymes. *Genes Dev.* **18**, 2172-81.
- Yang, H.Q., Tang, R.H. and Cashmore, A.R. (2000) The signalling mechanism of Arabidopsis CRY1 involves direct interaction with COP1. *Plant Cell* **13**, 2573-87.
- Yeh, K.C. and Lagarias, J.C. (1998) Eukaryotic phytochromes: light-regulated serine/threonine protein kinases with histidine kinase ancestry. *Proc Natl Acad Sci USA* **95**, 13976-81.
- Yeh, K.C., Wu, S.H., Murphy, J.T. and Lagarias, J.C. (1997) A cyanobacterial phytochrome two-component light sensory system. *Science* **277**, 1505-8.
- Zeidler, M., Bolle, C. and Chua, N-H. (2001) The phytochrome A specific component PAT3 is a positive regulator of *Arabidopsis* photomorphogenesis. *Plant Cell Physiol* **42**, 1193–1200.
- Zimmermann, P., Hirsch-Hoffmann, M., Hennig, L. and Gruissem, W. (2004) GENEVESTIGATOR. Arabidopsis microarray database and analysis toolbox. *Plant Physiol* **136**, 2621-32.

8. APPENDIX 1

Primers used in this study are described below.

Table 1. Primers used for identification of insertion lines

Experiment	Amplified Gene	Primer Name	Primer sequence (5' → 3')	
Identification of the position of the T-DNA insertion	<i>SCL21</i>	SCL Intron-f	CCCTTATCGACTTCCACCG	
		SCL21-1000	CGAGCAGCACTGCATGGCAA G	
	<i>SCL1</i>	SCL1 1110-f	GCTGAGGCAGATAGTTTCTAT CCAA	
		SCL1-3	CGAGAAGCGCTCTTTCAAGCT CTTG	
	<i>SCL5</i>	SCL1 TGA-rev	CGGTACCCCTCCAAGCTGAA GCAAC	
		SCL5 TGA-rev	CGGTACCCCTCCAAGCACAA GCCG	
	<i>PAT1</i>	PAT1 TGA-rev	TTTCCAAGCACACGGCGAAAC C	
	Identification of the homozygous lines	<i>SCL21</i>	SCL21 Xho	CCTCGAGAACTCTCCATGTGG CCTG
			SCL21 Kpn	CGGTACCGATTGGAACATTGC CGTG
		<i>SCL1</i>	SCL1-1500	GAGGCTTACGAATACTACTCA G
SCL1-1900			CCTCTGGTAATAATACATGGA GATG	
SCL1 Prom-f			CACCAGTGCGTACTGTCGTAG GCAC	
SCL1 ATG-rev			CCACAGTTTGTTCACCATTG AG	
SCL1 ATG-f			CGTCGACATGGTGAACAAAC TGTG	
SCL1 TGA-rev			CGGTACCCCTCCAAGCTGAA GCAAC	
<i>SCL5</i>		SCL5 ATG-f	GCTCGAGATGGAAGCTACTCA GAAAC	
		SCL5 TGA-rev	CGGTACCCCTCCAAGCACAA GCCG	
<i>PAT1</i>		PAT1 ATG-f	CACCATGTACAAGCAGCCTAG ACAAG	
		PAT1 TGA-rev	TTTCCAAGCACACGGCGAAAC C	

Table 2. Primers used for the identification of homozygous lines

Experiment	Insertion	Primer Name	Primer Sequence (5' → 3')
Identification of the insertion site	SALK left-border	SALK LB1	GTTCACGTAGTGGCCATCG
	SAIL left-border	SAIL LB1	GAAATGGATAAATAGCCTTGC TTC

Table 3. Primers used for analysis of the resistance gene

Experiment	Resistance gene	Primer Name	Primer Sequence (5' → 3')
Analysis of the resistance	<i>BAR</i>	Basta-f	CCAGAACGACGCCCGGCCG
	<i>BAR</i>	Basta-rev	GTCATCAGATCTCGGTGACGG
	<i>KAN</i>	Kana-f	CTCGTCAAGAAGGCGATAGAAG
	<i>KAN</i>	Kana-rev	GGCAGGATCTCCTGTCATCTC

Table 4. Primers used for RT-PCR

Experiment	Amplified gene	Primer Name	Sequence Primer (5' → 3')
RT-PCR	<i>SCL21</i>	SCL21-f	CCCTTATCGACTTCCACCG
		SCL21-rev	GATTCGAACATTGCCGTG
	<i>PAT1</i>	PAT1-f	GAACCTCTCCATGTGGCCTG
		PAT1-rev	GCACACGAGGCAACCAAATC
	<i>SCL13</i>	SCL13-f	CTCCCATTCAACAATAATTTCTTCA
		SCL13-rev	CCAGCAATACACTACACAGCTC
	<i>18S rRNA</i>	18S rRNA-f	GCTCAAAGCAAGCCTACGCTCTGG
		18S rRNA-rev	GGACGGTATCTGATCGTCTTCGAGC

Table 5. Primers used for Northern analysis

Experiment	Amplified Gene	Primer Name	Primer Sequence (5' → 3')
Northern Blot	<i>CAB</i>	CAB-f	CGAGCCATTAACCACGTAAGC
Northern Blot	<i>CAB</i>	CAB-rev	GAGACCATTGTTGAGGCGGCCAT
Northern Blot	<i>CHS</i>	CHS-f	CTCTTACAATGTTCTTGGAGATG
Northern Blot	<i>CHS</i>	CHS-rev	GCTTCTTGGTCTCCGTCCTTC
Northern Blot	<i>XTR7</i>	XTR-f	GCTGCGGCTTGACAGCCTC
Northern Blot	<i>XTR7</i>	XTR-rev	GATCTTGACAATGTACAATGG

Table 6. Primers used for generation of RNAi and antisense lines

Experiment	Amplified Gene	Primer Name	Primer sequence (5' → 3')
Generation of RNAi lines	<i>SCL21</i>	SCL21pTOPO-f	CACCAACTCTCCATGTGGCCTG
		SCL21pTOPO-rev	GATTCGAACATTGCCGTG
	<i>PAT1</i>	PAT1pTOPO-f	CACCGACTTCAGCGTATGCTC
		PAT1pTOPO-rev	GCACACGAGGCAACCAAATC
Generation of antisense lines	<i>SCL13</i>	SCL13-f	GCTCTAGAATGGAAGCCACAGT CAAAATATTC
		SCL13-rev	GGTACCTCATTCTGACCCTCCAT TTC

Table 7. Primers used for GFP fusions

Experiment	Amplified gene	Primer Name	Primer Sequence (5' → 3')
GFP fusions	<i>SCL1</i> full-length	SCL1-f	GGGGACAAGTTTGTACAAAAAAGCAGGCT CCATGGTGGAACTGTGGTTAGAG
		SCL1-rev	GGGGACCACTTTGTACAAGAAAGCTGGGT CCCTCCAAGCTGAAGCAACGATTAAG
	<i>SCL5</i> full-length	SCL5-f	GGGGACAAGTTTGTACAAAAAAGCAGGCT CCATGGAAGCTACTCAGAAACATATG
		SCL5-rev	GGGGACCACTTTGTACAAGAAAGCTGGGT CCCTCCAAGCACAAGAAGGATAAGAG

Table 8. Primers used for promoter analysis

Experiment	Amplified gene	Primer Name	Primer Sequence (5' → 3')
Promoter-GUS fusions	<i>SCL1</i>	SCL1 Prom-f	CACCAGTGCCTACTGTCTGTTAGGCAC
		SCL1 ATG-rev	CCACAGTTTGTCCACCATTTCAG
	<i>SCL21</i>	SCL21 Prom-f	CACCGCAACAACTGAACAAG
		SCL21 Prom-rev	CAGCTATCTCTGGCAGGGCTG
	<i>SCL13</i>	SCL13 ATG-f	CACCGTCTGTCTCTTCTCTGGTAC
		SCL13 intron-rev	GCTGAAGAAATTTGTTGAATGGG
		SCL13 5'-UTR-f	CCAGCAATACACTACACAGCTC
		SCL13 ATG-rev	CACCTCCATTCAACAAATTTCTTCG

Table 9. Primers used for Two-Hybrid analysis

Experiment	Amplified gene	Primer Name	Sequence Primer (5' → 3')
Yeast Two-Hybrid	<i>SCL21</i> full-length	SCL21-f	GGGGACAAGTTTGTACAAAAAAGCAGGC TCGATGGACAATGTAAGAAGTTCAATAAT G
		SCL21-rev	GGGGACCACTTTGTACAAGAAAGCTGGG TATCACTTCCATGCACAAGATGAC
	<i>SCL21</i> deletion N-term	SCL21 delIN-f	CACCATGGTGGAGCCAATATCAAG
		SCL21 delIN-rev	TCACTTCCATGCACAAGATGAGAC
	<i>PAT1</i> full-length	PAT1-f	GGGGACAAGTTTGTACAAAAAAGCAGGC TCGTACAAGCAGCCTAGACAAGAG
		PAT1-rev	GGGGACCACTTTGTACAAGAAAGCTGGG TACATTTCCAAGCACAAGGAGC
<i>SEUSS-LIKE</i>		TH77900-f	GGGGACAAGTTTGTACAAAAAAGCCTCG ATGCAGTACCTATATCATCAGC
		TH77900-rev	GGGGACCACTTTGTACAAGAAAGCTGGG TATCATGACTTCCAAGAATATCCTC

Table 10. Primers used for analysis sequence of the different constructs

Vector Name	Primer Name	Primer Sequence (5' → 3')
PGEM	T7 promoter-f	ATTTAGGTGACACTATAGAAT
	SP6 promoter-rev	ATTTAGGTGACACTATAG
PTOPO	M13-f	GTAAAACGACGGCCAG
	M13-rev	GTCCTTTGTCGATACTG
PENTR4	pENTR4-f	GTGACCTGTTCGTTGCAAC
	pENTR4-rev	GAGACACGGGCCAGAGCTGC
pDONR207	pDONR 207-f	CGCGTTAACGCTAGCATGGATCTC
	pDONR 207-rev	GTAACATCAGAGATTTTGAGACAC
pDONR201	pDONR 201-f	CGCGTTAACGCTAGCATGGATCTC
	pDONR 201-rev	GTAACATCAGAGATTTTGAGACAC
pDONR221	M13-f	GTAAAACGACGGCCAG
	M13-rev	GTCCTTTGTCGATACTG
pK7GWIWG2/pB7GWIWG2	T35S RNAi	GCGGACTCTAGCATGGCCG
	INTRON1-RNAi	GCAGGTCAGCTTGACACTGAAC
	INTRON2-RNAi	GCCGTAAGAAGAGGCAAGCG
	P35S RNAi	CGTAAGGGATGACGCACAATCC
PKGWFS7	P35S RNAi	CGTAAGGGATGACGCACAATCC
	T35S RNAi	GCGGACTCTAGCATGGCCG
pK7FWG2	P35S RNAi	CGTAAGGGATGACGCACAATCC
	T35S RNAi	GCGGACTCTAGCATGGCCG
	GFP-rev	CGGTGAACAGCTCCTCGCCC
pDEST 22	pDEST22-f	CGGTCCGAACCTCATAACAACCTC
	pDEST-rev	AGCCGACAACCTTGATTGGAGAC
pDEST 32	pDEST32-f	AACCGAAGTGCGCCAAGTGTCTG
	pDEST-rev	AGCCGACAACCTTGATTGGAGAC

ACKNOWLEDGEMENT

This dissertation was performed in the laboratories of Prof. Dr. R. G. Herrmann at the Botanisches Institut (Department für Biologie I) of the Ludwig-Maximilian-Universität in Munich. I would like to thank Prof. Dr. R.G. Herrmann for giving me the opportunity to work in his laboratory. In particular, I would like to thank him for the critical discussion of this thesis.

I would like to express my sincere gratitude to my supervisor PD Dr. Cordelia Bolle for giving me the possibility to work in her group, without her this work could not have been done. I thank Cordelia for introducing me into the interesting topic “photobiology” and giving me exciting projects, for her ideas and stimulating discussions we had during this time, for her enormous enthusiasm and patience, for her intensive theoretical and practical supervision during the experimental work, for her permanent support and understanding and for letting me benefit from her enormous scientific knowledge. Von ganzem Herzen: Vielen Dank für alles, Cordelia!

In particular, Petra, I thank you for all the time spent together, for nice and funny talks not only in the lab, but also outside. I am thankful for your help, care and support during my work.

I would like to thank especially Christine Matzenbacher, Anina Neuman and Elli Gerick for their excellent technical advices during my work. I am grateful to Ingrid Duschaneck for helping with sequencing, Martina Reymers for helping with the yeast transformation and Uli Wißnet for taking care of the plants. I would like to thank all of them for the fun and enjoyable moments we spent together in the lab.

I would like also to thank for technical help of Dr. Lina Lezhneva at the LightCycler and Dr. Katrin Amann for Northern analysis.

Many thanks to all my colleagues, especially to Julia, Cristina, Katrin, Giusy, Lina, Won, Pavan, Lada, Irina P., Irina S., Uwe, Martha, Stephan and Jefferson for creating a nice working atmosphere.

Adela, I thank you for the nice, funny and also “bad” time spent together in the third floor. Muchas gracias por tu apoyo, por tus consejos, por los cafes y sobretudo por tu “buen rollo”, sin ti en muchos momentos seguro que hubiera abandonado!! Muchas gracias!!

My deepest thanks to my parents for encouraging me to learn at a young age and providing their love, care and support at every moment. Also my deepest thanks to my sisters, they are always providing me with love and support. Muchas gracias papas sin vuestro amor y apoyo nunca hubiera llegado a donde he llegado!ah! y no teneis que ser siempre tan pesados....lo veis.... al final lo he acabado!!!! Muchas gracias por todo lo que me habeis dado, os quiero!

My last thanks to Ralf. To meet him was the first step towards this work.

A la meva filla, la Selma.

CURRICULUM VITAE

PERSÖNLICHE DATEN

Name: Patricia Torres Galea
Geburtsdaten: 09/ 01/ 1975 Terrassa, Spanien
Staatsangehörigkeiten: Spanisch
Familienstand: verheiratet, ein Kind
Adresse: Mittlerer Graben 8
86152 Augsburg
Telefon: (0)821/8006494
e-mail: patriberga99@yahoo.es

SCHULAUSSBILDUNG

1981-1989 Grundschole, „Col.legi Public Sant Joan“, Berga, Spanien
1989-1993 Gymnasium, „Sant Tomas d‘Aquino, IES Gironella“, Spanien
Juni 1993 allgemeine Hochschulreife: Abitur (PAAU, Spanien)

UNIVERSITÄTSAUSBILDUNG

1993 – 2002 Studium der Biologie (Grundstudium) an der „Universitat Autònoma de Barcelona, UAB“, Spanien
Februar 2002 akademischer Grad: „Licenciado en Biología“, Diplom-Biologin/
Hauptfach Molekular und Pflanzenphysiologie
seit April 2002 Promotion im Department für Biologie I/Bereich Physiologische
Botanik der LMU Muenchen bei Prof. Dr. R. G. Herrmann, in der
Arbeitsgruppe von PD Dr. Cordelia Bolle
Arbeitsgebiet: „The role of GRAS proteins in light signalling“

Veröffentlichungen

Journal:

Torres-Galea P, Huang LF, Chua NH and Bolle C (2006). The GRAS protein SCL13 is a positive regulator of phytochrome-dependent red light signalling, but can also modulate phytochrome A responses. *Mol Gen Genomics* **276**, 13-30.

Eine zweite Veröffentlichung zum Thema „Function of SCL21 and PAT1 in the Phytochrome A Signal Transduction“ ist derzeit in Vorbereitung.

Poster Presentationen:

Patricia Torres-Galea and Cordelia Bolle. “The role of SCL21 GRAS protein in phytochrome A signal transduction”. September 2003 auf dem “International plant photobiology meeting” in Marburg, Deutschland.

Patricia Torres-Galea and Cordelia Bolle. “The role of GRAS proteins in phytochrome signal transduction”. Juli 2004 auf dem “15th International Conference on Arabidopsis Research” in Berlin, Deutschland.

Patricia Torres-Galea and Cordelia Bolle. “The role of GRAS proteins in light signalling”*. August 2005 auf dem “2nd Tri-national Arabidopsis meeting” in Neuchatel, Schweiz.

* Posterpreis von der Zeitschrift “Current Opinion in Plant Science”

Kurse

Microarray Workshop. September 2004, Zürich, Schweiz.

Ehrenwörtliche Versicherung

Hiermit versichere ich, dass die vorliegende Dissertation das Ergebnis eigenständigen Arbeit ist und dass ich dieses Manuskript persönlich verfasst habe. Zudem habe ich keine anderen als die angegebenen Quellen und Hilfsmittel verwendet.

Zudem erkläre ich, dass ich keine früheren Promotionsversuche unternommen habe.

München, Juli 2007

Patricia Torres Galea